THE UNIVERSITY
of EDINBURGH

Interplay between S-nitrosylation and SUMOylation in plant immunity

Michael J. Skelly

Doctor of Philosophy

University of Edinburgh

2014

Abstract

Post-translational protein modifications (PTM) vastly increase the complexity and functional diversity of the proteome, to precisely regulate crucial cellular processes. The plant immune system is composed of complex signalling networks that are influenced by various PTMs. Activation of plant immunity is associated with a rapid burst of nitric oxide (NO), which can covalently modify cysteine thiols within target proteins by a process termed S-nitrosylation to form S-nitrosothiols (SNOs), constituting a redox-based PTM. Another key PTM involved in plant immunity is SUMOylation, an essential mechanism involving the conjugation of the small ubiquitin-like modifier (SUMO) peptide to lysine residues within target proteins.

Although the targets and mechanisms of S-nitrosylation and SUMOylation are becoming evident, how these key PTMs are themselves regulated remains obscure. Work presented in this thesis reveals that during plant immune signalling, the sole *Arabidopsis thaliana* SUMO conjugating enzyme, SUMO CONJUGATING ENZYME 1 (SCE1), is S-nitrosylated at a highly conserved, but previously uncharacterized cysteine. S-nitrosylation of SCE1 was shown to inhibit its SUMO conjugating activity *in vitro* and mutational analysis revealed that the site of this modification, Cys139, is not required for enzyme activity but rather constitutes a redox-sensitive inhibitory switch. Generation and characterization of transgenic *Arabidopsis* plants overexpressing both wild-type and mutant forms of SCE1 revealed that Cys139 is required for efficient immunity against bacterial pathogens. Furthermore, after immune activation, S-nitrosylation of this residue inhibits global SUMOylation of proteins. These results provide evidence of a novel means of crosstalk between S-nitrosylation and SUMOylation in the context of plant immunity.

The abundant cellular antioxidant, glutathione (GSH), is S-nitrosylated to form S-nitrosoglutathione (GSNO), which is thought to constitute a stable reservoir of NO bioactivity. In *Arabidopsis*, GSNO levels are controlled by the enzyme S-NITROSOGLUTATHIONE REDUCTASE 1 (GSNOR1), which indirectly

influences the levels of protein SNOs. In this study, transgenic plants overexpressing FLAG-epitope tagged GSNOR1 were generated in various mutant backgrounds, including *nitric oxide overproducer 1* (*nox1*), to further investigate the roles of GSNOR1 and NO in plant immunity. It was shown that ectopic GSNOR1 expression completely recovers developmental and disease susceptibility phenotypes of *gsnor1*, but not *nox1* mutant plants, highlighting *in vivo* differences between accumulation of GSNO and free NO. Surprisingly, elevated NO levels in *nox1* plants promote S-nitrosylation of GSNOR1, inhibiting its enzymatic activity. This suggests a previously unreported means by which NO might regulate its own bioavailability.

Further work in this study revealed that recombinant GSNOR1 can be SUMOylated *in vitro*, which appeared to increase its enzymatic activity. Several potential SUMO modification sites were identified within GSNOR1 and mutational analysis revealed that at least one of these, Lys191, is SUMOylated. Co-immunoprecipitation experiments revealed that transgenic GSNOR1 might be SUMOylated *in vivo*, although the site(s) and biological function of SUMOylation were not identified. Nonetheless, these results reveal another possible layer of interplay between S-nitrosylation and SUMOylation.

Lay Summary

Plants possess a complex immune system that provides resistance against a diverse range of pests and pathogens. Inside plant cells, immune responses are controlled by various modifications of molecules known as proteins. Work presented in this thesis reveals that two different types of these protein modifications can regulate each other, and that these interactions play important roles in immune responses, growth, and development in the model plant, *Arabidopsis thaliana*. Use of model organisms, such as *Arabidopsis*, allows rapid genetic modification in order to study fundamental biological processes. As such, the findings of this thesis can potentially be translated into other species, including crop plants and humans, as many of the mechanisms studied exist in both plants and animals. Therefore, novel regulatory mechanisms uncovered in this work may provide benefits in the context of food security and medicine.

Declaration

I hereby declare that except where explicitly stated in the text*, the work presented here is my own and has not been submitted in any form for any degree at this or any other university.

Michael J. Skelly

*Data shown in Figure 3-1 (A and B) were produced by Saad Malik. Data shown in Figures 6-1 and Figure 6-2 (A) were produced by Lucas Frungillo. Permission has been gained from both parties for inclusion in this thesis.

Acknowledgements

Firstly, I would like to thank the Biotechnology and Biological Sciences Research Council for funding my PhD. I am also grateful to the Biochemical Society and the James Rennie Bequest for the award of travel grants that allowed me to attend and present my work at the 24th International Conference on Arabidopsis Research in Sydney, Australia.

I am grateful to my supervisor Gary Loake, for his encouragement and allowing me the freedom to develop my own ideas throughout my PhD.

I thank Steven Spoel for hosting me for my first year lab rotation and sharing many materials and valuable thoughts over the last four years.

I am grateful to Saad Malik for his previous work on the S-nitrosylation of SCE1 and for the generation of numerous constructs for recombinant protein expression, which were invaluable for many of my experiments.

Thanks to our collaborators in Brazil, Lucas Frungillo and Ione Salgado. It was a pleasure to work with you and I hope to again in the future.

A big thanks to all the IMPS staff who keep the department running smoothly.

Thanks to all members of the Loake lab, past and present, it has been fun working with you all.

Finally, a huge thanks to Sarah and all of my family and friends for their support and encouragement over the last four years.

Thanks!

Contents

List of Figures

List of Tables

List of abbreviations

ABA	abscisic acid
Asc	ascorbate
ATG	AUTOPHAGY
ATP	adenosine triphosphate
avr	avirulence
AzA	azelaic acid
BST	biotin switch technique
CA	carbonic anhydrase
CaMV	cauliflower mosaic virus
cDNA	complementary DNA
CFU	colony forming units
Cys	cysteine
CysNO	S-nitrosocysteine
DEA/NO	diethylamine NONOate
DA	abietane diterpenoid dehydroabietinal
DTT	dithiothreitol
EDS1	enhanced disease susceptibility 1
EIX	ethylene-inducing xylanase
ESD4	EARLY IN SHORT DAY 4
ET	ethylene
ETI	effector-triggered immunity
FAD	flavin adenine dinucleotide
G3P	glycerol-3-phosphate
Glu	glutamic acid
GSH	reduced glutathione
GSNO	S-nitrosoglutathione
GSNOR	S-NITROSOGLUTATHIONE REDUCTASE
GSSG	oxidized glutathione
GST	glutathione S-transferase
H_2O_2	hydrogen peroxide
HEN	hepes, EDTA, neocuproine buffer
His	histidine
hpi	hours post-infection
HPY2	HIGH PLOIDY 2
HR	hypersensitive response
HSF	heat shock factor
IP	immunoprecipitation
JA	jasmonic acid
Lys	lysine
MAMP	microbial-associated molecular pattern
MAPK	mitogen-activated protein kinase
MC9	METACASPASE 9
MeSA	methyl salicylic acid
MMS21	METHYLMETHANESULFONATE SENSITIVE 21
MS	Murashige and Skoog media

NADH	nicotinamide adenine dinucleotide
NADPH	nicotinamide adenine dinucleotide phosphate
NB-LRR	nucleotide binding, leucine-rich repeat
NEDD8	neural precursor cell expressed
NEM	*N*-Ethylmaleimide
NH_3	ammonia
NIA	NITRATE REDUCTASE
NO	nitric oxide
NOS	nitric oxide synthase
nox1	nitric oxide overproducer 1
NPR1	NONEXPRESSOR OF PATHOGENESIS-RELATED GENES 1
NR	nitrate reductase
NTRA	NADPH-dependent thioredoxin reductase
O_2^-	superoxide
$ONOO^-$	peroxynitrite
PAMP	pathogen-associated molecular pattern
par2	*paraquat resistant 2*
PBS	phosphate-buffered saline
PCD	programmed cell death
PCNA	proliferating cell nuclear antigen
PCR	polymerase chain reaction
Pias3	protein inhibitors of activated STAT 3
PR	pathogenesis-related
PRR	pattern recognition receptor
PrxIIE	PEROXIREDOXIN II E
Pst	*Pseudomonas syringae* pv. tomato
PTI	PAMP-triggered immunity
PTM	post-translational modification
qPCR	quantitative real-time PCR
RanGAP1	RanGTPase activating protein 1
RBOH	respiratory burst oxidase homologue
ROI	reactive oxygen intermediate
RPM1	*RESISTANCE TO P. SYRINGAE PV MACULICOLA 1*
RST	reductive switch technique
RSUME	RWD-containing SUMOylation enhancer
RT	room temperature
RT-PCR	reverse transcriptase PCR
RUB	RELATED TO UBIQUITIN
SA	salicylic acid
SABP3	SA BINDING PROTEIN 3
SAE	SUMO activating enzyme
SAR	systemic acquired resistance
Sc	*Saccharomyces cerevisiae*
SCE1	SUMO CONJUGATING ENZYME 1
SDS	sodium dodecyl sulphate
SDS-PAGE	SDS-polyacrylamide gel electrophoresis
SEM	standard error of mean
*Sl*ERF4	*Solanum lycopersicum* ethylene responsive transcription factor 4

Smt3	suppressor of MIF two 3
SNO	S-nitrosothiol
SNP	single nucleotide polymorphism
SOH	sulphenic acid
SO_2H	sulphinic acid
SS	disulphide
SUMO	small ubiquitin-like modifier
SIZ1	SAP AND MIZ 1
T-SUMO	tomato SUMO
TGA	TGA-element binding bZIP transcription factor
TRX	thioredoxin
TTSS	type III secretion system
Tyr	tyrosine
Ub	ubiquitin
UBQ	*UBIQUITIN*
Ubc9	ubiquitin-conjugating enzyme 9
Ubl	ubiquitin-like protein
Ulp	ubiquitin-like protein protease
WB	western blot
WRKY	transcription factors containing a conserved WRKY domain
WT	wild-type

Chapter 1

1 Introduction

1.1 Post-translational protein modifications

The evolution of genomes takes place over millions of years, improving and adapting organisms to increase their chances of survival by adding, removing and editing genes. Each gene has a number of ways by which it can be transcribed, with diverse promoters, splicing variants and differential transcript lengths all contributing to a multitude of mRNA combinations that can originate from a single gene (Jensen, 2004). After these mRNAs are translated into proteins, there is a further exponential increase in the amount of possible gene products, facilitated by a plethora of post-translational modifications (PTMs) that allow dynamic control of protein function (Figure 1-1). PTMs are vital for organisms to maintain homeostasis in the face of ever-changing environments, providing a vast array of molecular switches that can be controlled rapidly to regulate cellular processes. The almost unlimited amount of protein variations that PTMs allow has been described as "Nature's escape from genetic imprisonment" (Prabakaran et al, 2012). Over 300 types of PTM have been described and range from the addition of small molecules to complex carbohydrates and even the addition of other proteins.

PTMs underpin almost all biological processes and their dysregulation is associated with a multitude of diseases and abnormalities not only in humans and other animals, but also in plants. Therefore, improving our understanding of PTMs and how they are regulated is of great importance to improve human health and maintain survival. With a rapidly growing global population, less land available for

agriculture, and limited water, improved crop production is required to keep up with intensifying demand (Ronald, 2011). Although plants are equipped with a sophisticated and efficient immune system, up to 16% of crops are lost globally each year to diseases caused by plant pathogens (Oerke et al, 2006). If this loss can be reduced it will greatly relieve the pressure on society to maintain food security in the coming decades. Dissecting the signalling pathways, and the regulation of PTMs involved in plant immunity will potentially uncover new mechanisms by which plants can be engineered with improved disease resistance. Furthermore, novel insights in to the plant immune system might lead to new discoveries in human immunity, thereby leading to the development of new therapeutic technologies.

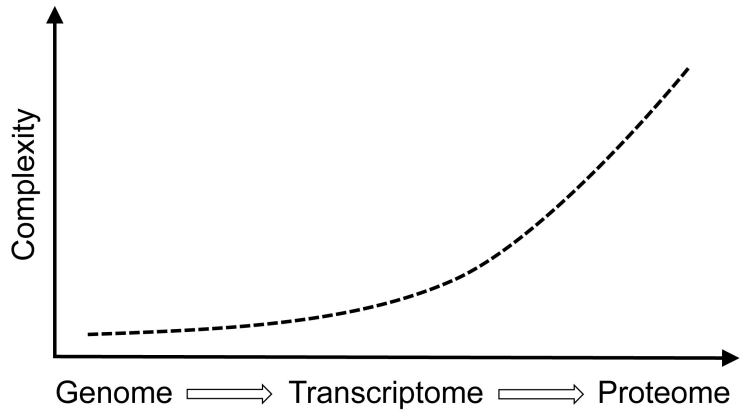

Figure 1-1 Post-translational modifications exponentially increase the complexity of the proteome

From the level of the genome to the proteome, the amount of possible gene products increases exponentially through post-translational modification of proteins. Adapted from Jensen et al (2004).

1.2 The plant immune system

To successfully grow and survive, plants must continuously resist attempted infection by a large variety of pathogens. Unlike animals, plants do not possess an adaptive immune system and do not have specific cells dedicated to providing immunity. However, plants have evolved a vast array of strategies to resist pathogen infection, from simple physical barriers and preformed antimicrobial compounds to a battery of inducible defence mechanisms. Phytopathogens must first subvert the cell wall, a complex and rigid structure that after defence activation, can be further strengthened at sites of attempted infection by the deposition of polysaccharides. If a pathogen manages to breach the cell wall, it will then encounter the plant innate immune system, which can be regarded as having two branches (Jones and Dangl, 2006). The first branch is triggered at the cell membrane where transmembrane pattern recognition receptors (PRRs) recognize molecular hallmarks of pathogens known as microbial- or pathogen-associated molecular patterns (MAMPs or PAMPs). This activates a relatively weak immune response termed PAMP-triggered immunity (PTI). Pathogens that have successfully evolved to counter this response can then secrete effector molecules into plant cells that suppress PTI. In some cases, these effectors are recognized by plant resistance (*R*)-gene products, triggering the second, more potent response of the immune system, termed effector-triggered immunity (ETI). This second branch of immunity commonly utilises NB-LRR proteins, named after their nucleotide binding (NB) and leucine rich repeat (LRR) domains. These NB-LRRs are the largest class of proteins encoded by the *R*-genes of plants. Pathogen genes encoding effectors that are recognized by the plant *R*-gene products can then be termed *avr*-genes as their recognition results in their avirulence.

This ‘gene-for-gene’ model (Flor, 1971) represents a long-fought evolutionary battle between plants and pathogens. After pathogen recognition, plants deploy a wide range of defence responses to resist attempted infection. To limit pathogen growth, plants often trigger programmed cell death (PCD) of plant cells at the site of attempted infection, known as the hypersensitive response (HR) (Dangl et al, 1996). This response is thought to cut off the availability of nutrients to pathogens provided by living plant cells.

Although plants lack a circulatory system, activation of immunity leads to the systemic transmission of signals throughout the plant, which protect distal tissues against potential secondary infections, a mechanism termed systemic acquired resistance (SAR) (Ross, 1961). The induction of SAR is mainly associated with ETI, although it can also be triggered by virulent pathogens (Mishina and Zeier, 2007; Kachroo and Robin, 2013). A key molecule in the establishment of SAR is the plant defence hormone, salicylic acid (SA). Pathogen recognition induces the production of SA, and this was originally proposed to be the mobile signal responsible for transduction of immunity to distal tissues. However, grafting experiments in tobacco revealed that although SA is required in distal tissues for the onset of SAR, it is not the signal that travels from the site of infection to distal tissues (Vernooij et al, 1994). Other small molecules produced after pathogen attack that promote SAR, and thus may constitute the aforementioned mobile signal(s) include methyl salicylic acid (MeSA), azelaic acid (AzA), glycerol-3-phosphate (G3P), and abietane diterpenoid dehydroabietinal (DA) (Fu and Dong, 2013; Kachroo and Robin, 2013). Although the identity of the mobile SAR signal remains a mystery, it is clear that SA is a key immune activator (Loake and Grant, 2007). SA accumulation induces the expression

of various *PATHOGENESIS-RELATED* (*PR*) genes in local and systemic tissues, encoding proteins with various antimicrobial functions that contribute towards SAR (van Loon and van Kammen, 1970; Fu and Dong, 2013). Other important plant hormones involved in immune signalling include jasmonic acid (JA) and ethylene (ET), although these are classically associated with defence against herbivores and necrotrophic pathogens, whereas SA is associated with defence against biotrophs. SA, JA and ET-signalling networks are extremely complex and can interact with each other antagonistically and synergistically, allowing plants to tailor their defence repsonses to the type of pathogen encountered (Verhage et al, 2010).

Activation of plant immunity is associated with the rapid production of nitric oxide (NO), and a parallel burst of reactive oxygen intermediates (ROIs), primarily superoxide (O_2^-) and hydrogen peroxide (H_2O_2). Critical for generation of the nitrosative and oxidative bursts are calcium ion (Ca^{2+}) influxes from the apoplast into the cytosol (Frederickson Matika and Loake, 2014). Both ROIs and NO, either alone or together, appear to function as key regulators of plant immunity (Delledonne et al, 2001; Scheler et al, 2013). A major means by which these small redox-active molecules exert their downstream biochemical activity is through post-translational modification of reactive cysteine residues within target proteins (Spadaro et al, 2010; Spoel and Loake, 2011; Skelly and Loake, 2013), discussed in more detail in the following sections of this chapter.

1.3 NO signalling in plant immunity

1.3.1 NO synthesis

Despite a wealth of evidence implicating a central role for NO in plant growth, development and environmental responses (Yu et al, 2014), a nitric oxide synthase (NOS), similar in structure to those found in animals, has yet to be identified in higher plants. These NADP(H)-dependent enzymes catalyze the formation of NO and citrulline from L-arginine. It is well established that mammals possess three isoforms of NOS; neuronal- (nNOS), endothelial- (eNOS) and inducible- (iNOS), the latter of which has been implicated in immune responses. A NOS similar to human eNOS in both sequence and structure was recently identified in *Ostreococcus tauri*, a single cell algae (Foresi et al, 2010). Purified recombinant protein from this predicted sequence was shown to exhibit similar catalytic kinetics to other NOS enzymes *in vitro*. Furthermore, *Escherichia coli* cells expressing *O. tauri* NOS showed increased levels of NO and cell viability, demonstrating the NOS activity of this enzyme. Although it is unlikely that they possess a protein structurally similar to these characterized NOS enzymes, higher plant extracts do appear to exhibit NOS-like activity (Cueto et al, 1996; Ninnemann and Maier, 1996; Delledonne et al, 1998; Durner et al, 1998). Accordingly, *Arabidopsis NO overproducer 1* (*nox1*) mutants that have elevated levels of NO (He et al, 2004) were originally described as *chlorophyll a*/*b binding protein* (*CAB*) *underexpressed 1* (*CUE1*), mutants that accumulate L-arginine and citrulline (Streatfield et al, 1999).

While a NOS in higher plants remains to be identified, other mechanisms by which plants can produce NO have been reported (Frohlich and Durner, 2011). A possible source is through the action of cytosolic nitrate reductases (NR), of which

two are found in *Arabidopsis*, NIA1 and NIA2, with NIA2 being responsible for the bulk of NR activity (Wilkinson and Crawford, 1991). These enzymes are primarily involved in reducing nitrate (NO_3^-), the main nitrogen source of plants, to nitrite (NO_2^-) in a NADPH-dependent fashion. However, NR also appears to be capable of producing NO both *in vitro* and *in vivo* independently of NOS activity (Rockel et al, 2002). It should be noted that the *in vivo* data from this study relied on artificial chemical stimulation of NR and so NR-derived NO production may not represent a physiologically relevant process. Furthermore, the production of NO by NR is inefficient and depends upon low O_2 levels and high concentrations of NO_2^- (Rockel et al, 2002). Further support for NR-mediated NO production came from a study examining the mechanisms of NO production during symbiosis between the legume *Medicago truncatula* and the Rhizobium *Sinorhizobium meliloti*. This study revealed that both plant and bacterial NRs contribute towards NO production in root nodules (Horchani et al, 2011).

1.3.2 S-nitrosylation

It is well established that NO levels are rapidly increased after pathogen recognition, and the downstream signalling mechanisms that translate NO accumulation into biological functions are now becoming evident. Being a gaseous free radical, NO is highly reactive and can modify thiols, tyrosine residues, metal centres and other reactive molecules such as ROIs (Leitner et al, 2009). S-nitrosylation, i.e. the addition of a NO moiety to a reactive cysteine thiol to form an S-nitrosothiol (SNO) has emerged as the principle mechanism by which NO conveys its bioactivity (Wang et al, 2006; Spadaro et al, 2010). This reversible, post-

translational protein modification was discovered in 1992 (Stamler et al, 1992) and has since been shown to regulate the activity, localization and conformation of a vast array of target proteins in plants and animals (Wang et al, 2006; Hess et al, 2005). S-nitrosylation is just one of many reversible redox-based modifications that can occur at reactive cysteine thiols with varying levels of oxidation, others include S-sulphenation (SOH), S-thiolation (SS, i.e. disulphide formation), and S-sulphination (SO_2H) (Spadaro et al, 2010; Spoel and Loake, 2011) (Figure 1-2).

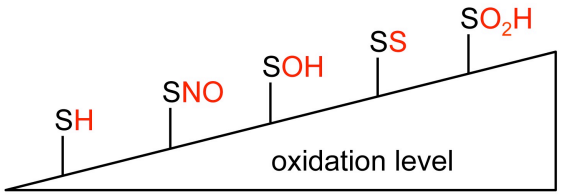

Figure 1-2 Redox-based cysteine modifications

Schematic diagram showing different redox-based modifications of cysteine thiols and their relative oxidation levels. Cysteine modifications depicted are unmodified free thiol (SH), S-nitrosylation (SNO), S-sulphenation (SOH), disulphide (SS) and S-sulphination (SO_2H). Adapted from Spadaro et al, 2010.

The small tripeptide glutathione (GSH), an important antioxidant and the most abundant cellular thiol, readily reacts with NO to form S-nitrosoglutathione (GSNO), a molecule thought to provide a relatively stable reservoir of NO bioactivity (Broniowska et al, 2013). NO can be released from GSNO or directly transferred to another thiol group by a mechanism termed transnitrosylation (Hess et al, 2005), therefore GSNO serves as a cellular NO donor. An enzyme conserved in

animals, plants and yeast, responsible for controlling GSNO levels is known as GSNO-reductase (GSNOR) and reduces GSNO to oxidized glutathione (GSSG) and ammonia (NH_3) (Liu et al, 2001). Although these enzymes are highly specific towards GSNO, they indirectly control the levels of protein SNOs by disrupting the GSNO:protein-SNO equilibrium (Liu et al, 2001) (Figure 1-3). Loss of GSNOR function in *Arabidopsis* leads to increased global SNO levels and compromised disease resistance (Feechan et al, 2005), confirming the importance of S-nitrosylation in plant immunity. Furthermore, SNO homeostasis appears to influence the accumulation of the immune activator SA, and the expression of SA-dependent defence genes (Loake and Grant, 2007; Feechan et al, 2005). Other studies have revealed that GSNOR is also a key regulator of plant development, cell death and thermotolerance (Kwon et al, 2012; Chen, 2009; Lee et al, 2008). Many proteins with important roles in plant immune signalling have now been identified as targets of S-nitrosylation and are discussed in the following section.

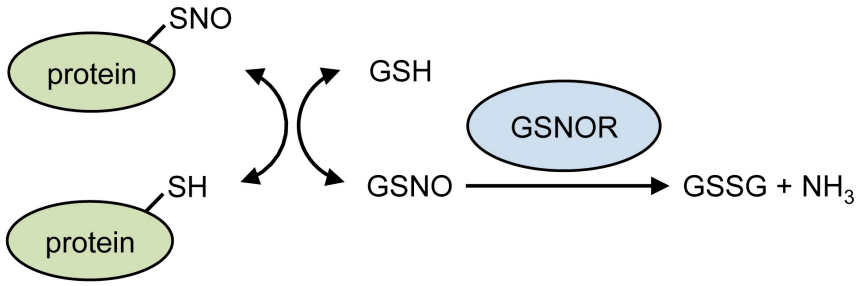

Figure 1-3 GSNOR indirectly controls protein-SNO levels

GSNOR has specific activity towards GSNO, reducing it to GSSG and NH3. Changes in GSNOR activity affect protein-SNO levels by disturbing the GSNO:protein-SNO equilibrium.

1.3.2.1 S-nitrosylation of plant defence-related proteins

The defence-related transcription co-activator NPR1 (NONEXPRESSOR OF PATHOGENESIS-RELATED GENES 1) is a central regulator of SA-mediated gene expression in *Arabidopsis*. NPR1 possesses many cysteine residues that facilitate the formation of high molecular-weight oligomers, mediated by intermolecular disulphide bonds. NPR1 oligomers are located in the cytoplasm but after pathogen infection, reduction of these disulphide bonds generates monomeric NPR1 to allow translocation to the nucleus where it exerts its co-activator function on many target genes (Mou et al, 2003). It was later shown that S-nitrosylation of NPR1 promoted its oligomerization and thus perturbed its transcriptional activity (Tada et al, 2008). S-nitrosylation of NPR1 was increased in *gsnor1-3* mutant plants, providing a molecular link between the elevated global SNO levels and the compromised disease resistance of these plants. Cellular redox status not only affects NPR1 but also its binding partners, the transcription factors TGA1 and TGA4, which possess intramolecular disulphide bonds at key cysteine residues that appear to block NPR1 interaction (Després et al, 2003). It was shown that reduction of these disulphide bonds leads to NPR1-TGA1/4 interaction and the subsequent activation by binding to target DNA (Després et al, 2003). A recent study revealed that these same cysteine residues can be S-nitrosylated and this may serve to prevent further oxidation of TGA1/4, enhancing their DNA-binding capacity (Lindermayr et al, 2010). There are now many lines of evidence suggesting the NPR1-TGA transcriptional regulation system is under complex redox-mediated control with S-nitrosylation appearing to play a key role (Spoel and Loake, 2011) (Figure 1-4).

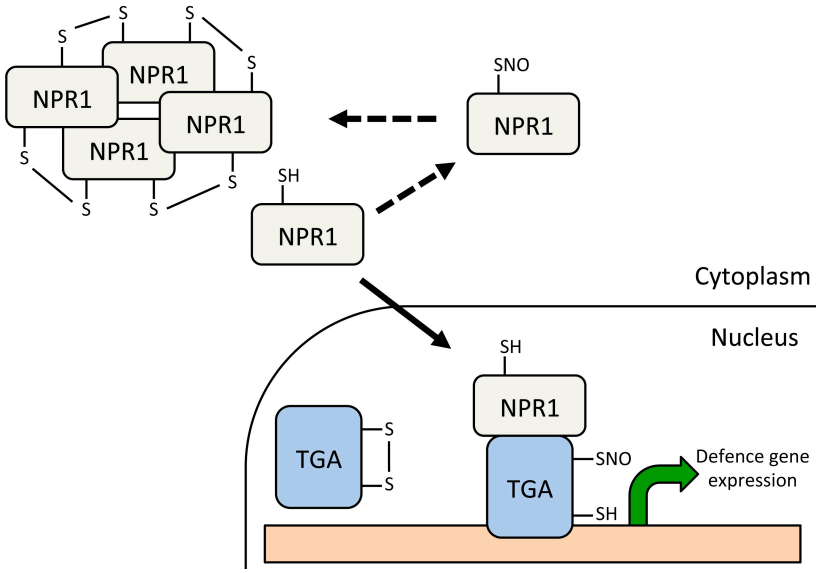

Figure 1-4 Redox regulation of the NPR1-TGA system

NPR1 forms high molecular weight oligomers in the cytoplasm, facilitated by intermolecular disulphide formation. Upon pathogen attack, reduction of these disulphide bonds allows monomeric NPR1 to translocate to the nucleus where it induces the expression of defence genes along with its cognate TGA transcription factors. S-nitrosylation of NPR1 is thought to promote its oligomerization while S-nitrosylation of TGAs may prevent formation of intramolecular disulphides, enhancing their DNA binding capacity. Source: Skelly and Loake, 2013.

Another S-nitrosylation target involved in SA signalling is SABP3 (SA BINDING PROTEIN 3) (Wang et al, 2009), a protein previously shown to exhibit carbonic anhydrase (CA) activity (Slaymaker et al, 2002). It was shown that S-nitrosylation of SABP3 was increased after infection with *Pseudomonas syringae* pv. tomato (*Pst*) DC3000 carrying the avirulence gene *avrB*, recognized by the resistance gene, *RESISTANCE TO P. SYRINGAE PV MACULICOLA 1* (*RPM1*) in wild-type (WT) Col-0 plants (Wang et al, 2009). S-nitrosylation of SABP3 appeared to inhibit both its SA binding capacity, and its CA activity. Interestingly, mutation of the site

of S-nitrosylation, Cys280, rendered SABP3 inactive suggesting that this residue is essential for protein function (Wang et al, 2009). Thus, S-nitrosylation of this cysteine has a potent effect on SABP3 activity. The CA activity of SABP3 was shown to be required for disease resistance, which raises a dilemma, since the nitrosative burst and subsequent S-nitrosylation of proteins is associated with activation of plant immunity. However, this might represent a negative feedback loop to regulate SA-mediated responses or could even be a strategy exploited by pathogens to suppress host immunity (Wang et al, 2009).

After activation of plant immunity, and the subsequent nitrosative and oxidative bursts, peroxynitrite ($ONOO^-$), a highly toxic agent, is consequently formed by NO reacting with O_2^-. Detoxification of $ONOO^-$ is essential to avoid damaging effects and in *Arabidopsis*, the enzyme that performs this process is PrxIIE (PEROXIREDOXIN II E) (Romero-Puertas et al, 2007). PrxIIE was shown to be S-nitrosylated, which inhibited its ability to detoxify $ONOO^-$ (Romero-Puertas et al, 2007). $ONOO^-$ has been shown to stimulate PCD in animals (Bonfoco et al, 1995) but not in plants, (Delledonne et al, 2001; Romero-Puertas et al, 2007). Thus, the S-nitrosylation of PrxIIE may serve as a regulatory mechanism that NO employs to control the levels of $ONOO^-$, but it is unknown whether this has a role in PCD and/or plant immunity. Caspases are proteins that are integrated into signalling cascades that induce PCD in humans. Caspase-3 has been shown to be basally S-nitrosylated at its active-site cysteine in human cells (Mannick et al, 1999). This S-nitrosylation suppressed the cysteine protease activity of caspase-3, which is required for triggering PCD. Upon induction of the PCD pathway, levels of S-nitrosylated caspase-3 decreased with a concurrent increase in intracellular caspase activity and

induction of PCD (Mannick et al, 1999). This may have some relevance to plants, as the *Arabidopsis* relative of caspase-3, MC9 (metacaspase 9), has also been identified as a target for S-nitrosylation. Similarly, this inhibited its proteolytic activity (Belenghi et al, 2007), although whether this process has a role in plant immunity remains obscure.

Generation of the oxidative burst by plants after immune activation has long been attributed to NADPH oxidase enzymes termed respiratory burst oxidase homologues (RBOHs). The *Arabidopsis* genome contains ten predicted *RBOH* genes (*RBOHA-RBOHJ*) (Torres et al, 2005), although RBOHD and RBOHF were shown to be the main generators of ROIs after pathogen recognition (Torres et al, 2002). A novel link between NO and ROIs was recently uncovered after RBOHD was identified as a target for S-nitrosylation during immune signalling (Yun et al, 2011). S-nitrosylation of RBOHD at Cys280 inhibited its NADPH oxidase activity *in vitro* and this cysteine was also S-nitrosylated *in vivo*. Accordingly, production of ROIs was shown to be decreased by elevated SNO levels in both *gsnor1-3* and *nox1* mutant plants. It was shown that S-nitrosylation of RBOHD Cys890 inhibited binding of its cofactor flavin adenine dinucleotide (FAD), and this effect was abolished in a C890A mutant protein. In further agreement, transgenic plants expressing a C890A mutant RBOHD showed increased levels of pathogen-induced ROI accumulation and cell death during the HR. These findings suggest a negative feedback loop by which the increasing NO levels during the HR promote S-nitrosylation of RBOHD at Cys890, attenuating its NADPH oxidase activity to prevent excessive ROI-induced cell death (Yun et al, 2011). Importantly, this cysteine reside is highly conserved from plants to humans and this study also showed

that recombinant human and *Drosophila melanogaster* NADPH oxidases can be S-nitrosylated at this site *in vitro*, suggesting that this mechanism of regulating cell death in immune responses may also operate in other eukaryotes (Yun et al, 2011).

1.3.2.2 Enzymatic denitrosylation by thioredoxins

As previously discussed, cellular redox status and GSNOR activity modulate global SNO levels. However, NO can be directly removed from target proteins by enzymes with denitrosylating activity. Thioredoxin (TRX) proteins are mainly associated with reduction of disulphide bonds, and indeed *Arabidopsis* TRX-h5 (TRX5) has been shown to facilitate the reduction and subsequent monomerization of NPR1 oligomers upon SA-mediated plant defence activation (Tada, 2008). Furthermore, TRX5 has been implicated in plant immunity in response to the toxic peptide victorin, produced by the Victoria blight fungus (Sweat and Wolpert, 2007), and is also upregulated in response to avirulent bacterial pathogens (Laloi et al, 2004). TRXs have since been shown to possess specific denitrosylating activity and together with thioredoxin reductase (TRX-reductase) can remove the NO from SNOs within target proteins (Benhar et al, 2008). A recent animal proteomic study revealed a list of S-nitrosylated proteins with diverse functions to be substrates for TRX/TRX-reductase-mediated denitrosylation (Benhar, 2010), thus further enhancing the notion that denitrosylation of proteins by TRX may have important roles in cellular signalling. However, whether or not there is a role for TRX-mediated denitrosylation in the context of plant immunity remains a mystery.

1.3.2.3 Identification of S-nitrosylated proteins in plants

Since S-nitrosylation of proteins after immune activation constitutes an important signalling mechanism, identifying new targets of this PTM will help to uncover the complexities of plant immunity. The highly labile nature of the S-NO bond makes it a technically challenging PTM to detect. Most research to date has relied on the biotin-switch technique (BST), where free cysteines are first blocked before SNOs are specifically reduced with ascorbate and switched with a biotin label (Forrester et al, 2009). This procedure allows detection of S-nitrosylated proteins with antibodies against biotin, or enrichment by streptavidin affinity purification. The first proteomic screen to identify S-nitrosylated proteins in *Arabidopsis* revealed a catalogue of proteins involved in a diverse range of cellular processes (Lindermayr et al, 2005). However, this study involved the application of exogenous GSNO and therefore does not represent a true list of endogenous S-nitrosylated proteins. A further proteomic analysis of plants undergoing HR only identified 16 proteins (Romero-Puertas et al, 2008) that did not include any of the defence-related targets of S-nitrosylation described previously in Section 1.3.2.1. Therefore, it is likely that due to its often transient nature (Hess et al, 2005), proteomic screens will be likely to miss many proteins that are regulated by S-nitrosylation and new targets for this PTM remain to be identified. More recent proteomic analyses have identified and monitored the levels of endogenous S-nitrosylated proteins in plants responding to salt and cold stress (Fares et al, 2011; Puyaubert et al, 2014). Again, none of the proteins previously mentioned in Section 1.3.2.1 were identified in these studies, although this could be expected due to the lack of immune activation in the plants tested. Thus, a more complete assembly of the SNO-proteome after immune

activation and the subsequent nitrosative burst is required to identify novel NO-regulated proteins involved in plant immune signalling.

1.4 Ubiquitin and ubiquitin-like proteins

Ubiquitin (Ub) and ubiquitin-like proteins (Ubls), including the small ubiquitin-like modifier (SUMO) are covalently conjugated to lysine residues within target proteins. Ub is a small protein of 76 amino acids that was first discovered in 1975 (Goldstein et al, 1975) and is conserved in all eukaryotic cells. Although Ub is classically known for its role in targeting substrate proteins for degradation by the 26S proteasome, it is now apparent that it also has other roles in various cellular processes including control of subcellular localization, chromatin structure, signal transduction and DNA damage responses (Komander and Rape, 2012). Since the discovery of Ub, other Ubls have been identified with various roles in cellular processes. Ubl subfamilies in plants include SUMO, RUB [RELATED TO UBIQUITIN, an orthologue of mammalian NEDD8 (neural precursor cell expressed, developmentally down-regulated 8)], ATG8 and ATG12 (AUTOPHAGY 8 and 12) (Miura and Hasegawa, 2010). These proteins are classified as Ubls by having both a similar three-dimensional structure to Ub and also having similar mechanisms of conjugation to target proteins (Dye and Schulman, 2007; Hochstrasser, 2009). The main structural characteristic of Ub and Ubls is the ‘Ub-fold' which is a globular domain consisting of an α–helix surrounded by four β-sheets (Figure 1-5). Ubls also possess flexible C-terminal domains by which they attach to lysine residues of substrate proteins. Remarkably, despite having such similar structures, the Ubls share little sequence homology to Ub with RUBs having approximately 60% sequence

similarity but the other subfamilies sharing less than 30% (Miura and Hasegawa, 2010).

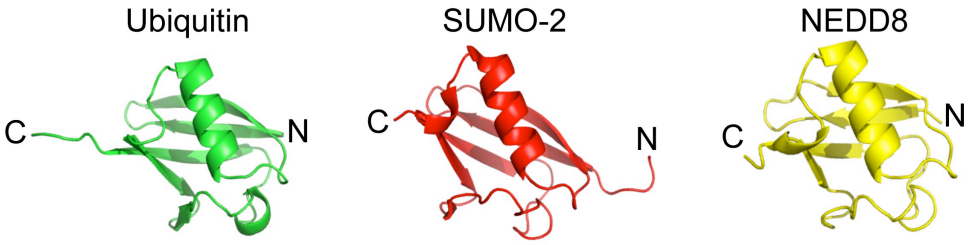

Figure 1-5 Structural similarities of Ub and Ubls

Cartoon representations of the crystal structures of mammalian Ub, SUMO-2 and NEDD8. Adapted from Dye and Schulman, 2007.

1.5 SUMOylation

SUMO was first identified in mammals in 1997 attached to RanGTPase activating protein 1 (RanGAP1), a protein implicated in nuclear transport and control of mitosis (Mahajan et al, 1997). Since its discovery, SUMO has become the best characterized of all the Ubls and its importance in various cellular processes has become evident. SUMO is present in all eukaryotes and is essential for viability (Hay, 2005; Saracco et al, 2007). Newly synthesised SUMO is formed as a precursor that must be matured through proteolytic cleavage to expose the C-terminal diglycine required for conjugation. SUMO is conjugated to target proteins via a pathway analogous to ubiquitination, involving three classes of enzymes known as E1, E2 and E3s. The SUMO activating enzyme (E1) is a heterodimeric complex and forms a high-energy thioester bond with the C-terminal carboxyl group of SUMO. Next,

SUMO is transferred to the SUMO conjugating enzyme (E2), which catalyzes the conjugation of SUMO to its targets. SUMO ligases (E3) enhance the efficiency of conjugation and may contribute to target specificity but are not required for SUMO conjugation *in vitro* (Desterro et al, 1999) (Figure 1-6).

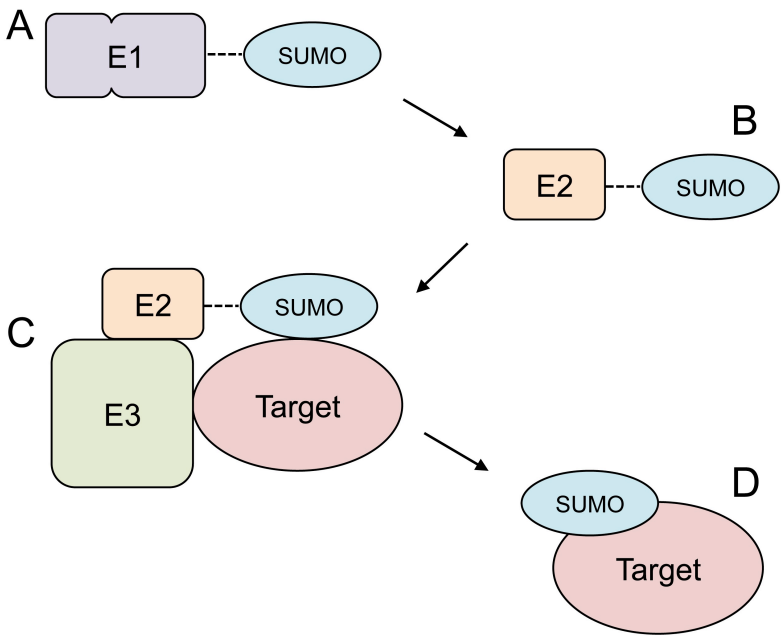

Figure 1-6 The SUMOylation cascade

(A) SUMO is first activated by forming a thioester bond with active site cysteine of the heterodimeric E1 enzyme. **(B)** The activated SUMO thioester is then transferred to the E2 conjugating enzyme. **(C)** The E2 can conjugate SUMO directly to its targets but E3 ligases are thought to have a role in presenting the target to the E2 as well as enhancing the efficiency of conjugation. **(D)** SUMO is covalently attached to lysine residues within target proteins by an isopeptide bond.

SUMO modification usually occurs at target lysine residues within the recognition sequence ψKXE, where ψ represents a large hydrophobic residue such as leucine, isoleucine or valine and X represents any amino acid (Rodriguez et al, 2001). This short sequence is recognised by the E2 enzyme and provides a binding site between the E2 and substrate protein (Bernier-Villamor et al, 2002). Although this is the consensus SUMO attachment site, SUMOylation can occur at other lysine residues within proteins and the existence of a ψKXE motif in a protein does not necessarily mean that it is a target for SUMO modification (Hay, 2005). SUMO is deconjugated from targets by SUMO-specific proteases, which also provide the previously mentioned proteolytic cleavage activity for SUMO maturation. These biochemical steps are analogous in yeast, mammals and plants although each system has its own set of SUMO machinery (Table 1-1). Yeast has only one SUMO gene, known as Smt3 (suppressor of MIF two 3) while in mammals, three SUMO paralogues (*SUMO 1-3*) are expressed, although SUMO2 and SUMO3 have not been functionally differentiated and differ in sequence by only three residues (Saitoh and Hinchey, 2000). A fourth SUMO gene exists in mammals (*SUMO4*) but no current evidence suggests it is expressed and thus is most likely a pseudogene (Hay, 2005). In *Arabidopsis*, eight SUMO genes exist (*SUM1-8*) although current evidence suggests that *SUM4*, *6*, *7* and *8* are all pseudogenes as these do not appear to be expressed and their coding sequences lack the C-terminal diglycine motif required for conjugation to target proteins (Kurepa et al, 2003; Saracco et al, 2007). SUM1 and SUM2 in *Arabidopsis* are homologues of mammalian SUMO2 and SUMO3 and likewise cannot be functionally differentiated.

As mentioned above, efficient conjugation of SUMO to target proteins requires E1, E2 and E3 enzymes as well as SUMO-specific proteases to cleave the proprotein and remove SUMO from targets. The *Arabidopsis* E1 complex is made up of either SAE1a or SAE1b, which are functionally redundant, and SAE2 (SUMO ACTIVATING ENZYME 1a, 1b and 2). Like other systems, *Arabidopsis* has only one SUMO E2, SCE1 (SUMO CONJUGATING ENZYME 1) and although yeast has four SUMO E3 ligases and mammals possess at least ten, only two have been identified in *Arabidopsis* to date. These are known as SIZ1 (SAP AND MIZ 1) and HPY2/MMS21 (HIGH PLOIDY 2 / METHYLMETHANESULFONATE SENSITIVE 21) (referred to herein as HPY2). SUMOylation is a dynamic and reversible process and SUMO-specific proteases have important roles in physiological processes. In *Arabidopsis*, twelve candidate SUMO-specific proteases were originally identified with similarity to *Saccharomyces cerevisiae* Ulp1 (ubiquitin-like protein protease 1) (Kurepa et al, 2003) although recent evidence suggests only four of these are expressed and active *in vivo* (ULP1c, ULP1d, ESD4 [EARLY IN SHORT DAY 4] and ELS1 [ESD4 LIKE SUMO PROTEASE 1]) (Colby et al, 2006; Chosed et al, 2006; Murtas et al, 2003; Hermkes et al, 2011; Miura et al, 2007; Miura and Hasegawa, 2010).

Since its discovery, the majority of research focused on SUMOylation and its associated processes has been centred on mammalian and yeast systems. However, recent years have seen major advances in understanding of the SUMOylation system in plants and in particular, *Arabidopsis*. Studies with loss-of-function and gain-of-function mutants have revealed that SUMOylation is an essential process that regulates plant signalling, development, and responses to hormones and the

environment, predominantly through transcriptional regulation of specific genes (Saracco et al, 2007; Miura et al, 2007). Recent proteomic studies in human cell cultures and *Arabidopsis* have revealed a diverse range of SUMO substrates mainly located in the nucleus, further supporting the role for SUMOylation in transcriptional regulation (Golebiowski et al, 2009; Miller et al, 2010; Elrouby and Coupland, 2010). Many studies have implicated SUMOylation in stress responses, with heat and oxidative stress in particular causing dramatic increases in SUMO conjugates (Saitoh and Hinchey, 2000; Kurepa et al, 2003). It should be noted that the main stress-responsive isoforms of SUMO are SUM1/2 in *Arabidopsis* and SUMO2/3 in mammals. Presumably these increases reflect global SUMO-mediated transcriptional activation of stress-responsive genes, either directly or indirectly, and/or repression of housekeeping genes to efficiently protect cells from stress-induced damage.

Table 1-1 The SUMOylation machinery of different species

	Yeast	Mammals	*Arabidopsis*
SUMO	Smt3	SUMO1	SUM1
		SUMO2	SUM2
		SUMO3	SUM3
			SUM4
			SUM5
			SUM6
			SUM7
			SUM8
E1	Aos1	Aos1	SAE1a
			SAE1b
	Uba2	Uba2	SAE2
E2	Ubc9	Ubc9	SCE1
E3	Siz1/Ull1	PIAS1	SIZ1
	Siz2/Nfi1	PIAS3	
		PIASxα	
		PIASxβ	
		PIASy	
	Mms21/Nse2	MMS21	HPY2/MMS21
	Zip3/Cst9		
		RanBP2	
		Pc2	
		HDAC4	
		Topors	
Protease	Ulp1	SENP1	ESD4
		SENP2	ELS1
		SENP3	ULP1b
		SENP5	ULP1c
			ULP1d
	Ulp2	SENP6	ULP2a
		SENP7	ULP2b

(Adapted from Miura and Hasegawa, 2010)

1.5.1 SUMO targets in plants

Proteomic studies have revealed a catalogue of proteins in *Arabidopsis* that are modified by SUMO both basally and under stressed conditions (Budhiraja et al, 2009; Miller et al, 2010, Elrouby and Coupland, 2010). Up to 357 substrates have so far been identified with most of these attributed to roles within the nucleus (Miller et al, 2010). Of the 357 conjugates identified by Miller et al, 80% contained at least one ψKXE motif while in the whole Arabidopsis proteome only 47% of proteins contain this motif, providing confidence that the proteins identified in this study are genuine SUMO targets (Miller et al, 2010). Interestingly, this study revealed that components of the SUMOylation machinery are SUMOylated (SUMO1, SAE2, SCE1, SIZ1 and ESD4), which may be an irrelevant consequence of the conjugation process, but could possibly indicate feedback mechanisms regulating SUMOylation. Many transcription factor families were represented by numerous members, including WRKYs (named for their conserved N-terminal amino acid sequence WRKY), and HSFs (heat shock factors). Other types of well-represented targets in the list include chromatin modifiers, DNA repair/maintenance proteins, RNA-related proteins, nuclear pore proteins and cell cycle regulators (Miller et al, 2010). Further proteomic screens for SUMO targets in plants under various stresses will likely reveal new substrates for this essential PTM. For example, monitoring the SUMO proteome after pathogen challenge might reveal key defence-related proteins that are SUMOylated or deSUMOylated during immune signalling.

1.5.2 SUMOylation and plant immunity

Many studies have implicated SUMOylation in plant immunity and in fact the first report of a plant SUMO was in relation to tomato defence against the fungus *Trichoderma viride* (Hanania et al, 1999). The authors discovered that T-SUMO (tomato-SUMO) interacted with EIX (ethylene-inducing xylanase), an elicitor from *T. viride* in a yeast two-hybrid screen. T-SUMO was shown to suppress EIX-induced ET biosynthesis and PCD in transgenic tobacco plants suggesting that SUMO may have a role in suppressing plant defence responses. Consistent with this hypothesis, a recent study suggested that SUMO1/2 suppress SA-dependent defence responses in *Arabidopsis* (van den Burg et al, 2010). The authors of this study generated transgenic plants expressing an artificial micro RNA (amiRNA) against *SUM2* (*amiR-SUM2*) to knockdown *SUM2* expression. This construct was then crossed in to *sum1-1* knockout plants to generate a *sum1-1 amiR-SUM2* plants, which exhibited reduced levels of global SUMOylation. Interestingly, these plants also showed a 10-fold increase in *PR-1* expression, a marker gene for SA-dependent defence activation, as well as increased resistance to *Pst* DC3000 and increased HR (van den Burg et al, 2010). Interestingly overexpression of *SUM1* or *SUM2* had a similar phenotype as the *sum1-1 amiR-SUM2* mutant, suggesting that tight regulation of SUM1 and SUM2 may be required to keep plant defence responses under control in the absence of pathogens. In the same study the authors also provide evidence that *SUM3* is involved in plant defence downstream of SA as its expression is widely induced by both SA and the bacterial PAMP flg22. Similarly, the SUMO E3 ligase SIZ1, has been shown to regulate SA-mediated immunity in *Arabidopsis*. Mutant *siz1* plants exhibit constitutive SAR and increased resistance against *Pst* DC3000

(Lee et al, 2007). Since global SUMOylation levels are dramatically decreased in *siz1* plants (Miura et al, 2005; Saracco et al, 2007), this further suggests a general role for SUMOylation in the suppression of plant immune responses against bacterial pathogens.

Bacterial pathogens have evolved strategies to suppress plant defence responses and many do this via the type III secretion system (TTSS) by which they can transfer virulence factors into host cells. The tomato pathogen *Xanthomonas campestris* expresses a type III effector, XopD that has been shown to be a SUMO-specific protease (Hotson et al, 2003). The authors showed in this study that XopD can deSUMOylate proteins *in planta* and is located to the nuclei of plant cells suggesting the targets of deSUMOylation are nuclear proteins. Further work from the same laboratory showed that XopD is required by *X. campestris* to effectively colonize plants by suppressing defence responses (Kim et al, 2008). This observation was somewhat contradictory to the idea that SUMOs suppress plant defence, since deSUMOylation would be expected to induce defence responses and not be advantageous to an invading pathogen. However, a SUMOylated target for XopD-mediated deSUMOylation has now been identified as *Solanum lycopersicum* ethylene responsive transcription factor 4 (*Sl*ERF4) (Kim et al, 2013). This work revealed that cleavage of SUMO from lysine 53 by XopD destabilises SlERF4, decreasing its levels and reducing host ET-mediated immune signalling to promote pathogen growth.

Geminiviruses are a large family of plant viruses that infect a variety of plants and cause significant crop losses (Mansoor et al, 2006). Geminiviruses employ a remarkable array of mechanisms to exploit host signalling pathways, including

targeting of the Ub and SUMO systems (Hanley-Bowdoin et al, 2013; Lozano-Durán et al, 2011; Castillo et al, 2003). Geminiviruses encode a protein essential for replication, AL1, that was shown to interact with *Nicotiana benthamiana* SCE1 (Castillo et al, 2003). Further work revealed that the interaction between AL1 and SCE1 is required for viral infection and that AL1 appears to increase the SUMOylation of selected host proteins *in vivo* (Sánchez-Durán et al, 2011). The identity of these host proteins has yet to be determined but it is possible that geminiviruses use this strategy to suppress host defence responses. SCE1 has also been shown to interact with the RNA polymerase, nuclear inclusion b (NIb) of *Turnip mosaic virus* (TuMV) (Xiong and Wang, 2013). Like geminivirus AL1, this interaction was required for viral infection suggesting that SCE1 is a target for numerous viruses during plant infection.

More evidence suggesting a role for SUMOylation in plant immunity comes from the observation that some SUMO substrates are also phosphorylated by mitogen-activated protein kinases (MAPKs) that phosphorylate transcription factors regulating defence gene expression (van den Burg and Takken, 2010). MPK4 and MPK3/6 phosphorylate five defence-related WRKY transcription factors (WRKY3, 4, 6, 33, and 72) and the defence-related transcription factors EIN3 (ethylene-insensitive 1), EIL1 (EIN3-like) and ERF104 (ethylene-responsive element-binding family). These transcription factors were also identified in a proteomic catalogue of SUMO substrates in *Arabidopsis* (Miller et al, 2010). This overlap suggests that crosstalk between SUMOylation and MAPK phosphorylation might exist in plant defence signalling. Similar convergence of these pathways has been described in mammals (Yang and Sharrocks, 2006) making this a plausible scenario. WRKYs

generally act as activators of defence genes but overexpression of WRKY4 suppresses pathogen-induced *PR-1* expression, suggesting they can also act as transcriptional repressors (Lai et al, 2008). An interesting model was proposed by van den Burg and Takken, by which SUMOylation of WRKYs can convert them from transcriptional activators to repressors, whereas phosphorylation can activate them (van den Burg and Takken, 2010). However this is a speculative theory and further elucidation of these signalling networks will be required before an evident model emerges for this mechanism.

1.5.3 Regulation of SUMOylation

Although the biological functions and substrates of SUMOylation are becoming more apparent, how the system itself is regulated remains poorly understood. If global SUMOylation increases after stress then presumably there must be mechanisms in place to trigger this change. SUMOylation can be regulated at the substrate level by competing with other post-translational modifications, particularly those that also attach to lysine residues in target proteins such as acetylation and ubiquitination, but also by phosphorylation (reviewed in Bossis and Melchior, 2006b). Indeed, some SUMO targets contain a phosphorylation-dependent SUMOylation motif (PDSM) that consists of a phosphorylation site downstream of the classical ψKXE sequence (Hietakangas et al, 2006). Modulating the levels of the SUMO conjugation machinery can also influence global SUMOylation. Upregulation of the SUMO E1 and E2 enzymes has been associated with human calcium-induced keratinocyte differentiation (Deyrieux et al, 2007). After inducing cell differentiation with exogenous application of Ca^{2+}, the authors of this study

showed that this increases both mRNA and protein levels of SAE1 and Ubc9. This upregulation increases global SUMOylation of proteins that if inhibited, results in aberrant cell differentiation (Deyrieux et al, 2007). Furthermore, ectopic expression of Ubc9 in mice was shown to increase global SUMOylation and protect mice from hypoxia-induced brain damage (Lee et al, 2011).

Binding of other proteins and molecules to components of the SUMOylation machinery has also been reported to alter SUMO conjugate levels. The adenovirus CELO (chicken embryo lethal orphan) expresses a protein Gam1 that has been shown to reduce host E1 levels by binding to its subunits and recruiting Cullin-RING Ub ligases leading to its proteasomal degradation (Boggio et al, 2004; Boggio et al, 2007). SUMO E2 enzymes are also targets for some viruses with a recent study reporting that HPV (human papillomavirus) E6 proteins bind to Ubc9 promoting its proteasomal degradation to decrease global host SUMOylation levels (Heaton et al, 2011). There are also various examples of endogenous proteins binding to E2 enzymes and sequestering them to regulate SUMOylation, including the yeast DNA repair protein Rad60 and human NIP45 (nuclear factor-interacting protein 45) (Prudden et al, 2009; Sekiyama et al, 2010). The interaction between SUMO and the conjugation machinery can also be manipulated by binding partners and small molecules to regulate SUMOylation. Ginkgolic acid and its analog, ancaric acid have been reported to inhibit protein SUMOylation *in vitro* and *in vivo* by directly binding to the E1 and preventing the formation of a SUMO-E1 intermediate (Fukuda et al, 2009). In contrast, SUMOylation can be enhanced by the binding of other proteins to the conjugation machinery as exemplified by the mammalian protein RSUME (RWD-containing SUMOylation enhancer) (Carbia-Nagashima et al, 2007). The

authors of this study showed that RSUME interacts with Ubc9, enhancing its thioester bond formation with SUMO and increasing SUMOylation of IKB (inhibitor of kappa B) and HIF-1α (hypoxia-inducible factor 1 α) both *in vitro* and in cultured human cells. Furthermore, it was shown that RSUME is induced by hypoxia thus providing a molecular link between a stress-stimulus and increased SUMOylation.

Members of the SUMO conjugation machinery can themselves be targets for PTMs. As mentioned previously, many studies have reported that oxidative stresses such as the application of exogenous hydrogen peroxide (H_2O_2) to mammalian cells dramatically increases global SUMOylation (Saitoh and Hinchey, 2000). However, the concentrations of H_2O_2 used in these studies are not relevant under physiological or even pathophysiological conditions *in vivo*. At lower concentrations, such as those found within cells, H_2O_2 had the opposite effect causing a dramatic decrease of SUMOylation levels (Bossis and Melchior, 2006a). The authors of this study showed that this decrease was due to direct inhibition of SUMO conjugation by the formation of a reversible disulphide bridge between the catalytic cysteine residues of the E1 subunit, Uba2 and the E2, Ubc9. Interestingly at these levels of H_2O_2 (1 mM) the active site cysteine residues of SUMO protease enzymes were unaffected and thus the balance of SUMOylation/deSUMOylation was shifted towards the unconjugated species. It remains unclear as to what the cellular benefits are to inhibit SUMOylation under conditions of oxidative stress.

Crosstalk between S-nitrosylation, SUMOylation and ubiquitination has been reported in a study which showed that S-nitrosylation of the SUMO E3 ligase, protein inhibitors of activated STAT 3 (Pias3), enhanced its interaction with a ubiquitin E3 ligase, Tripartite motif-containing protein 32 (Trim32). This was shown

to stimulate the ubiquitination and proteasomal degradation of Pias3, leading to decreases in global SUMOylation within human cells (Qu et al, 2007). This study also revealed that the SUMO E2 could be S-nitrosylated with exposure to exogenous GSNO but this did not appear to affect its activity (Qu et al, 2007).

Covalent attachment of SUMO to lysine residues within the SUMO conjugation machinery has also been reported. SUMOylation of a lysine located in the active site domain of the E1 subunit, SAE2, was shown to inhibit SUMOylation of target proteins (Truong et al, 2012). This study suggested that deSUMOylation of SAE2 rapidly provides a pool of active E1 enzyme and this may contribute to the increase in SUMO conjugates observed after heat shock. Mammalian and yeast Ubc9 were both shown to be SUMOylated, although the modification site was different between species (Knipscheer et al, 2008). SUMOylation of mammalian Ubc9 was shown to alter its specificity towards substrates, enhancing the SUMOylation of some targets, but inhibiting the SUMOylation of others (Knipscheer et al, 2008). A further study revealed that SUMOylation of yeast Ubc9 inhibits its SUMO-conjugating activity, but enables it to act as a cofactor with non-SUMOylated Ubc9 to promote the assembly of poly-SUMO chains (Klug et al, 2013).

Post-translational modification of the SUMO E2 enzyme is now emerging as a key mechanism by which SUMOylation can be regulated. A recent study revealed that Ubc9 is phosphorylated by cyclin-dependent kinase 1 (CDK1) *in vitro*, which elevated its SUMO-conjugating activity (Su et al, 2012). Ubc9 has also been shown to be acetylated *in vivo*, which selectively inhibited the SUMOylation of a subset of SUMO substrates (Hsieh et al, 2013). The deacetylase, SIRT1 was shown to remove this modification from Ubc9 under hypoxic conditions to modulate SUMOylation of

these targets. This suggests that the acetylation and deacetylation of Ubc9 serves as a dynamic switch to specifically regulate SUMOylation of target proteins (Hsieh et al, 2013).

The examples highlighted above demonstrate that post-translational modification of the SUMO conjugation machinery can specifically regulate the SUMOylation of target proteins in yeast and mammals. It is unknown if similar regulation exists in plants, but since the mechanisms of SUMOylation and the conjugation machinery is highly conserved across all species it is likely this might be the case. Because SUMOylation appears to have a key role in mediating plant immunity, it is possible that PTMs triggered by immune activation may regulate this system.

1.6 Aims and objectives of this study

Post-translational modification of proteins by S-nitrosylation and SUMOylation are two mechanisms that clearly play important roles in plant immunity. Improving our understanding of how these modifications are regulated during immune signalling will further reveal the complexities of defence strategies employed by plants to resist pathogen infection. Studies in mammalian systems have revealed that the SUMO E2 enzyme is a key target to regulate SUMOylation. Previous unpublished work by Saad Malik showed that the *Arabidopsis* SUMO E2, SCE1, could be S-nitrosylated *in vitro*. Work presented in this thesis aims to establish whether this modification occurs *in vivo*, and how it affects the activity of SCE1. Activation of plant immunity is associated with increased levels of NO, and a concurrent increase in protein S-nitrosylation. Thus, S-nitrosylation of SCE1 might

constitute a convergence of two key immune signalling mechanisms, S-nitrosylation and SUMOylation. The model plant, *Arabidopsis* provides a powerful genetic tool that can be easily transformed to generate transgenic lines. This technique will be utilised to generate plants overexpressing SCE1 to examine the influence of modulating SCE1 levels on SUMOylation.

While SCE1 is a key enzyme regulating SUMOylation, GSNOR is a master regulator of S-nitrosylation. Further work in this study aims to generate and characterise transgenic *Arabidopsis* plants overexpressing GSNOR1. These plants will be crossed with other mutant lines, including *nox1*, to generate tools for further study of NO signalling in plant immunity. Although GSNOR1 has been implicated in plant immunity and other important processes, how the activity of the protein might be regulated is currently unknown. Work presented in this thesis aims to uncover any PTMs that might target GSNOR1. In particular, GSNOR1 will be tested as a SUMO substrate, as this enzyme may provide another point where S-nitrosylation and SUMOylation converge.

Chapter 2

2 Materials and Methods

Unless otherwise stated, all chemicals and oligonucleotides used were supplied by Sigma-Aldrich, UK, and all restriction enzymes used in cloning procedures were supplied by New England Biolabs (NEB), UK. All primer sequences are written as 5' to 3'. Unless stated, for all cloning procedures, One Shot® TOP10 Chemically Competent *E. coli* cells (Life Technologies) were used according to the manufacturers' instructions. In all instances, H_2O refers to autoclaved double-distilled water.

2.1 Plant growth conditions

All *Arabidopsis* plants described were grown under long day conditions (16 hour photoperiod) on soil in controlled growth rooms at 65% humidity and 22°C unless otherwise stated. Seeds were stratified at 4-8°C in the dark for 2 days before moving to growth rooms. Plants were grown in a soil mix composed of peat moss, vermiculite and sand at a ratio of 4:1:1 respectively, and illumination was provided by general fluorescent tube lighting at an intensity of 70-100 μmol $m^{-2}sec^{-1}$. For plants grown under sterile conditions, seeds were sterilized by washing in 100% ethanol for 2 mins before incubating in 50% household bleach for 20 mins. After removal of bleach, seeds were washed at least 3 times with sterile H_2O before use. For growth in liquid media, sterilized seeds were stratified in sterile H_2O before adding to ½ strength Murashige and Skoog (½ MS) (Murashige and Skoog, 1962) media containing 1% (w/v) sucrose at pH 5.8. Flasks containing seeds were shaken gently under the same light and temperature conditions as above to prevent clumping

of seedlings. Sterilized seeds for plants grown on plates were resuspended in sterile 0.1% agar and spread on to plates containing the same ½ MS media as above but with the addition of 0.4% agar. Plated seeds were then stratified before placing under lighting conditions as above.

2.2 Plasmid constructs for generation of transgenic plants

All primers used to generate the following constructs are listed in Table 2-1. For the *35S::FLAG-SCE1* and *35S::FLAG-SCE1-C139S* lines, the coding sequence of the relevant genes were amplified using Phusion high-fidelity polymerase (NEB, UK) from previously cloned constructs (Saad I. Malik, unpublished data) with the addition of the nucleotide sequence CACC at the 5' end, necessary for TOPO® cloning (Life Technologies). The PCR products were gel-purified and cloned into the pENTR™/D-TOPO® vector according to the manufacturers' instructions. Resulting clones were selected on Kanamycin plates and validated by sequencing. Subsequently, positive clones were digested with *Mlu*I prior to Gateway® cloning into the pEarleyGate 202 vector (Earley et al, 2006) by LR reaction (Life Technologies). Recombinant clones were selected and the coding sequences were verified as in frame with both the Cauliflower Mosaic Virus (CaMV) *35S* promoter and the N-terminal FLAG sequence contained within the pEarleyGate 202 plasmid by sequencing. The construct for the *35S::FLAG-GSNOR1* lines was produced as above with the exception that the initial PCR product for TOPO® cloning was amplified from *Arabidopsis* cDNA and cloned into the pENTR™/SD/D-TOPO® vector.

Table 2-1 Primers used for TOPO® cloning

Amplicon	Primer sequences
SCE1 coding sequence	**F** - CACCATGGCTAGTGGAATC **R** - TTAGACAAGAGCAGGATACTG
SUMO1 coding sequence	**F** - CACCATGTCTGCAAACCAGG **R** - TCAGCCTCCAGTCTGATGGA
GSNOR1 coding sequence	**F** - CACCATGGCGACTCAAGGTCAG **R** - TCATTTGCTGGTATCGAGGACACA
SCE1 promoter	**F** - CACCCCTGCAAAAACTGCTTC **R** - AAACGACCACGAGCGATTCCA

2.3 Plant transformation and selection

All plant transformations were performed using the well-established floral dip technique (Clough and Bent, 1998). After transgenes of interest were successfully cloned in the plant expression vector pEarleyGate 202 (see above), these plasmids were used to transform *Agrobacterium tumifaciens* strain GV3101 (pMP90) (Koncz and Schell, 1986). After selection of positive clones carrying the transgenes, approximately 6-week old flowering plants were transformed according to the original protocol (Clough and Bent, 1998).

Plants transformed with pEarleyGate 202 were selected for resistance to the herbicide BASTA by spraying 10-day old seedlings with 120 μg/l BASTA at least three times. Further confirmation of transformation was performed by western blot against FLAG. Segregation analysis of BASTA resistance in the T_2 generation to confirm plants had single insertions of transgenes was carried out under sterile conditions using plates with ½ MS media containing 10 μg/ml glufosinate ammonium.

2.4 Genomic DNA extraction from plant tissue

Genomic DNA was isolated from plants by first grinding leaf tissue in CTAB (cetyl trimethylammonium bromide) buffer (100 mM Tris-HCl pH8, 1.5 M NaCl, 20 mM EDTA pH8, 2% CTAB) and heating at 65°C for 20 mins. Next, an equal volume of chloroform was added and samples were centrifuged at 13,000 rpm for 2 mins. The aqueous layer was collected and added to an equal volume of isopropanol before mixing and centrifuging at 13,000 rpm for 15 mins. The supernatant was then removed from the pelleted DNA and pellets were carefully washed in 70% ethanol before drying and resuspending in H_2O for subsequent PCR analyses.

2.5 PCR genotyping of plants

All T-DNA insertion lines were obtained from the Nottingham Arabidopsis Stock Centre (NASC) and were identified by PCR genotyping using two sets of primers; one set for gene-specific amplification (Table 2-2) and another set to verify the presence of the T-DNA insertion with a left border primer appropriate to the collection it was obtained from, namely SALK (Alonso et al, 2003) or GABI-Kat (Kleinboelting et al, 2012) (Table 2-3), and the reverse gene-specific primer.

Table 2-2 T-DNA lines and genotyping primers

Gene	Published name	T-DNA insertion	Gene-specific primers	References
SCE1	*sce1-6*	SALK_071596	**L** - TTTCCGACCATTCTGTTTGAC **R** - AAGGGAAGAGACTGGTGAAGC	Sarraco et al, 2007
SIZ1	*siz1-2*	SALK_065397	**L** - GAGCTGAAGCATCTGGTTTTG **R** - CACGACAGATGAAGCATTGTG	Miura et al, 2005

Table 2-3 Left border primers for T-DNA insertion genotyping

Mutant collection	Primer name	Sequence
SALK	LBb1.3	ATTTTGCCGATTTCGGAAC
GABI-Kat	o8409	ATATTGACCATCATACTCATTGC

The *par2-1* line is a point mutation in the *PAR2* gene (Chen et al, 2009) and was genotyped using different forward primers overlapping the single-nucleotide polymorphism (SNP). The wild-type forward primer only amplified a product if the *par2-1* SNP was absent, whereas the *par2-1* forward primer only amplified a product if the *par2-1* SNP was present (Table 2-4). DNA from heterozygous plants produced a PCR product with both sets of primers.

Table 2-4 *par2-1* genotyping primers

Primer name	Sequence
WT forward	GAAAACAGCTGGTGCTTCAAGGATCATTAG
par2-1 forward	GAAAACAGCTGGTGCTTCAAGGATCATTTA
Reverse	TTTTACATGGATGACTTACCTTGTGACAGCACT

2.6 Total RNA extraction and RT-PCR

To extract total RNA, 200 mg of plant leaf tissue was ground to a fine powder in liquid nitrogen before adding 0.5 ml of TRIzol® RNA isolation reagent and vortexing. Samples were then centrifuged at 13,000 rpm at 4°C for 5 mins to collect plant debris. The supernatant was collected and incubated at RT for 5 mins followed by the addition of 200 µl chloroform and a further 5 min incubation at RT. Samples were then spun at 13,000 rpm at 4°C for 15 mins, the aqueous layer containing RNA was retained and added to 500 µl isopropanol. Next, samples were incubated at RT for 10 mins at RT before spinning at 13,000 rpm at 4°C for 10 mins to pellet the precipitated RNA. Pellets were washed with 70% ethanol, dried then resuspended in H_2O for cDNA synthesis.

Before cDNA synthesis, RNA samples were quantified using a NanoDrop spectrophotometer (Thermo Scientific) and appropriate dilutions were made to ensure all samples contained equal amounts of RNA. Reverse transcription was performed using an Omniscript RT Kit (Qiagen) according to the manufacturers' instructions and 2 µl of the resulting cDNA was used for each PCR reaction of 25 cycles. All primers for RT-PCR were designed using AtRTPrimer (Han and Kim, 2006) and are listed in Table 2-5.

Table 2-5 Primers used for RT-PCR

Gene	Primer sequences	Product size (bp)
SCE1	**F** - ATGGTGTGGCATTGCACTATACCTG **R** - GCGGGATTCGGTGTGTCAAGTAA	263
GSNOR1	**F** - CAAGCTGGTGAGGTTCGGATCAA **R** - CAACAGTGCCAAGACCGAAAATGG	523
UBQ10	**F** - GATCTTTGCCGGAAAACAATTGGAGGATGGT **R** - CGACTTGTCATTAGAAAGAAAGAGATAACAGG	484
PR-1	**F** - GGTGACTTGTCTGGCGTCTC **R** - ACCTCACTTTGGCACATCCG	151

2.7 Quantitative real-time PCR

Total RNA from *Arabidopsis* leaf tissue was isolated with a plant RNA isolation kit (Agilent Technologies) according to the manufacturer's instructions. 1 μg of RNA was used to synthesize cDNA using Omniscript RT (Qiagen) according to the manufacturer's instructions. Real-time PCR was performed using SYBR Green I Master, in a LightCycler 480 system (Roche). Relative quantification of gene expression was calculated using the $2^{-\Delta\Delta Ct}$ method (Livak et al, 2001) using *UBQ5* as an internal reference gene. Primers used to amplify *PR-1* were as follows; F–CTAAGGGTTCACAACCAGGC, R–AAGGCCCACCAGAGTGTATG, and *UBQ5*; F–CCAAGCCGAAGAAGATCAAG, R–ACTCCTTCCTCAAACGCTGA.

2.8 Pathogen infection experiments

The bacterial plant pathogen *Pst* DC3000 was grown overnight from a glycerol stock in 5 ml LB media containing 5 mM $MgSO_4$ and 50 μg/ml Rifampicin. Media for the growth of *Pst* DC3000 carrying the *avrB* gene also contained 50 μg/ml Kanamycin. 1 ml of overnight culture was centrifuged at 4000g for 10 mins and resuspended in 1 ml of 10 mM $MgSO_4$. From this suspension, the necessary dilutions were made in 10 mM $MgSO_4$ to acquire the desired optical density of bacterial suspension. For bacterial growth assays, plants were inoculated with a suspension of OD_{600} = 0.0002, corresponding to 10^5 colony-forming units per ml (cfu/ml). For analysis of defence gene expression, plants were inoculated with a suspension of OD_{600} = 0.002, corresponding to 10^6 cfu/ml. Finally, for protein assays, plants were inoculated with a higher amount of bacteria, at OD_{600} = 0.02, corresponding to 10^7

cfu/ml. All mock inoculations were made with 10 mM $MgSO_4$. Four-week old plants were inoculated by needle-less syringe infiltration of the abaxial leaf surface.

For measurement of bacterial growth, a single disc per plant was cut from infected leaves at the stated times and ground in 10 mM $MgSO_4$. Serial dilutions were made and then spread on LB plates containing the appropriate antibiotics. Plates were incubated at 30°C for two days before colonies were counted. Bacterial growth expressed as cfu/cm^2 of leaf tissue was then calculated and the results were presented as the mean of 6 biological replicates.

2.9 Isolation and treatment of protoplasts

Protoplasts were isolated from 3-5 week old plants using the described tape-*Arabidopsis* sandwich protocol (Wu et al, 2009). Protoplasts were counted using a haemocytometer and necessary dilutions were made for equivalent loading in experiments. All treatments were carried out on freshly isolated protoplasts on the same day. Heat-shock and GSNO treatments were performed on 1 ml of suspended protoplasts in 6-well tissue culture plates. Samples were then transferred to 15 ml Falcon tubes and centrifuged at 200g for 2 mins to pellet the protoplasts. Supernatant was removed and pellets were frozen in liquid nitrogen then stored at -80°C until protein extractions and western blots analyses.

2.10 Protein extraction from plant tissue and protoplasts

Leaf tissue was weighed for equal loading, ground in liquid nitrogen then thawed in extraction buffer (50 mM Tris-HCl pH 7.5, 150 mM NaCl, 5 mM EDTA, 0.1% Triton X-100 and 0.2% Nonidet P-40) freshly supplemented with protease

inhibitors [50 μg/ml TPCK (N-tosyl-L-phenylalaninyl-chloromethylketone), 50 μg/ml TLCK (N-alpha-tosyl-L-lysinyl-chloromethylketone) and 0.5 mM PMSF (phenylmethanesulfonyl fluoride)] (Spoel et al, 2009). Samples were centrifuged at 13,000 rpm at 4°C for 15 mins to remove plant debris and the supernatant was collected. Protein was extracted from protoplasts by thawing frozen pellets in the same extraction buffer and vortexing before centrifugation.

2.11 Immunoprecipitation of FLAG-tagged proteins from plants

FLAG-tagged proteins from transgenic plants were immunoprecipitated by first extracting protein from leaf tissue as previously described in 2.9, with the addition of 2.5 mM *N*-Ethylmaleimide (NEM) in the extraction buffer. Protein extracts were then filtered through 0.45 μm filters (Millipore) to remove any solid plant material. Next, ANTI-FLAG M2 affinity gel was added to the total protein extracts according to the manufacturers' instructions. After incubation overnight at 4°C, the beads were washed five times with 1X PBS, and FLAG-tagged proteins were eluted by adding SDS-PAGE sample buffer and boiling.

2.12 Recombinant protein expression and purification

All constructs for the N-terminal 6xHis-tagged *Arabidopsis* SUMOylation machinery in the pQE70 vector (Qiagen) were generated, and expression conditions of each protein in the M15 (pRep4) *E. coli* strain optimized previously by Saad Malik (unpublished). Constructs for 6xHis-tagged TRX5 and NTRA in the vectors pET24c and pETG10a respectively, were obtained from Steven Spoel (unpublished) and expressed in the BL21 (DE3) *E. coli* strain. For all proteins above, expression

was induced in bacterial cultures with the addition of 1 mM IPTG and after 3-6 hours cells were pelleted by centrifugation at 6000g for 15 mins. Supernatant was removed and pellets were stored at -80°C until cell lysis and protein extraction.

Cells were resuspended in lysis buffer (50 mM $KHPO_4$ pH 8, 300 mM NaCl, 10 mM Imidazole, 1 mg/ml lysozyme, 25 U/ml Benzonase nuclease, 0.1% Triton-X-100, 10 mM β-mercaptoethanol, 50 μg/ml TPCK, 50 μg/ml TLCK and 0.5 mM PMSF) and incubated with gentle rocking at room temperature for 30 mins. The lysate was then centrifuged at 4°C at 15,000 rpm for 15 mins and the supernatant collected. His-tagged proteins were then purified by gravity-flow method using HisPur Cobalt Resin (Thermo Scientific) columns according to the manufacturers' instructions. Immediately after elution, proteins were dialyzed against appropriate buffers using Slide-A-Lyzer dialysis cassettes (Thermo Scientific) to remove excess Imidazole.

Recombinant N-terminal GST-tagged GSNOR1 was generated from the pENTR™/SD/D-TOPO® vector clone mentioned in 2.2. The coding sequence of GSNOR1 was recombined in to the pDEST15 expression vector (Life Technologies) by LR reaction. GST-GSNOR1 expression was induced in BL21 (DE3) cells by addition of 0.5 mM IPTG and cultures were incubated overnight at 20°C until centrifugation as above. Cells were then resuspended in 1X PBS (140 mM NaCl, 2.7 mM KCl, 10 mM Na_2HPO_4, 1.8 mM KH_2PO_4, pH 7.3) supplemented with 1 mg/ml lysozyme, 25 U/ml Benzonase nuclease, 0.1% Triton-X-100, 50 μg/ml TPCK, 50 μg/ml TLCK and 0.5 mM PMSF. After incubation with gentle rocking at room temperature for 30 mins, lysates were centrifuged at 4°C at 15,000 rpm for 15 mins and the supernatant collected. GST-tagged protein was purified by gravity-flow

using Glutathione Sepharose 4B (GE Healthcare) columns according to the manufacturers' instructions.

Proteins were quantified by the well-established Bradford Assay (Bradford, 1976) with bovine serum albumin (BSA) (NEB, UK) used for protein standards. All proteins were aliquoted in small volumes to avoid repeated freeze-thaw cycles and stored with 10% glycerol at -80°C.

2.13 Site-directed mutagenesis

All site-directed mutagenesis reactions were performed using the QuikChange II XL kit (Agilent Technologies) according to manufacturers' instructions. Primers used are listed in Table 2-6 with the altered codons underlined. To create the SCE1-C94S/C139S double mutant protein, the primers used were originally designed by Saad Malik to make each single mutant. The SCE1-C139S - pENTR™/D-TOPO® mentioned in section 2.2 was used as a template to introduce the C94S mutation. After validating the correct sequence, this construct was then used as a template to clone SCE1-C94S/C139S into the pET-28a(+) expression vector between the *Eco*RI and *Sal*I restriction sites using the following primers:

Forward - CGGAATTCATGGCTAGTGGAATCGC

Reverse - ACGCGTCGACTTAGACAAGAGCAGGATACTG

After sequencing the clones to verify the correct mutation, the construct was cloned in to BL21 (DE3) cells and the recombinant protein was produced as in 2.11.

The K191R mutation of GSNOR1 was introduced in the pENTR™/SD/D-TOPO® vector clone mentioned in 2.2, the mutation was then verified by sequencing before LR reactions. For production of recombinant GST-tagged GSNOR1, the

construct was recombined in to the pDEST15 vector exactly as described in 2.11, while for generation of transgenic plants it was recombined in to the pEarleyGate 202 vector as described in 2.2.

Table 2-6 Primers used for site-directed mutagenesis

Gene	Mutation	Primer sequences
SCE1	C94S	**F** - CCATCTGGAACTGTCAGTCTCTCTATCCTTAAC **R** - GTTAAGGATAGAGAGACTGACAGTTCCAGATGG
GSNOR1	K191R	**F** - GTTTGGAATACTGCAAGAGTAGAACCAGGGTCA **R** - TGACCCTGGTTCTACTCTTGCAGTATTCCAAAC

2.14 SDS-PAGE and western blots

For SDS-PAGE, protein samples were added to a 4X stock of sample buffer to give a final concentration of 50 mM Tris-HCl pH 6.8, 2% SDS, 0.02% bromophenol blue and 10% glycerol with or without 50 mM dithiothreitol (DTT). Next, samples were heated at 70°C for 10 mins before separating on gels of appropriate polyacrylamide percentage. For Coomassie Blue staining, gels were washed in H_2O before incubating in staining solution (0.25% Brilliant Blue R, 40% methanol, 7% acetic acid) for 30 mins. Gels were then destained overnight in destaining solution (40% methanol, 10% acetic acid) and photographed.

For western blots, proteins were transferred on to nitrocellulose membranes either overnight at a constant voltage of 20V or for 1-2 hours at 90V. Before blocking, membranes were stained with Ponceau S (0.1% Ponceau S, 5% acetic acid) for 1 min then rinsed in H_2O to remove background staining. Photographs were taken before the stain was removed by washing in PBS + 0.1% tween (PBS-T).

Membranes were blocked for 1 hour at room temperature using 5% dried skimmed milk in PBS-T before antibody incubation. Primary antibodies used are indicated in the figure legends and were incubated either at 4°C overnight or for 1-2 hours at room temperature. Appropriate secondary antibodies coupled to horseradish peroxidase (HRP) were used to detect bands with SuperSignal West Pico/Dura Chemiluminescent Substrate (Thermo Scientific) and exposure to X-ray films. All antibodies were obtained commercially (Table 2-7) and were diluted in 5% dried skimmed milk / PBS-T.

Table 2-7 List of antibodies used

Primary antibody	Host species	Manufacturer
anti-SUMO1	rabbit	Abcam
anti-SCE1	rabbit	Abcam
anti-S5a	rabbit	Abcam
anti-FLAG M2	mouse	Sigma
anti-His	mouse	Cell Signaling Technology
anti-GST	mouse	Aviva Systems Biology
anti-Biotin HRP-linked	goat	Cell Signaling Technology

Secondary antibody	Host species	Manufacturer
anti-rabbit IgG HRP-linked	goat	Cell Signaling Technology
anti-mouse IgG HRP-linked	goat	Cell Signaling Technology

2.15 S-nitrosylation and denitrosylation assays

S-nitrosylation of proteins was detected using the biotin switch procedure essentially as described (Jaffrey and Snyder, 2001) but with some modifications. For the *in vitro* denitrosylation assay, recombinant SCE1 was incubated with 500 μM

GSNO for 20 mins in the dark before removal of GSNO by Zeba desalting spin columns (Thermo Scientific). Reactions were set up in 100 µl volumes of HEN buffer (200 mM HEPES, 1 mM EDTA pH7.7, 0.1 mM neocuproine) containing 50 µM SCE1 and stated additional components at the following concentrations; 5 µM TRX5, 0.2 µM NTRA and 20 mM NADPH. UV-treated control samples were exposed to UV light in a DNA gel transilluminator for 5 mins. Denitrosylation reactions were incubated at RT in the dark for 1 hr before samples were directly used for biotin switch. Free cysteines were blocked by alkylating with 25 mM NEM in the presence of 2.5% SDS at 50°C for 20 mins. NEM was removed from samples by acetone precipitation before SNOs were reduced and labelled by adding sodium ascorbate to a concentration of 25 mM and Biotin-HPDP (Thermo Scientific) to a concentration of 0.4 mM and incubating at room temperature for 1 hour. Proteins were acetone precipitated again and the pellets dissolved in 1X SDS-PAGE sample buffer. Samples were resolved on gels and transferred to membranes as described in 2.13 before total SCE1 was detected by Ponceau S staining and SNO-SCE1 was detected by western blot against biotin.

In vivo S-nitrosylation assays were performed by grinding 250-500 mg of plant leaf tissue per sample in liquid nitrogen and adding to extraction buffer (HEN + 0.5% Triton X-100 supplemented with the protease inhibitors described in 2.9). Samples were centrifuged at 13,000 rpm at 4°C for 15 mins to remove plant debris and the supernatant was collected and filtered before performing the biotin switch as above, until the second acetone precipitation. After biotinylating protein-SNOs, a portion of each sample was collected and kept as the total or input. The remaining sample was used for pull-down of biotinylated (SNO) proteins using Streptavidin

immobilized on agarose beads according to a described protocol (Forrester et al, 2009). Both input and SNO-samples were separated by SDS-PAGE before western blot analyses against specific proteins as described.

2.16 Reductive-switch assay

The reductive-switch assay was adapted from the biotin-switch described in 2.15. Protein extracts were prepared and free cysteines blocked by exactly the same method. The first difference between the reductive switch and the biotin switch occurred after the first acetone precipitation. After resuspending the protein pellet in HENS 1% (1% SDS in HEN buffer), DTT was added to a final concentration of 2 mM and samples were incubated at room temperature for 10 mins to allow oxidized cysteines to be reduced. This was followed by another acetone precipitation to remove DTT and biotin-HPDP was then added to each sample at 0.4 mM final concentration. Biotinylation and subsequent streptavidin pull-down were performed exactly as in 2.15.

2.17 *in vivo* SUMOylation assays

Seedlings were grown in liquid media as described in 2.1 until they were approximately 2 weeks old. For heat-shock treatments, flasks containing seedlings were moved to a 37°C water bath, ensuring the bottom of the flasks were submerged in water, and incubated for the stated times. For H_2O_2 treatments, H_2O_2 was added directly to the media to a final concentration of 5 mM and mixed to ensure all seedlings were exposed. Immediately after treatments, seedlings were removed from media and dried with paper towels. Seedlings were then weighed and frozen in liquid

nitrogen ready for grinding and protein extraction in the extraction buffer described in 2.9, supplemented with 2.5 mM NEM to inactivate SUMO proteases. Proteins were resolved on pre-cast 4-15% gradient gels (Biorad) before western blot against SUMO1.

2.18 *in vitro* SUMOylation assays

Analysis of SUMO-SCE1 thioester formation was adapted from a described protocol (Alontaga et al, 2012). All proteins were dialyzed against reaction buffer (50 mM Tris-HCl, 100 mM NaCl and 10 mM $MgCl_2$). Reactions were set up in 20 µl volumes of reaction buffer containing 0.5 µM SAE1a, 0.5 µM SAE2, 1 µM SCE1 and 2.5 µM SUMO1 and kept on ice. Thioester formation was started by adding an ATP-regenerating mix (2 mM ATP, 10 mM creatine phosphate disodium salt, 3.5 U/ml creatine kinase and 6 U/ml inorganic pyrophosphatase) (Tatham et al, 2001) and incubating samples at 30°C for the stated times. Reactions were stopped with the addition of SDS-PAGE sample buffer without DTT and samples were heated at 70°C for 10 mins before SDS-PAGE and western blot against SCE1.

Formation of poly-SUMO chains *in vitro* was analyzed by setting up the same reactions as for the thioester assay but incubating the samples at 30°C for longer times, stated in each figure, and DTT was added to the sample buffer before SDS-PAGE and western blot against SUMO1. GST-GSNOR1 was SUMOylated *in vitro* by adding purified GST-GSNOR1 to a final concentration of 3 µM in the same reaction mixtures and incubation at 30°C for the stated times. GST-GSNOR1 was detected by western blot against GST or assayed for GSNOR activity as described in 2.20.

2.19 *in vitro* SCE1 dimerization assay

Reactions were made up to a 65 µl volume in the buffer described in 2.17 including 100 µg of purified SCE1, and H_2O_2 at the stated concentrations. Samples were incubated at RT for 30 mins before splitting into two 30 µl volumes and adding to SDS sample buffer with or without 50 mM DTT. Proteins were separated by SDS-PAGE, transferred to nitrocellulose membranes and visualized by Ponceau S staining as described in 2.13.

2.20 GSNOR activity assay

The activity of GSNOR was assayed spectrophotometrically by measuring the rate of NADH oxidation in the presence of GSNO essentially as previously described (Feechan et al, 2005) but with some modifications. In the case of recombinant protein, 1 µg GST-GSNOR1 was used in each reaction. SUMOylation reactions were passed through Micro Bio-Spin P-30 Gel Columns (Biorad) to remove small molecules and proteins of molecular weight < 40 kDa before GSNOR activity assays. For plant extracts, protein was extracted in HE buffer (25 mM HEPES, 1 mM EDTA pH7.7) with the addition of the protease inhibitors described in 2.9. Protein content was quantified by Bradford assay and samples were diluted accordingly to include 100 µg of total protein per reaction. For all GSNOR activity assays, proteins were incubated in 1 ml of HE buffer with the addition of 350 µM NADH with or without 350 µM GSNO and NADH oxidation was measured by following the absorbance at 340 nm for 5 minutes and calculating the rate using the extinction coefficient of NADH (6.22 $L.mol^{-1}.cm^{-1}$). Specific GSNOR activity was determined by subtracting the NADH oxidation in the absence of GSNO from the

oxidation in the presence of GSNO. All samples were tested for linearity and protected from light throughout.

2.21 Protein structure modelling and analysis

Protein structures were viewed and analysed using PyMOL software (PyMOL Molecular Graphics System, Version 1.5.0.5 Schrödinger, LLC). The crystal structures of human Ubc9 (Tong et al, 1997) and tomato GSNOR1 (Kubienova et al, 2013) were downloaded from the Protein Data Bank (http://www.rcsb.org/pdb) with the PDB codes 1U9B and 4DLA respectively. The predicted structure of *Arabidopsis* SCE1 was modelled using Phyre protein structure prediction (Kelley and Sternberg, 2009).

2.22 Densitometry analysis of western blots

Images of X-ray films from western blots were scanned using a standard desktop scanner and processed using ImageJ software (Schneider et al, 2012). Comparisons or ratios of samples are stated in the figure legends.

2.23 Measurement of rosette surface area

Photographs of plants next to a white square of known surface area were taken with a standard digital camera. The amount of pixels in the white square for each photograph was measured using Adobe Photoshop software and compared to the amount of pixels in each selected leaf surface area. The ratio of pixels was then used to calculate the surface area of each plant in cm^3.

Chapter 3

3 Redox-regulation of SCE1

3.1 Background

Post-translational modification of proteins by SUMO is an essential mechanism regulating a myriad of cellular processes. Although the targets of SUMOylation are becoming apparent, how the mechanism is itself regulated remains largely unknown. As discussed in Chapter 1, the SUMO conjugation machinery can be targeted by various molecules and modifications in order to regulate SUMOylation. It is now becoming evident that SUMOylation is implicated in plant defence against bacterial pathogens and thus regulation of this process during immune signalling may provide a means to fine-tune defence responses. A hallmark of immune activation in higher eukaryotes is the rapid synthesis of both NO and ROIs. Current evidence suggests that these small, redox-active molecules exert their downstream signalling functions by post-translational modification of target proteins. Reactive cysteine thiols can be reversibly modified with varying degrees of oxidation. Importantly, enzyme function can be regulated by these modifications and in particular, S-nitrosylation of proteins has been shown to underpin immune responses in both plants and animals.

SUMO, unlike Ub, relies on a sole E2 enzyme, SCE1, for its conjugation to targets and it can be expected that SCE1 is under tight regulatory control. Since SCE1 contains four cysteines including its active site residue, Cys94, it was hypothesized that this enzyme could be a target for redox-based post-translational modification. Indeed, previous work (Saad Malik, unpublished data) showed that this

enzyme was S-nitrosylated *in vitro* at Cys139 (Figure 3-1). Work presented in this chapter aims to build on this finding by examining the effect of S-nitrosylation on the activity of SCE1 and investigating whether this essential enzyme is redox-regulated *in vivo*. Furthermore, the importance of redox-regulation of SUMOylation in plant immune signalling will be investigated and discussed.

3.2 S-nitrosylation of SCE1 *in vitro*

3.2.1 SCE1 is S-nitrosylated at Cys139 *in vitro*

Previous work by Saad Malik identified Cys139 SCE1 as a target for S-nitrosylation *in vitro* by utilizing the biotin-switch technique (BST). As shown in Figure 3-1 (A), purified, recombinant SCE1 was efficiently S-nitrosylated *in vitro* by two different NO-donors, GSNO and CysNO (Saad Malik). Mass-spectrometry analysis revealed Cys139 to be the sole site of S-nitrosylation and this was further confirmed by site-directed mutagenesis of the cysteine residues within SCE1, with only the C139S mutation preventing detection by biotin switch (Figure 3-1 (B)) (Saad Malik). Structural modelling of SCE1 based on its mammalian homologue Ubc9 revealed that this cysteine is likely solvent-exposed and therefore accessible for modification, unlike Cys44 and Cys76 which are both located in the interior of the protein structure with their side chains orientated inwards, and Cys94 which sits within the active-site cleft (Figure 3-1(C)). Importantly, Cys139 is highly conserved in higher eukaryotes (Figure 3-2) suggesting it may have a functional role. Interestingly, *Sc*Ubc9 only contains an active site cysteine and does not possess the other three that are conserved in diverse species.

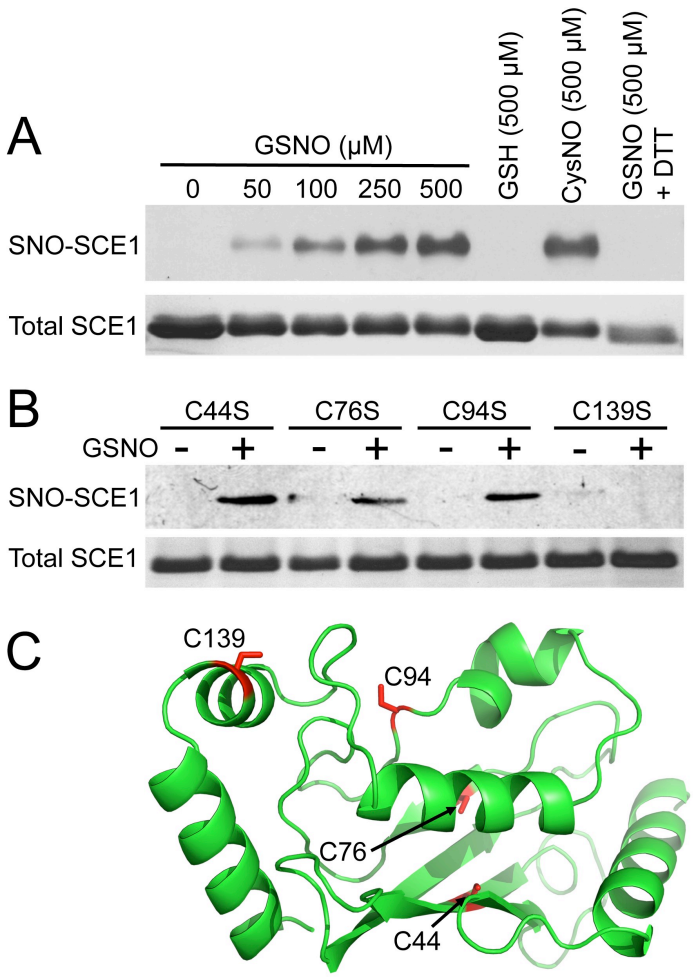

Figure 3-1 SCE1 is S-nitrosylated at Cys139 *in vitro*

(A) Purified recombinant SCE1 was incubated with the stated concentrations of NO-donors or GSH before the BST. The presence of 20 mM DTT in the final lane serves as a negative control for S-nitrosylation. Total SCE1 is detected by Coomasie staining while SNO-SCE1 is detected by western blot against biotin. **(B)** Each cysteine mutant form of SCE1 was incubated with either 100 μM GSH or GSNO as in (A) before the BST. **(C)** The structure of SCE1 was modelled based on its mammalian homologue Ubc9 and the location of the cysteine residues shown in red.

N.B. Data shown in parts A and B were produced by Saad Malik.

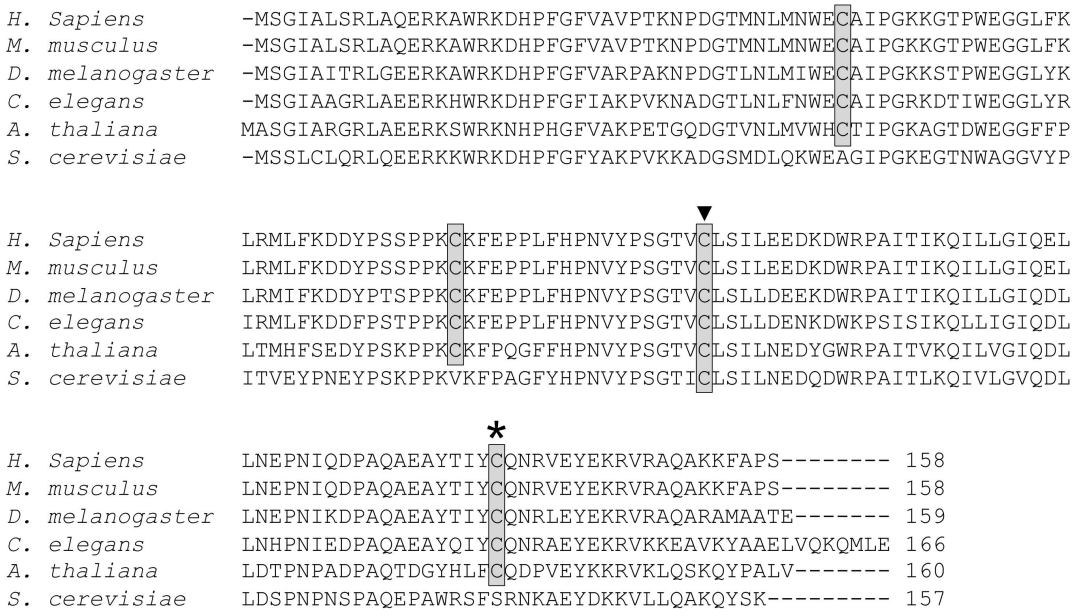

Figure 3-2 Sequence alignments of SUMO E2 enzymes from multiple eukaryotes

Sequences of SUMO E2 enzymes from various species were aligned using the ClustalW2 software (www.ebi.ac.uk/Tools/msa/clustalw2/) (Larkin et al, 2007). Cysteines are shown in shaded boxes with the active site residue marked with an arrowhead and the equivalent residues to SCE1 Cys139 marked with an asterisk.

3.2.2 S-nitrosylation of SCE1 inhibits its E2 activity *in vitro*

After identifying Cys139 of SCE1 as a site of S-nitrosylation *in vitro*, it was then necessary to establish whether this modification affected its enzymatic activity. To test this, *in vitro* SUMOylation reactions were set up using purified recombinant SAE1a, SAE2, SCE1 and SUMO1. First, all proteins were tested for activity by performing an *in vitro* SUMOylation reaction without any treatment to SCE1. Since SUMO1 possesses an internal SUMOylation motif and can form polymeric SUMO chains (Colby et al, 2006), the formation of these chains was used as a measure of E2

activity. As shown in Figure 3-3, SUMOylation occurs rapidly in the presence of ATP. Poly-SUMO chains are not detected as distinct bands but rather as a smear probably because *Arabidopsis* SAE2 and SCE1 are themselves modified by SUMO as previously reported (Miller et al, 2010). Therefore poly-SUMO chains and mono-SUMOylated substrates will likely be present with various molecular weights. As expected, the increase in SUMO-conjugates is accompanied by a decrease in the detectable amount of free SUMO. From this experiment, the time points of 10 minutes and 30 minutes were chosen for future assays.

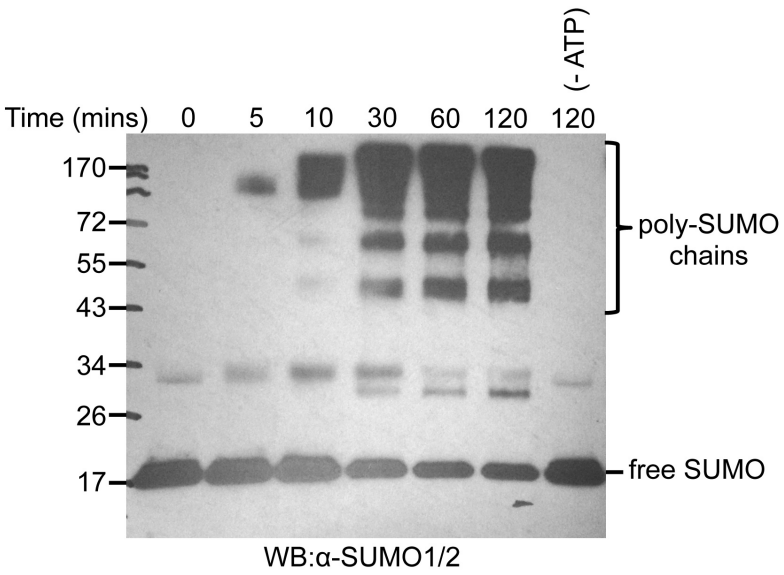

Figure 3-3 *in vitro* SUMOylation assay

Arabidopsis SAE1a, SAE2, SCE1 and SUMO1 and an ATP-regeneration mix were incubated at 30°C for the stated times and SUMO-conjugation observed by reducing SDS-PAGE and western blot against SUMO1/2. The –ATP sample serves as negative control for ATP-dependent SUMOylation.

After confirming that the recombinant SUMOylation machinery was active, the effect of SCE1 S-nitrosylation was then examined. As shown in Figure 3-4 (top panel), both SCE1 and the mutant SCE1-C139S protein are equally capable of rapidly forming SUMO1-chains in the presence of ATP. Therefore it appears that mutation of Cys139 to Ser does not affect enzyme activity *in vitro*. However, if SCE1 is pretreated with the NO-donor, GSNO, its ability to form SUMO1-chains is inhibited at both the 10- and 30-minute time points after addition of ATP (Figure 3-4, bottom panel). This effect is not observed if SCE1-C139S pretreated with GSNO, suggesting specific modification of Cys139 is inhibiting its E2 activity.

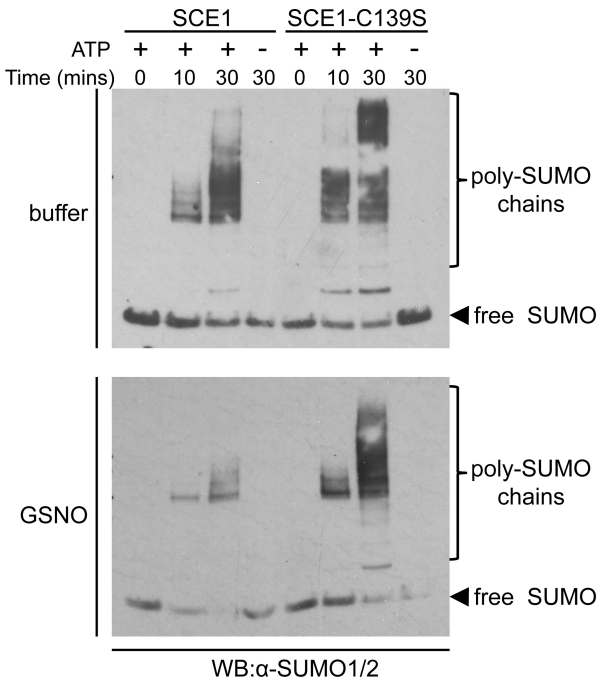

Figure 3-4 GSNO pre-treatment of SCE1 inhibits its E2 activity *in vitro*

SCE1 or SCE1-C139S were incubated with HEN buffer or 500 μM GSNO for 20 mins in the dark before adding to *in vitro* SUMOylation reactions and incubating at 30°C for the stated times. The –ATP samples serve as negative controls for ATP-dependent SUMOylation. This experiment was repeated three times with similar results.

Since SUMO first forms a thioester with the E1 heterodimer before it is transferred to the active site of SCE1, it was next tested whether the observed inhibition by S-nitrosylation was occurring during this stage of the SUMOylation process. To do this, *in vitro* SCE1-SUMO1 thioester formation assays were performed in which ATP is added to reaction mixtures containing the E1, E2 and SUMO1. Formation of the SCE1-SUMO1 thioester is then observed by non-reducing SDS-PAGE and western blot against SCE1. As expected, SCE1-C139S was capable of forming a thioester bond with SUMO1 and was perhaps even more efficient at this than WT SCE1 (Figure 3-5).

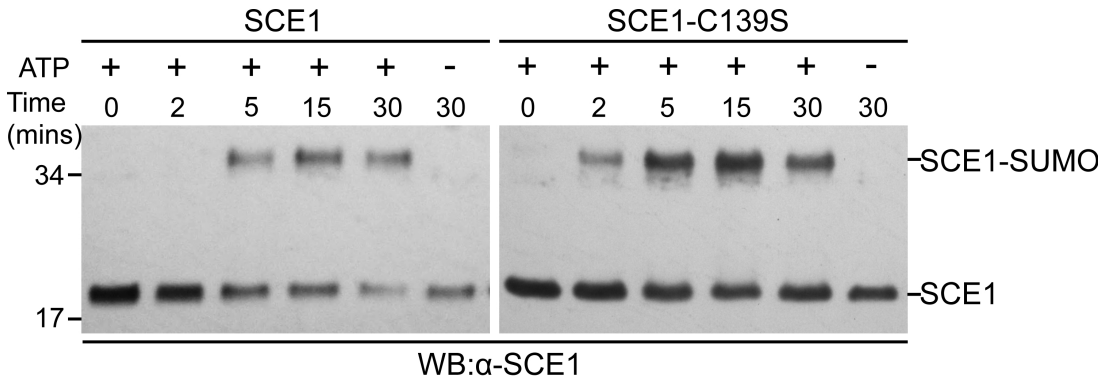

Figure 3-5 SCE1-C139S efficiently forms a SUMO thioester *in vitro*

SCE1 or SCE1-C139S were added to a reaction mix containing the E1 heterodimer and SUMO1 before the addition of ATP and incubation at 30°C for the stated times. The SCE1-SUMO1 thioester was observed by western blot against SCE1 after non-reducing SDS-PAGE.

Pretreatment of both SCE1 and SCE1-C139S with either GSH or GSNO had no effect on *in vitro* thioester formation (Figure 3-6) suggesting that the inhibition of poly-SUMO chain formation after GSNO incubation observed in Figure 3-4 is occurring at the transfer of SUMO to its substrate(s).

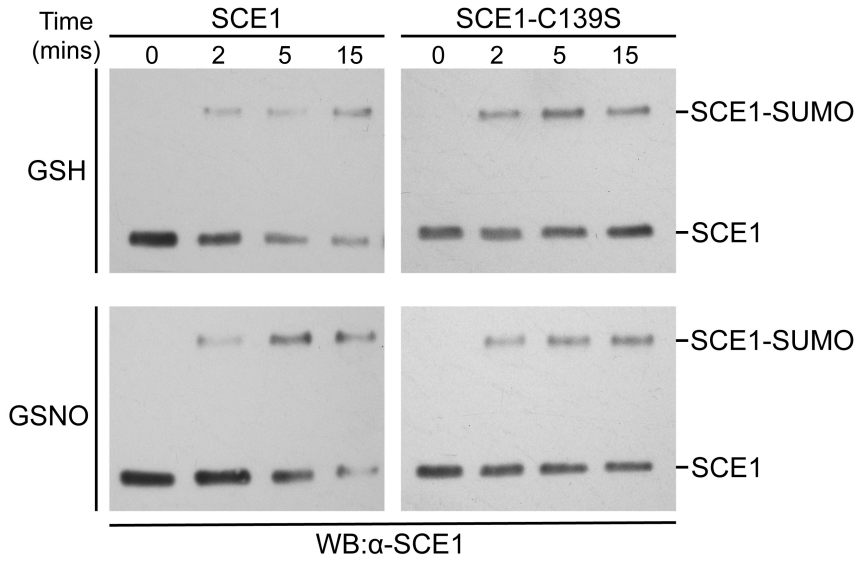

Figure 3-6 S-nitrosylation of SCE1 has no effect on thioester formation *in vitro*

SCE1 or SCE1-C139S were incubated with either 500 μM GSH or GSNO for 20 mins in the dark before adding to *in vitro* thioester assay reactions as in Figure 3-5.

3.2.3 SCE1 is an *in vitro* substrate for TRX-mediated denitrosylation

Protein S-nitrosylation in some cases has been suggested to be under regulatory control of enzymes with denitrosylation activity, including thioredoxins. Since SCE1 is S-nitrosylated *in vitro* at Cys139 it was next tested whether TRX5 can remove this NO modification. Thioredoxins require the action of NADPH-dependent

thioredoxin reductase (NTRA) to recycle and perform more than one round of denitrosylation. After S-nitrosylating recombinant SCE1 with 200 μM GSNO, combinations of either TRX5, NTRA or both were added to the reaction mixture and left at room temperature for 1 hour before conducting the BST to detect S-nitrosylation. As shown in Figure 3-7, TRX5 in combination with NTRA is capable of completely denitrosylating SCE1 at least *in vitro*.

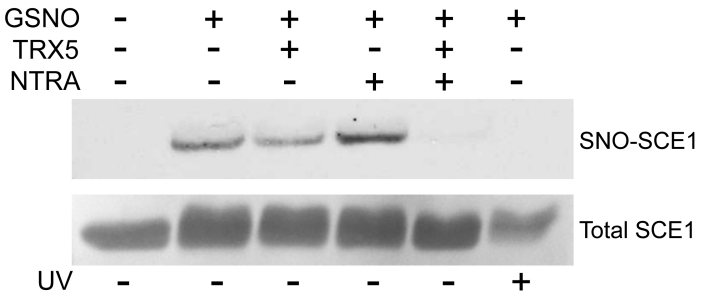

Figure 3-7 SCE1 is denitrosylated by TRX5 *in vitro*

Recombinant SCE1 was incubated with 200 μM GSNO for 20 minutes before the shown combinations of recombinant TRX5 and NTRA were added to total reaction volumes of 100μl. NADPH was added to the samples containing TRX5 and NTRA. The UV-treated sample serves as a negative control for SNO formation. After biotin switch, proteins were analyzed by non-reducing SDS-PAGE and western blot against biotin for SNO-SCE1. Total SCE1 was detected by Ponceau S staining of the membrane.

3.3 SCE1 is S-nitrosylated and further oxidized *in vivo*

3.3.1 Endogenous SNO-SCE1 is undetectable *in vivo*

After identifying SCE1 as an *in vitro* target for S-nitrosylation it was next tested if SNO-SCE1 could be detected *in vivo* by applying the BST to plant protein

extracts. Under resting conditions, no SNO-SCE1 was detected in either WT or *gsnor1-3* plants, which have elevated global SNO levels (Feechan et al, 2005) (Figure 3-8 (A)). To establish if endogenous SCE1 can be S-nitrosylated, exogenous GSNO was applied to plant extracts before the BST. Surprisingly, as shown in Figure 3-8 (B), the addition of 1 mM GSNO did not result in any detection of SNO-SCE1. This could be due to a number of possibilities; the cysteines are blocked by other modifications or inaccessible due to protein folding, reducing agents in the plant extracts are preventing the GSNO from S-nitrosylating proteins, other proteins are more efficiently S-nitrosylated than SCE1, or the antibodies used against endogenous SCE1 are not sensitive enough to detect SNO-SCE1.

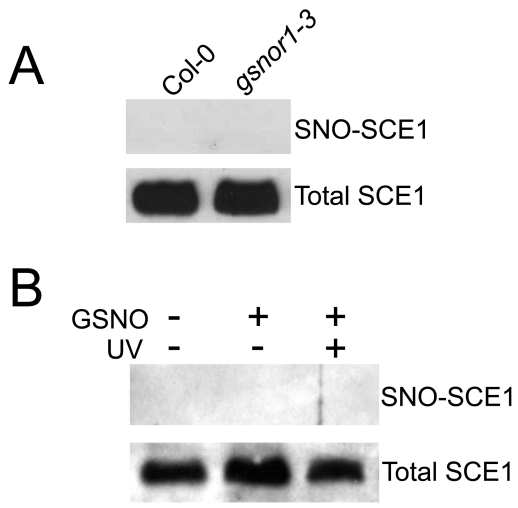

Figure 3-8 Endogenous SCE1 is not S-nitrosylated *in vivo*

(A) Protein extracts from the stated plants were subjected to the BST and S-nitrosylated proteins were enriched by Streptavidin affinity pull-down before reducing SDS-PAGE and western blot against SCE1. **(B)** Protein extract from wild-type plants was incubated with 1 mM GSNO in the dark for 20 mins before the BST and detection of SCE1 as in (A).

3.3.2 Production of FLAG-SCE1 transgenic plants

To facilitate alternative immunodetection of SCE1, generation of transgenic plants expressing epitope-tagged SCE1 was required. Due to its small size, reliable detection by western blot, and the fact it contains no cysteines the FLAG-tag was chosen (Einhauer and Jungbauer, 2001). Loss-of-function *sce1* T-DNA insertion mutants are embryonic lethal (Saracco et al, 2007) so heterozygous *sce1* plants were transformed with the *35S::FLAG-SCE1* constructs to attempt to rescue the lethality and replace all endogenous SCE1 with the transgenic FLAG-tagged versions. However, no homozygous *sce1* plants were recovered (in over 50 genotyped) in subsequent generations from heterozygous *sce1* parents in the T_1 generation. This suggests that either the FLAG-tagged proteins are inactive *in vivo* or that the expression pattern under the control of the *35S* promoter is not appropriate to substitute for endogenous *SCE1* expression. Numerous (>15) independent transgenic lines containing insertion(s) at single loci were isolated constitutively expressing either FLAG-SCE1 or FLAG-SCE1-C139S under the control of the CaMV *35S* promoter. These plants were analyzed for expression levels by semi-quantitative RT-PCR and western blot against both FLAG and SCE1. As shown in Figure 3-9 (A), top panel, *35S::FLAG-SCE1* line #4 and *35S::FLAG-SCE1-C139S* line #1 both express the *SCE1* transgenes at a comparable level when analysed by western blot against FLAG. The lack of a band detected by anti-FLAG in the Col-0 sample demonstrates that this is a specific means to detect transgenic FLAG-SCE1. When analysed by western blot against SCE1, endogenous SCE1 is detected in both transgenic lines and Col-0, but the FLAG-tagged transgenic SCE1 is also detectable at a higher molecular weight and at much higher levels (Figure 3-9 (A), middle

panel). RNA was extracted from these plants and analysed by RT-PCR confirming that *SCE1* expression was elevated to similar levels in the transgenic lines (Figure 3-9 (B)). After these two lines were confirmed as suitable tools for biochemical analysis of FLAG-SCE1 and FLAG-SCE1-C139S, they were chosen to isolate plants homozygous for the transgene in a WT background and were used for all future experiments.

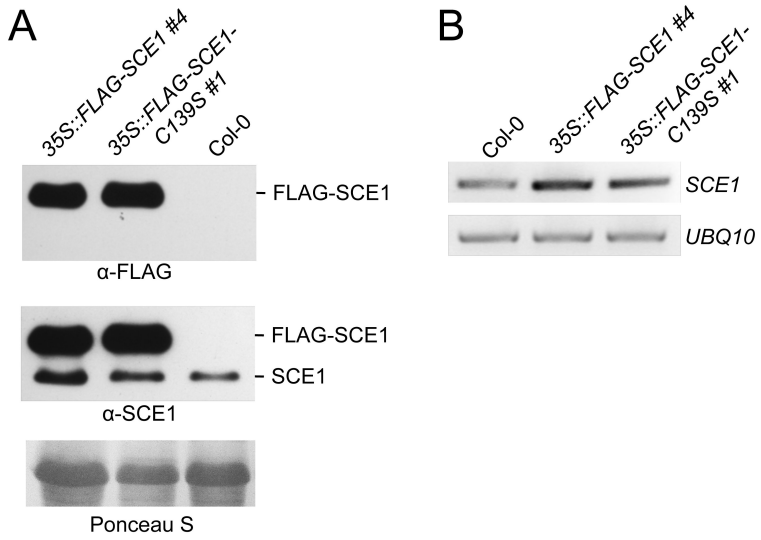

Figure 3-9 Expression of FLAG-SCE1 in transgenic lines

(A) Plant protein extracts from the stated lines were analysed by reducing SDS-PAGE and western blot using the stated antibodies. Ponceau S staining of the large subunit of Rubisco is included as a loading control. **(B)** Expression of *SCE1* was determined in the stated lines by semi-quantitative RT-PCR. The constitutively expressed *UBQ10* was included as a loading control.

3.3.3 S-nitrosylation of FLAG-SCE1

After generating *35S::FLAG-SCE1* plants, protein extracts from these were subjected to BST analyses to further investigate *in vivo* S-nitrosylation of SCE1. As shown in Figure 3-10, very little SNO-FLAG-SCE1 was detected under resting

conditions but pre-incubating the extracts with 1 mM GSNO did result in detection. This confirmed that FLAG-SCE1 produced *in vivo* can be S-nitrosylated.

Global SNO levels are increased in *Arabidopsis* upon recognition of pathogen infection (Feechan et al, 2005; Yun et al, 2011) and so the BST was performed on *35S::FLAG-SCE1* and *35S::FLAG-SCE1-C139S* plants that had previously been challenged with both virulent *Pst* DC3000, and *Pst* DC3000 carrying the avirulence gene *avrB*. Low levels of SNO-SCE1 were detected in non-inoculated plants (Figure 3-11 (A and B), control sample) while SNO-SCE1 levels were dramatically increased at 6 hours post-infection (hpi) with both virulent and avirulent *Pst* DC3000, suggesting that S-nitrosylation of SCE1 occurs in response to pathogen challenge (Figure 3-11 (A and B)). A negative control was included for each sample in which ascorbate was omitted during the BST, thus revealing any non-specific background biotinylation and was taken into account in the quantification shown in Figure 3-11 (B). S-nitrosylation of SCE1 in response to pathogen infection was absent in *35S::FLAG-SCE1-C139S* plants (Figure 3-11 (A)) suggesting that Cys139 is also the site of modification *in vivo*.

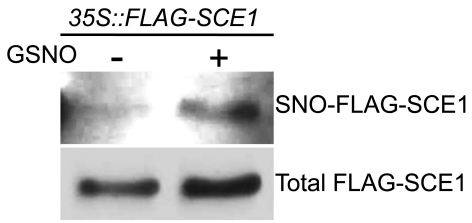

Figure 3-10 S-nitrosylation of FLAG-SCE1

Protein extracts from *35S::FLAG-SCE1* plants were subjected to the BST with or without pre-incubation with 1 mM GSNO where stated. Total and SNO-FLAG-SCE1 were detected by western blot against FLAG.

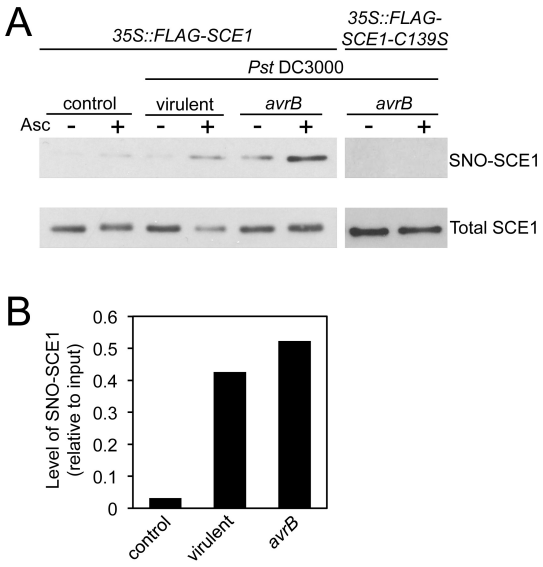

Figure 3-11 SCE1 is S-nitrosylated at Cys139 following *Pst* DC3000 infection

(A) Protein extracts from untreated (control), or *Pst* DC3000-inoculated plants of the stated lines were subjected to the BST and both SNO-SCE1 and Total SCE1 were detected by western blot against FLAG. The omission of ascorbate (-Asc) represents a negative control for each sample. **(B)** The levels of SNO-SCE1 in *35S::FLAG-SCE1* plants in (A) were quantified by densitometry and represented as a ratio of the respective inputs, with the –Asc background subtracted from each sample.

3.3.4 SCE1 is further oxidized at Cys139 *in vivo*

3.3.4.1 Development of the reductive-switch technique

Although S-nitrosylation of SCE1 was detected after pathogen challenge, the fact that addition of exogenous GSNO to plant extracts failed to S-nitrosylate endogenous SCE1 to detectable levels (Figure 3-8 (B)) suggests that the availability of Cys139 for this modification was low. To test whether Cys139 of SCE1 exists in a

more highly oxidized state, the BST was adapted to detect all DTT-sensitive cysteine modifications, including SOH and SS as well as S-nitrosylation. In the BST, ascorbate is used to specifically reduce all SNOs, allowing biotinylation of "newly-freed" cysteines. For the reductive-switch technique (RST), ascorbate is replaced by 2 mM DTT to reduce all cysteine modifications. DTT is then removed by acetone precipitation before biotin labelling (Figure 3-12).

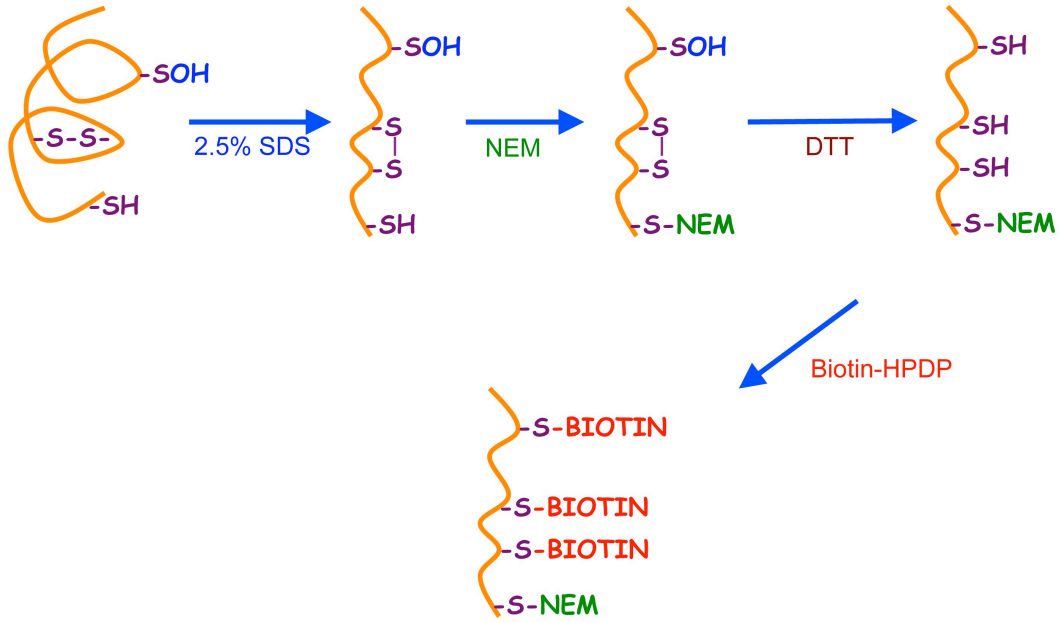

Figure 3-12 Reductive-switch technique

Cartoon schematic of the RST. Proteins are first unfolded by the addition of SDS to access cysteines buried within the structure. Next, free thiols are irreversibly blocked by alkylating with NEM. DTT is then added to reduce oxidized cysteines before these are labelled with Biotin-HPDP in the final step.

To confirm that this procedure was capable of reducing and then subsequently labelling oxidized cysteines, it was applied to protein extracts from WT plants as a proof of concept experiment. As shown in Figure 3-13, proteins are only

biotinylated and enriched by Streptavidin pull-down when the DTT step is included. This suggests that the blocking step is efficient and also that the DTT is efficiently removed by acetone precipitation thus allowing disulphides to form between newly-freed thiols and biotin-HPDP.

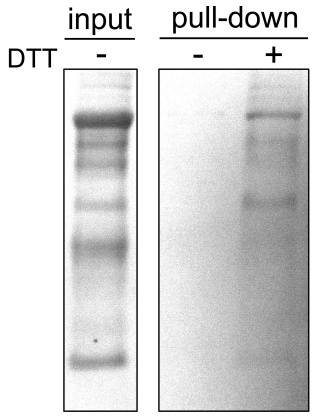

Figure 3-13 Reductive-switch technique on plant extracts

Protein extract from Col-0 plants was subjected to the RST. DTT +/- represents presence or omission of the DTT-step in the RST. Proteins were separated by reducing SDS-PAGE, transferred to a nitrocellulose membrane and visualized by Ponceau S staining.

3.3.4.2 SCE1 is oxidized at Cys139 under resting conditions

After confirming that the RST was suitable for detecting proteins with oxidized cysteines, the technique was applied to protein extracts from *35S::FLAG-SCE1* and *35S::FLAG-SCE1-C139S* plants. Addition of DTT before biotin-labelling allowed enrichment and detection of FLAG-SCE1 but not FLAG-SCE1-C139S from plant extracts under resting conditions (Figure 3-14), suggesting that as well as S-nitrosylation, further oxidative modification can occur at Cys139. However, the RST

is a non-specific procedure and the signal detected could represent a number of reversible oxidative states of SCE1.

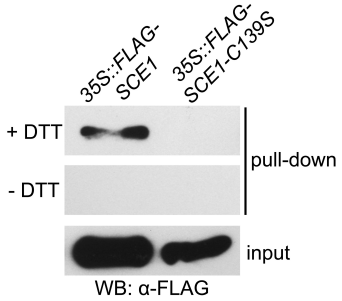

Figure 3-14 SCE1 is oxidized at Cys139 *in vivo*

Protein extracts from the stated lines were subjected to the RST. The –DTT samples served as a negative control in which the DTT step is omitted, thus oxidized cysteines are not reduced and not biotinylated. Proteins were analysed by reducing SDS-PAGE and western blot against FLAG.

3.3.4.3 SCE1 oxidation increases after pathogen challenge

Since S-nitrosylation of SCE1 at Cys139 appeared to increase after infection with *Pst* DC3000 (*avrB*) it was tested whether the oxidation detected by RST in Figure 3-14 was also affected by pathogen challenge. At 6 hours post-infection, the level of oxidized SCE1 is increased in WT plants (Figure 3-15 (A)), although the total level of SCE1 also appeared to be increased. However, quantification of the gel revealed that the ratio of oxidized to total SCE1 was increased approximately four-fold after pathogen infection. The same experiment was then performed on extracts from *35S::FLAG-SCE1* plants in which expression of the transgene is constitutive. As expected, the level of total FLAG-SCE1 was not significantly increased after

pathogen challenge, but the level of oxidized FLAG-SCE1 was increased 6 hours post-infection (Figure 3-15 (B)). The level of oxidized FLAG-SCE1 had returned to resting levels 24 hours post-infection suggesting that the increase in oxidation is an early event in response to attempted pathogen infection.

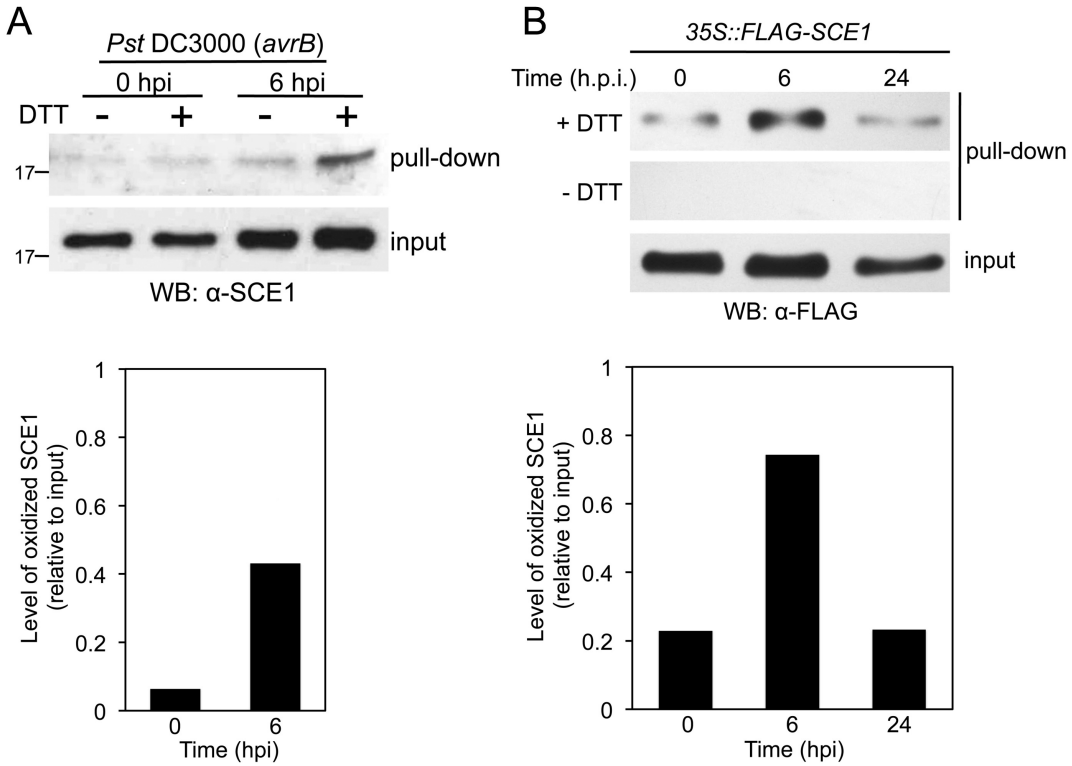

Figure 3-15 SCE1 oxidation increases after *Pst* DC3000 (*avrB*) infection

(A) WT protein extracts were subjected to the RST at the stated hpi with *Pst* DC3000 (*avrB*) before reducing SDS-PAGE and western blot against SCE1. Quantification of the blot by densitometry is shown below. –DTT values were subtracted as background from the +DTT samples and the ratio of pull-down over input is shown. **(B)** Protein extracts from *35S::FLAG-SCE1* plants were subjected to the RST as in (A) but analysed by western blot against FLAG.

3.4 SCE1 forms oligomers *in vitro*

Since the RST allows detection of all DTT-sensitive cysteine modifications including disulphides, it was tested whether SCE1-C139S was capable of forming disulphide-mediated dimers *in vitro*. As shown in Figure 3-16 (left panel), SCE1 and SCE1-C139S can both spontaneously form DTT-sensitive dimers, trimers and oligomers that are stimulated by H_2O_2. Dimerization of various E2 enzymes has been previously reported (David et al, 2010) although the function of, and residues that facilitate this has remained unknown. The formation of a disulphide between the active-site cysteines of mammalian Ubc9 and the E1 subunit Uba2 has previously been reported (Bossis and Melchior, 2006a). Thus, it was hypothesized that the active site cysteine of SCE1, Cys94, is responsible for the dimerization observed in Figure 3-16 (left panel). Unexpectedly, SCE1-C94S is also capable of forming dimers although perhaps less efficiently than wild-type SCE1 and the SCE1-C139S mutant (Figure 3-16, middle panel). This suggests that the active-site cysteine is not solely responsible for the disulphide-mediated dimerization and oligomerization observed *in vitro*. Indeed, if both Cys94 and Cys139 are mutated then the ability of SCE1 to form dimers is completely abolished (Figure 3-16, right panel) suggesting that as expected, these are the only cysteines in SCE1 that are redox-active.

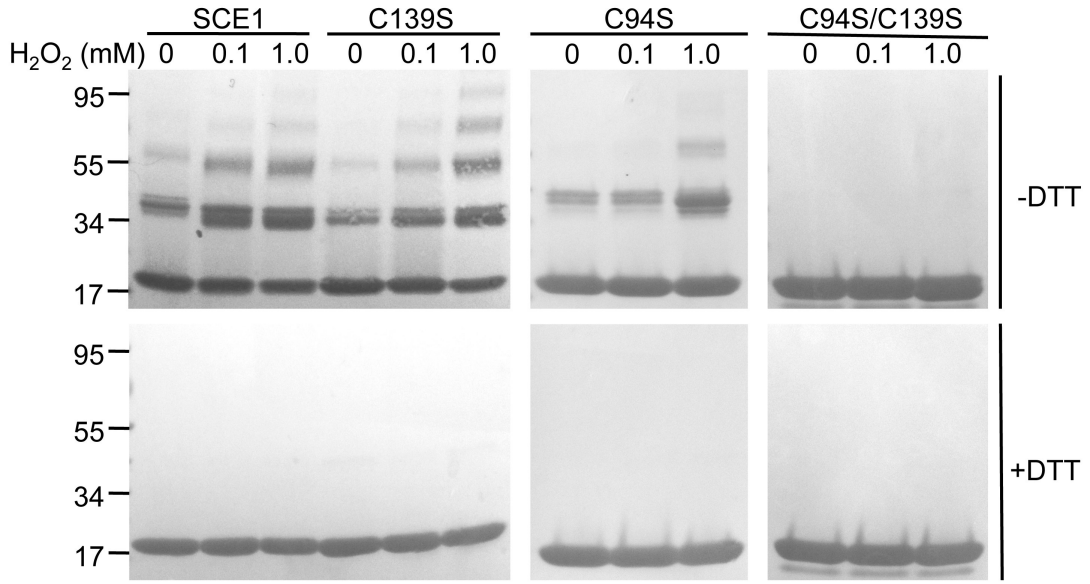

Figure 3-16 SCE1 forms Cys94- and Cys139-mediated DTT-sensitive oligomers *in vitro*

The stated forms of recombinant SCE1 were incubated at room temperature for 30 mins in buffer containing the stated concentrations of H_2O_2. Proteins were analysed by non-reducing (top panels), or reducing (bottom panels) SDS-PAGE and transferred to nitrocellulose membranes for Ponceau S staining.

3.5 Investigating the effect of the SCE1-C139S mutation *in vivo*

3.5.1 FLAG-SCE1 and FLAG-SCE1-C139S are active *in vivo*

A possible reason that the *35S::FLAG-SCE1* and *35S::FLAG-SCE1-C139S* transgenes do not rescue the embryonic lethality of the *sce1* mutant is that the transgenic proteins are inactive. To test if this was the case, a co-immunoprecipitation experiment was performed to examine the ability of transgenic FLAG-tagged SCE1 and SCE1-C139S to form thioester bonds with SUMO *in vivo*. As shown in Figure 3-17, SUMO1/2 co-immunoprecipitates with both FLAG-SCE1 and FLAG-SCE1-C139S at the expected size from plant protein extracts. Addition of

DTT to the loading buffer reduces the thioester bond and allows the detection of free SUMO. However, a SCE1-SUMO complex is still detectable in the presence of DTT and this likely represents the SUMOylated form of SCE1, which has been previously reported in *Arabidopsis* (Garcia-Dominguez et al, 2008; Miller et al, 2010).

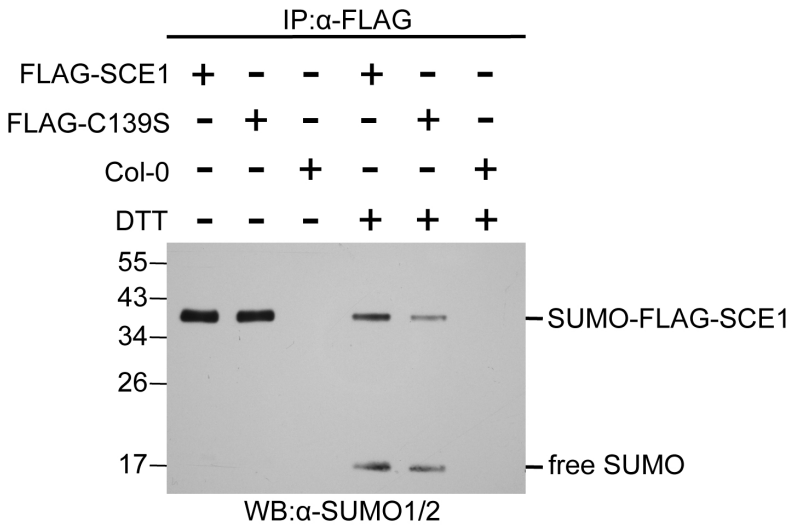

Figure 3-17 FLAG-SCE1 and FLAG-SCE1-C139S both form SUMO thioesters *in vivo*

Protein extracts from either *35S::FLAG-SCE1*, *35S::FLAG-SCE1-C139S* or Col-0 plants were subjected to FLAG immunoprecipitation before analysis by non reducing (-DTT) or reducing (+DTT) SDS-PAGE and western blot against SUMO1/2. Col-0 plant extracts were included as a negative control for the FLAG immunoprecipitation.

3.5.2 Overexpression of FLAG-SCE1 and FLAG-SCE1-C139S increases global SUMOylation *in vivo*

Since the *35S::FLAG-SCE1* lines have high levels of SCE1 compared to WT, *in vivo* heat shock-induced SUMOylation assays on liquid-grown seedlings as

described previously (Kurepa et al, 2003) were performed to establish if overexpression of *Arabidopsis* SCE1 affects global SUMOylation levels. As shown in Figure 3-18, SUMO conjugates were dramatically increased after 15 minutes of incubation at 37°C in Col-0 seedlings. The increase in conjugates was matched by a decrease in the amount of detectable free SUMO. In plants overexpressing FLAG-SCE1 and FLAG-SCE1-C139S, the amount of SUMOylation after heat-shock was more pronounced, and within 15 minutes no free SUMO was detectable compared to WT. Furthermore, plants overexpressing FLAG-SCE1-C139S appear to be more efficient than those overexpressing FLAG-SCE1, with significantly more SUMO-conjugates detectable after 15-minute and 1 hour incubations at 37°C (Figure 3-18). Interestingly, more SUMO-conjugates appear to be present in *35S::FLAG-SCE1*-C139S under resting conditions, suggesting that modification of this cysteine constitutes an inhibitory switch. This is consistent with the observation that the C139S mutant form of SCE1 was more active in forming thioesters *in vitro* (Figure 3-5).

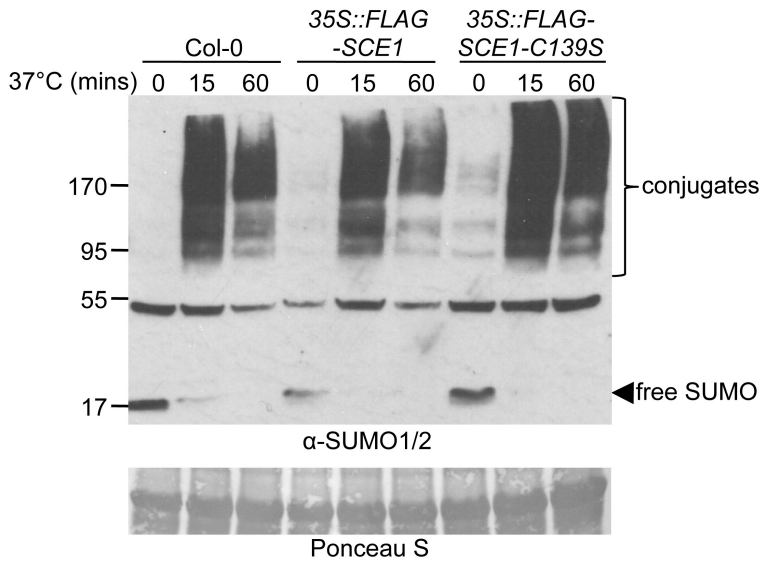

Figure 3-18 Overexpression of both FLAG-SCE1 and FLAG-SCE1-C139S increases heat-shock induced SUMOylation in *Arabidopsis* seedlings

Liquid-grown seedlings of the stated lines were exposed to 37°C for the indicated times before freezing in liquid nitrogen. Proteins were extracted and separated by reducing SDS-PAGE before western blot against SUMO1/2. Ponceau S staining of the large subunit of Rubisco indicates equal loading.

3.5.3 Plants overexpressing FLAG-SCE1-C139S are susceptible to virulent and avirulent *Pst* DC3000

After establishing that SCE1 S-nitrosylation and further oxidation at Cys139 is involved in immune activation, we next tested whether plants overexpressing the FLAG-C139S mutant form were affected in their resistance to both virulent and avirulent forms of *Pst* DC3000. As shown in Figure 3-19 (A), *35S::FLAG-SCE1-C139S* plants are more susceptible to infection by *Pst* DC3000, as compared to WT and *35S::FLAG-SCE1* plants which both showed similar levels of pathogen growth 3 days post-infection. Similarly, as shown in Figure 3-19 (B) only *35S::FLAG-SCE1-*

C139S plants exhibited less resistance to *Pst* DC3000 (*avrB*). These data suggest that Cys139 of SCE1 is required for both basal immunity and *R*-gene mediated resistance and thus redox signalling facilitated by this conserved cysteine may regulate immune responses in plants. Although the *35S::FLAG-SCE1* and *35S::FLAG-SCE1-C139S* lines are in a WT background and thus also express endogenous *SCE1*, the overexpression of FLAG-SCE1-C139S might be acting in a dominant-negative fashion. Indeed, it has recently been shown that overexpression of SCE1 with its active site cysteine (Cys94) mutated in a WT background inhibits SUMOylation and results in plants having a similar phenotype to *siz1* mutants (Tomanov et al, 2013). A similar dominant-negative effect has been reported in human cells with overexpression of mutant Ubc9 decreasing SUMOylation (Mo et al, 2002).

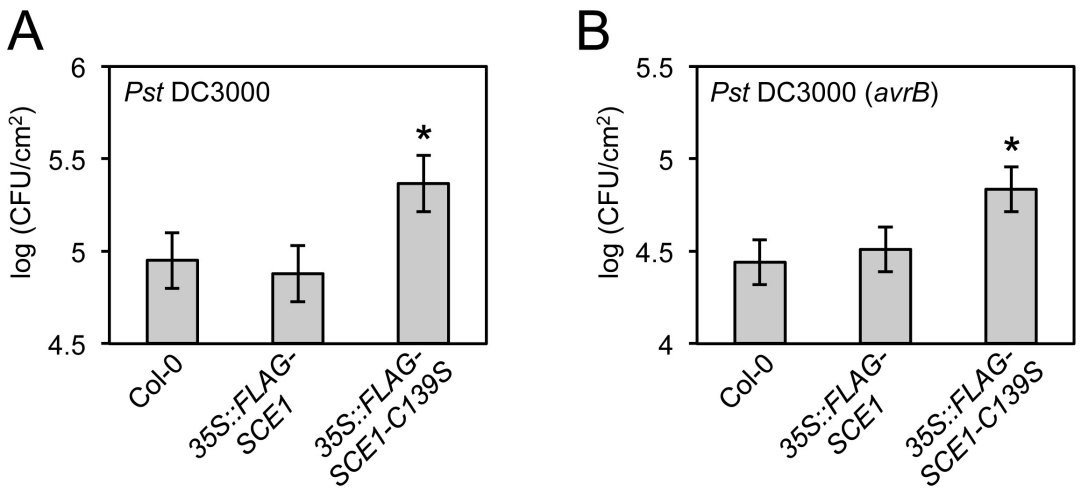

Figure 3-19 Cys139 of SCE1 is required for resistance to *Pst* DC3000

The stated lines were inoculated with **(A)** *Pst* DC3000 or **(B)** *Pst* DC3000 (*avrB*) and leaf discs were assayed for bacterial growth at 3 dpi. Data points represent mean ± SEM (n=6), with asterisks indicating significant difference from the Col-0 sample (Student's *t* test, $P < 0.05$). This experiment was repeated four times with similar results.

After uncovering that *35S::FLAG-SCE1-C139S* plants are susceptible to *Pst* DC3000, the activation of the defence gene *PR-1* after infection was analysed by semi-quantitative RT-PCR. As shown in Figure 3-20, in WT plants, *PR-1* transcript levels have increased to a detectable level at 6 hpi, with a strong induction at 12 hpi in response to both virulent (A) and avirulent (B) *Pst* DC3000. *35S::FLAG-SCE1* plants show a similar response to WT, but *35S::FLAG-SCE1-C139S* plants appear to have a delayed response with no detectable *PR-1* transcripts evident at 6 hpi and a much fainter band detected at 12 hpi when compared to WT and *35S::FLAG-SCE1* plants. To further investigate this, the activation of *PR-1* after *Pst* infection was analysed by quantitative real-time PCR (qPCR). As shown in Figure 3-21, *PR-1* expression is strongly induced in WT and *35S::FLAG-SCE1* plants at 12 hpi. In contrast, *PR-1* expression was severely compromised at 12 hpi in *35S::FLAG-SCE1-C139S* plants (Figure 3-21). Together with the increased susceptibility of *35S::FLAG-SCE1-C139S* plants, this suggests that redox modification of this cysteine is required for plants to mount an efficient immune response against *Pst* DC3000 infection.

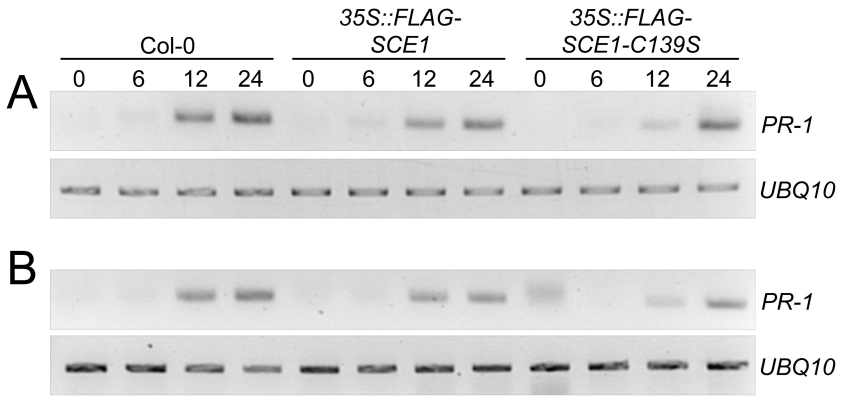

Figure 3-20 *PR-1* expression is delayed in *35S::FLAG-SCE1-C139S* plants following *Pst* DC3000 infection

The stated lines were inoculated with **(A)** *Pst* DC3000 or **(B)** *Pst* DC3000 (*avrB*) and RNA was extracted from leaf tissue for cDNA synthesis and RT-PCR analysis of the given genes. Numbers above the panels represent hours post-infection. *UBQ10* expression was analysed as a constitutively expressed control gene.

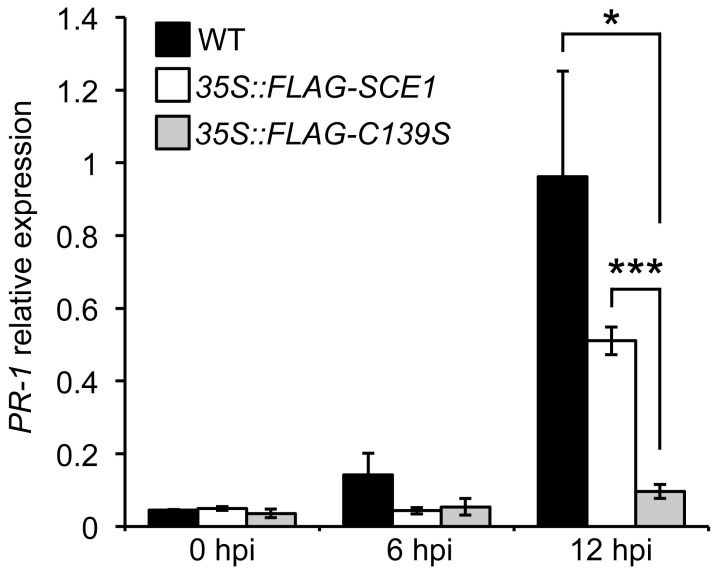

Figure 3-21 *PR-1* expression is strongly reduced in *35S::FLAG-SCE1-C139S* plants following *Pst* DC3000 infection

Plants of the stated lines were inoculated with *Pst* DC3000 and leaf tissue was harvested at the stated times. The expression of *PR-1* was analysed using qPCR and normalized against the constitutively expressed *UBQ5*. Data points represent mean ± SEM (n=3) of three independent biological samples while asterisks represent significant differences between the indicated samples (Student's *t* test,* $P < 0.05$, *** $P < 0.0001$).

3.5.4 Plants overexpressing FLAG-SCE1-C139S have increased SUMO conjugate levels after pathogen infection

Since *35S::FLAG-SCE1-C139S* plants showed susceptibility to *Pst* DC3000, it was tested whether global SUMOylation is affected in this line after infection. Similar to previously reported (Lee et al, 2007), *Pst* DC3000 infection has no observable effect on global SUMOylation in WT plants, with similar results observed for *35S::FLAG-SCE1* plants (Figure 3-22). Strikingly, in *35S::FLAG-SCE1-C139S* plants, SUMO conjugate levels were dramatically increased after

infection with virulent *Pst* DC3000 and also *Pst* DC3000 (*avrB*) (Figure 3-22) suggesting that Cys139 is required to suppress SUMOylation after pathogen infection. In contrast to heat-shock induced SUMOylation assays (Figure 3-18), increased SUMOylation after infection in *35S::FLAG-SCE1-C139S* plants was not accompanied by a concurrent decrease in free SUMO levels (Figure 3-22). Free SUMO levels remained unchanged in WT plants after infection. As expected, free SUMO levels were lower in *35S::FLAG-SCE1* plants compared to WT but remained unchanged after infection. Unexpectedly, free SUMO levels increased with infection in *35S::FLAG-SCE1-C139S* plants alongside the increase in SUMO conjugates. This suggests that in *35S::FLAG-SCE1-C139S* plants, SUMO protein levels are upregulated. Perhaps the pool of free SUMO in these plants is so depleted due to increased E2 activity that more SUMO is being produced in an attempt to counteract this.

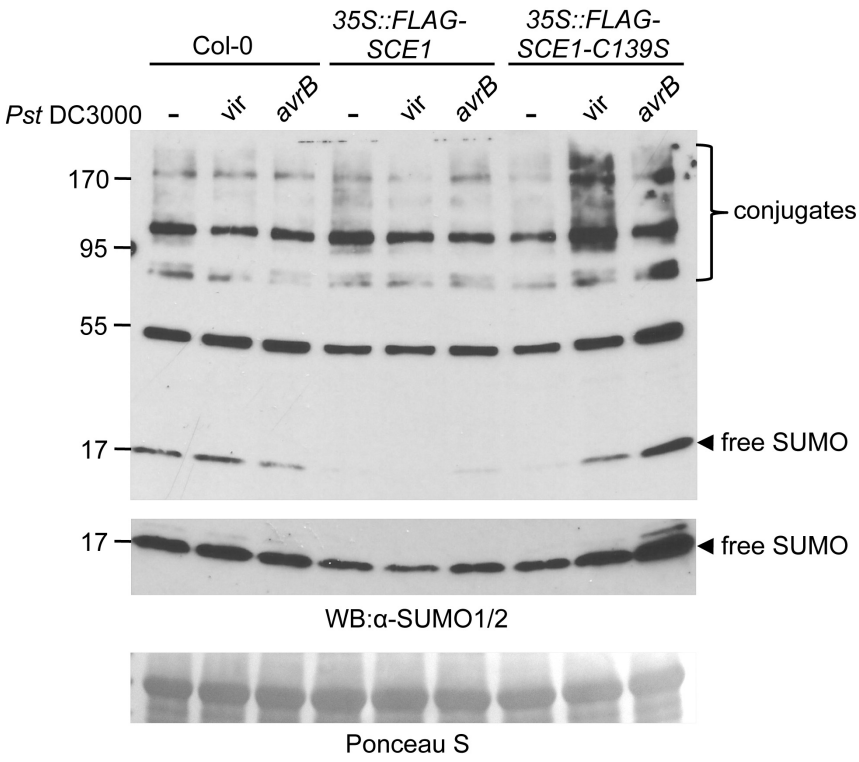

Figure 3-22 Global SUMOylation is increased in *35S::FLAG-SCE1-C139S* plants after *Pst* DC3000 infection

The stated lines were either not inoculated (-) or inoculated with either virulent (vir) or avirulent (*avrB*) *Pst* DC3000 and leaf tissue collected at 6 hpi. Protein extracts were then analysed by reducing SDS-PAGE and western blot against SUMO1/2. The middle panel is a longer exposure time of the top panel showing free SUMO levels. Ponceau S staining of the large subunit of Rubisco indicates equal loading.

3.6 Global SUMOylation is affected by SNO levels

3.6.1 Global SUMOylation in *gsnor1-3* and *nox1* seedlings

After establishing that S-nitrosylation of SCE1 inhibits its activity *in vitro* and that Cys139 is a target for redox-based post translational modifications *in vivo*, global SUMOylation was analysed in *gsnor1-3* and *nox1* (*cue1*-6 allele, herein referred to as *nox1* (Streatfield et al, 1999; He et al, 2004)) mutant seedlings, which

both exhibit elevated global SNO levels (Feechan et al, 2005; Yun et al, 2011). As shown in Figure 3-23 (A) heat shock and H_2O_2 treatment both induce similar levels of SUMOylation in WT and *gsnor1-3* seedlings. Under resting conditions, *gsnor1-3* plants appear to have lower levels of SUMO conjugates than WT although the levels of free SUMO are comparable between the two lines. A more pronounced difference was observed between WT and *nox1* seedlings (Figure 3-23 (B)) but unexpectedly, SUMOylation appears to be increased in *nox1* plants, both under resting conditions and with heat shock and H_2O_2 treatment.

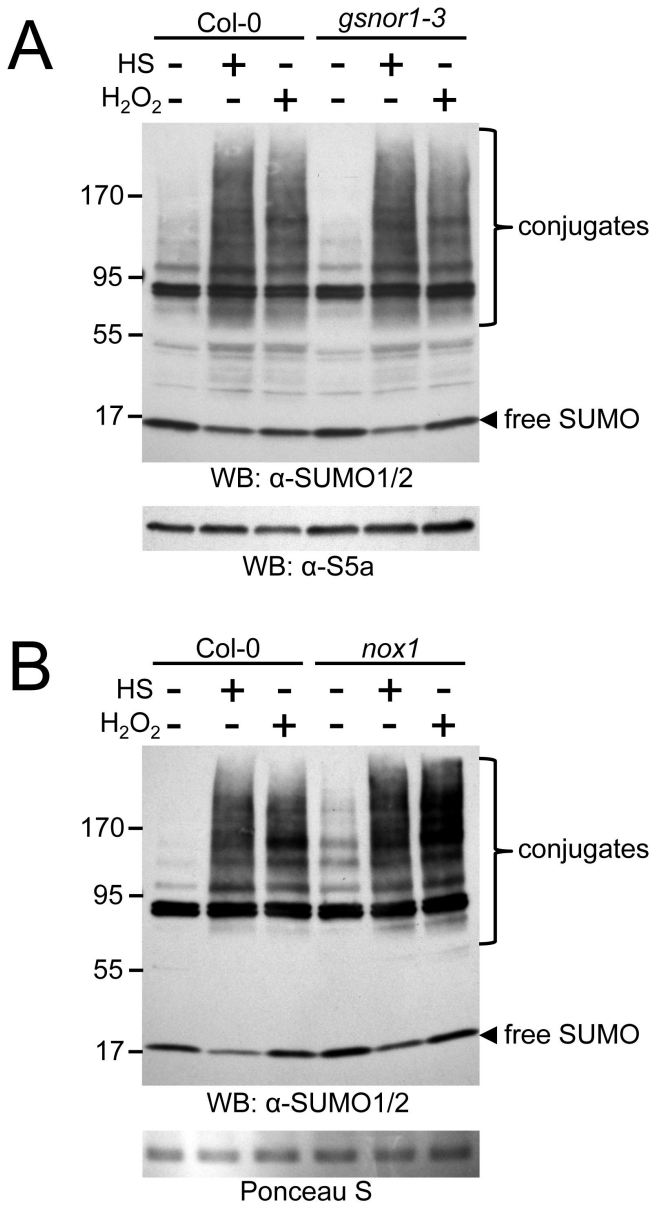

Figure 3-23 Global SUMOylation in *gsnor1-3* and *nox1* seedlings

Liquid-grown seedlings of the stated lines were exposed to 37°C or 5 mM H_2O_2 for 1 hour before freezing in liquid nitrogen. Proteins were extracted and separated by reducing SDS-PAGE before western blot against SUMO1/2. Loading controls are provided by **(A)** western blot against the proteasomal subunit S5A and **(B)** Ponceau S staining of the large subunit of Rubisco.

3.6.2 GSNO treatment inhibits SUMOylation in protoplasts

In order to further test the effect of S-nitrosylation on SUMOylation, protoplasts were isolated from WT and *gsnor1-3* plants and used to monitor SUMOylation after heat shock, with or without pre-treatment with GSNO. Rather than using whole plants or seedlings, it was hypothesized that more GSNO would be capable of accessing the intracellular space in protoplasts, without the need to bypass the cell wall. As shown in Figure 3-24, heat shock induces SUMOylation in WT and *gsnor1* protoplasts but pre-treatment with GSNO inhibits this response. GSNO treatment also appears to reduce levels of SUMO conjugates under resting conditions. Unexpectedly, compared to WT, *gsnor1-3* protoplasts have dramatically higher levels of SUMO-conjugates both under resting conditions and after heat-shock. Interestingly, the inhibitory effect of GSNO treatment appears to be heightened in *gsnor1-3*, suggesting that the increased SUMOylation observed in this line may be unrelated to SNO levels.

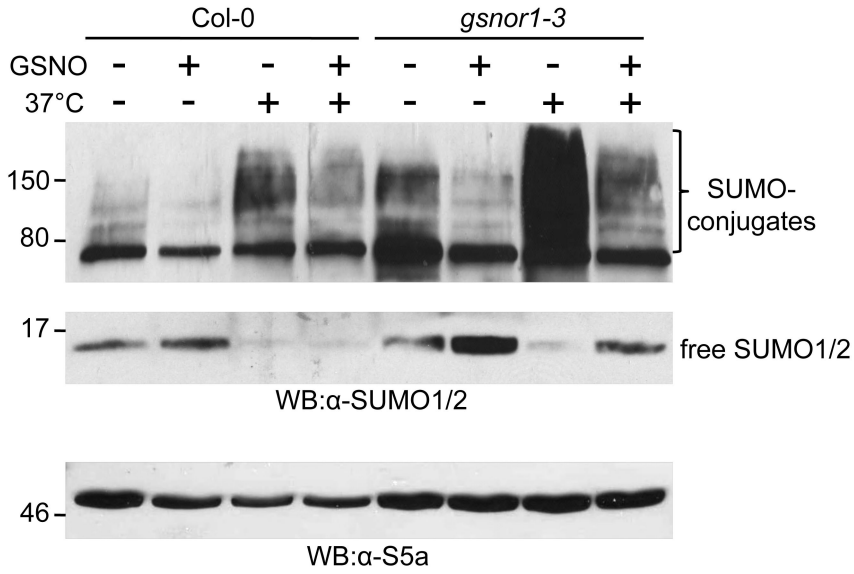

Figure 3-24 GSNO inhibits SUMOylation in protoplasts

Protoplasts were isolated from 4-week old plants of the stated genotypes and incubated with or without 1 mM GSNO in the dark for 5 mins before a 30 min heat shock treatment. Protoplasts were pelleted, frozen in liquid nitrogen and proteins extracted before analysis by reducing SDS-PAGE and western blot against SUMO1/2 or the proteasome subunit S5a.

3.7 Discussion

3.7.1 Inhibition of SCE1 by S-nitrosylation

S-nitrosylation of proteins is now known to be a key post-translational modification and is proposed to be one of the predominant means by which NO exerts its cellular biochemical activity. The effect of S-nitrosylation on the enzymatic activity of a protein can be directly mediated through modification of active site Cys residues (Hess et al, 2005). The findings of this thesis and previous work (Saad Malik, unpublished) provide compelling evidence that Cys139 is the only S-nitrosylation site of SCE1 both *in vitro* and *in vivo*. Since this residue is not located in or around the active site of SCE1, how does S-nitrosylation at this cysteine cause

inhibition of enzyme activity? In a mutational study of *S. cerevisiae* Ubc9, residues close to this area were shown to be important for Smt3-Smt3 conjugate formation (Bencsath et al, 2002). Similar to S-nitrosylation of SCE1 at Cys139, these same mutations did not have any effect on Ubc9-Smt3 thioester formation. The fact that S-nitrosylation of SCE1 at Cys139 does not affect SUMO thioester formation suggests that it does not interfere with binding to the E1 complex. This is not surprising since a well-defined region of the Ubc9 N-terminal has been identified as the binding site for E1:E2 noncovalent interactions (Benscath et al, 2002; Tatham et al, 2003 (a); Knipscheer et al, 2007; Capili and Lima, 2007) and Cys139 is located at a distant site near the C-terminus. Although there are currently no structures available for components of the *Arabidopsis* SUMOylation machinery, data from the structure of human Ubc9 in complex with the SUMO substrate RanGAP1 revealed that residues close to Cys138 on the same α-helix are important for interaction with RanGAP1 (Bernier-Villamor et al, 2002). Mutation of a conserved tyrosine to phenylalanine (Y134F) dramatically reduced the ability of Ubc9 to conjugate SUMO to RanGAP1 suggesting this residue plays an important role. As shown in Figure 3-25, structural modelling of SCE1 based on Ubc9 places the side chain of Tyr134/135 close to the side chain of Cys138/139 at a distance of 4 Å and 3.6 Å in Ubc9 and SCE1 respectively. Strikingly, overlaying the Ubc9 and predicted SCE1 structures shows remarkable conservation of secondary structure suggesting similar mechanisms of regulation. A possible means of S-nitrosylation of Cys139 inhibiting SUMOylation is by interfering with interactions between Tyr135 and the target protein, which in the case of data presented in this study, is SUMO1.

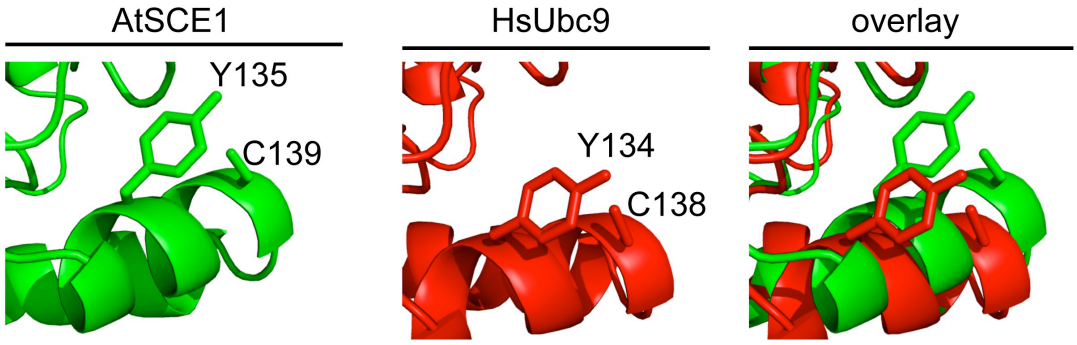

Figure 3-25 Orientation of SCE1 Tyr135 and Cys139 side chains

The predicted structure of SCE1 showing the proximity and orientation of Tyr135 and Cys139 compared with the equivalent resides of human Ubc9.

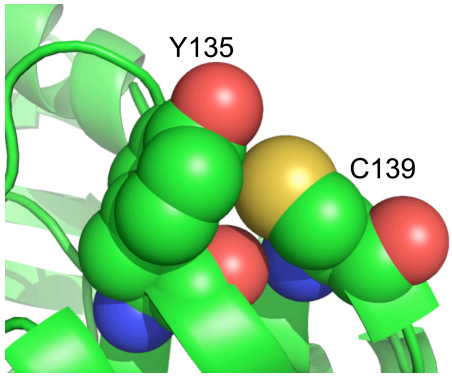

Figure 3-26 Electron densities of Tyr135 and Cys139

The electron densities of Tyr135 and Cys139 are represented by spheres with the rest of the protein shown as cartoon representation. Carbons are shown in green, oxygens in red, nitrogens in blue and sulphur in yellow. Hydrogens are omitted for clarity.

This is plausible in terms of the electron density around the side chains of Tyr135 and Cys139, which almost overlap while Cys139 is in its thiol state (Figure 3-26). Presumably the presence of an S-nitrosothiol here could cause reorientation of

these residues due to its increased size compared to a free thiol group. The α-helix containing Tyr135 and Cys139 packs tightly against a loop containing an asparagine (Asn125) that is highly conserved in SUMO E2s across all kingdoms suggesting it has an important functional role. Perhaps S-nitrosylation of Cys139 disrupts packing of the helix and this loop. This model is reminiscent of a structural study examining S-nitrosylation of Myoglobin purified from blackfin tuna. The authors compared the crystal structures of unmodified and S-nitrosylated myoglobin and found that *in vitro* S-nitrosylation of a surface-exposed cysteine resulted in a reversible conformational change in which a helix and a loop were "wedged" apart (Schreiter et al, 2007). However, if either of these models is true for SCE1 it would be expected that S-nitrosylation of Cys139 is a mechanism occurring in both humans and *Arabidopsis* due to the high conservation of these residues. In contrast, it has previously been reported that Ubc9 is S-nitrosylated at Cys75 in mammalian HEK293 cells, and that this S-nitrosylation did not affect its E2 activity (Qu et al, 2007). The authors of this study only tested S-nitrosylation of Ubc9 after treating cells with GSNO and based their identification of Cys75 purely on a lack of signal detected by biotin switch when Ha-tagged Ubc9-C75S was ectopically expressed in cells. Various crystal structures of Ubc9 show that Cys75 is located inside the protein structure and not solvent exposed making it unlikely to be S-nitrosylated. The evidence for S-nitrosylation of *Arabidopsis* SCE1 at Cys139 appears stronger, with *in vitro* data showing that Cys139 is the sole site of this modification as suggested by mass spectrometry analysis and site-directed mutagenesis (Saad Malik, unpublished). Furthermore the data presented in this thesis suggests that Cys139 is also the only site of S-nitrosylation *in vivo*, in response to pathogen recognition.

3.7.2 Further oxidation of SCE1 at Cys139

Although SCE1 is S-nitrosylated at Cys139 *in vivo* in response to pathogen challenge, further data presented in this thesis suggest that this is not the only oxidative modification occurring at this cysteine. SCE1 forms DTT-sensitive oligomers *in vitro* that are dependent on Cys94 and Cys139 (Figure 3-16). However, these oligomers are not detected *in vivo* and thus are probably an *in vitro* phenomenon. These experiments did provide more evidence that as well as the active site Cys94, the only other cysteine available for redox-based modification is Cys139. Furthermore, the fact that no dimers of SUMO E2s have been crystallized suggests that they do primarily exist as monomers. The fact that the RST detected higher levels of SCE1 than the BST, as exemplified by a signal readily detected for the RST from plants under resting conditions (Figure 3-14) suggests that a more oxidative modification than S-nitrosylation is present. However, due to its lack of specificity, the RST will also detect S-nitrosylation and there is no evidence that the signal detected does not represent this. Perhaps using DTT at a concentration of 1 mM and at room temperature effectively reduces SNOs without reducing more oxidized cysteines. To determine the exact redox-based modifications of specific cysteines *in vivo* would provide significant difficulty as these modifications may occur transiently and at very low levels.

3.7.3 Mutation of Cys139 of SCE1 compromises disease resistance

The effect of mutating Cys139 in the context of plant immunity became apparent by analysis of the overexpressor line *35S::FLAG-SCE1-C139S*, which showed increased susceptibility to both virulent and avirulent *Pst* DC3000 (Figure 3-

19). Furthermore, *35S::FLAG-SCE1-C139S* plants were compromised in activation of *PR-1* expression (Figures 3-20 and 3-21). These data suggest that Cys139 of SCE1 might play a role in immune signalling following bacterial infection. Combined with the *in vitro* evidence that S-nitrosylation of SCE1 inhibits its activity, that SCE1 is S-nitrosylated *in vivo* following pathogen infection, and that global SUMOylation levels are increased in *35S::FLAG-SCE1-C139S* plants following infection, this leads to a potential model by which SUMOylation is regulated through pathogen-induced redox-regulation of SCE1 (Figure 3-27). In this model, increasing levels of NO induced by attempted bacterial pathogen infection lead to S-nitrosylation of SCE1 at Cys139. This results in a decrease in SUMO conjugation by SCE1, relieving negative regulation of disease resistance by SUMOylation.

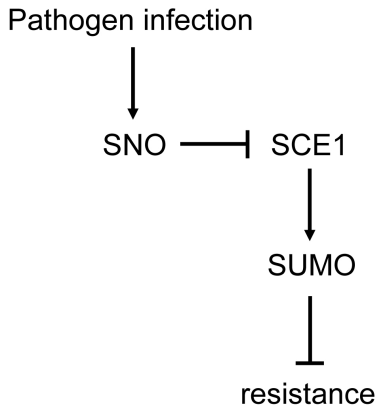

Figure 3-27 A model for redox-regulation of SCE1 in plant immunity

Simplified schematic diagram showing that increased S-nitrosylation of SCE1 after pathogen infection leads to activation of immune signalling.

For this model to be valid, the notion that SUMOylation negatively regulates disease resistance against bacterial pathogens must be true. This is perhaps a generalization based on data from plants with altered global SUMOylation such as *siz1* mutants (Lee et al, 2007) and plants with altered expression of *SUM1* and *SUM2* (van den Burg et al, 2010). van den Burg et al suggest that in non-infected plants, SUMO1/2 conjugation represses plant defence activation (van den Burg et al, 2010). If active suppression by SUMOylation is required to prevent immune activation, this suggests that defence responses are primed and ready for rapid induction. Thus the model proposed in this thesis constitutes a molecular mechanism by which the nitrosative burst after pathogen attack is perceived and translated into immune activation.

Chapter 4

4 Investigating the effects of SCE1 overexpression

4.1 Background

The *35S::FLAG-SCE1* transgenic plants described previously in Chapter 3 appeared to have increased levels of global SUMOylation (Figure 3-18). Since SUMOylation is known to play a major role in stress responses, manipulation of this complex system could potentially improve tolerance to stresses in plants. Previous work has suggested that SUMOylation may be under strict regulation, with both overexpression and knockdown of *Arabidopsis SUM1* having similar phenotypes in the context of SA-mediated plant immunity (van den Burg et al, 2010). Data presented in this thesis showed that *35S::FLAG-SCE1* plants exhibit WT levels of resistance to both virulent and avirulent *Pst* DC3000 (Figure 3-19). Previous work in mice has shown that overexpression of Ubc9 increases global SUMOylation and protects transgenic mice from ischemic brain damage (Lee et al, 2011). However, overexpression of SUMO E2s as a therapeutic strategy must be approached with caution as it has been shown that ectopic Ubc9 expression promotes tumour growth and metastasis of cancer cells in mice (Zhu et al, 2010). Interestingly this effect is independent of the SUMO-conjugating activity of Ubc9 since overexpression of a mutant Ubc9 that cannot SUMOylate proteins had the same effect. Furthermore, it has been reported that Ubc9 is expressed at high levels in many types of cancer cells from human patients (Moschos et al, 2010) and so at least in mammals, high levels of SUMO E2 enzyme may have more negative effects than positive. However,

whether this is the case in plants is unknown and modulating SCE1 levels as a strategy to engineer plant tolerance to stresses is worthy of investigation.

4.2 Confirmation of increased SUMOylation in *35S::FLAG-SCE1* transgenic plants

To further confirm that global SUMOylation is increased in *35S::FLAG-SCE1* plants, an *in vivo* SUMOylation assay similar to Figure 3-18 was repeated on *Arabidopsis* seedlings. As shown in Figure 4-1 (A), SUMO-conjugates are increased in *35S::FLAG-SCE1* plants compared to WT after both 15- and 60 minute heat shock treatments. The differences in SUMOylation are even more apparent when free SUMO1/2 levels are observed. A 15 minute heat shock resulted in a ~25% decrease in free SUMO1/2 levels in WT, but a ~90% decrease in *35S::FLAG-SCE1* plants (Figure 4-1 (B)) suggesting that *35S::FLAG-SCE1* plants utilize the available pool of free SUMO much more rapidly than WT. After a 60 minute heat shock, free SUMO was decreased by ~85% in WT and virtually undetectable in *35S::FLAG-SCE1* plants. It has previously been reported that overexpression of SCE1 in *Arabidopsis* did not affect global SUMO conjugate levels (Lois et al, 2003) although this study only tested plants under resting conditions. The data presented in Figure 4-1 is in agreement with this, as both free SUMO and SUMO-conjugate levels are similar in untreated plants. Therefore, overexpression of SCE1 appears to have a more pronounced effect on SUMOylation in response to heat stress.

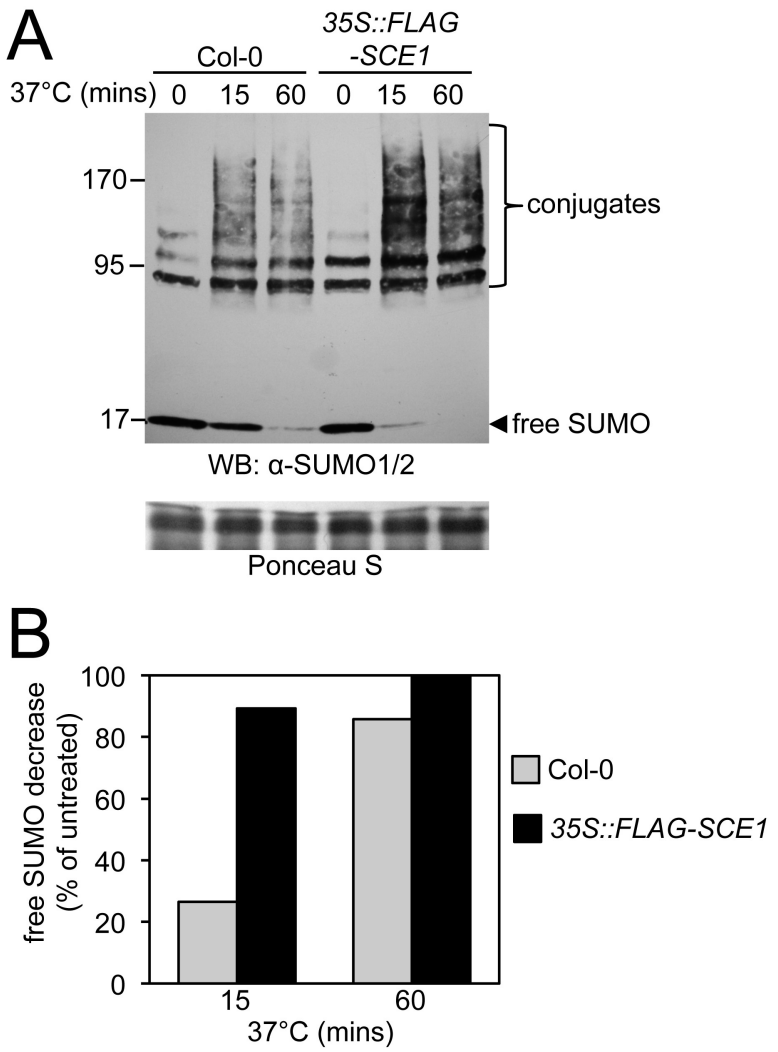

Figure 4-1 Overexpression of FLAG-SCE1 increases heat-shock induced SUMOylation in *Arabidopsis* seedlings

(A) Liquid-grown seedlings of the stated lines were exposed to 37°C for the indicated times before freezing in liquid nitrogen. Proteins were extracted and separated by reducing SDS-PAGE before western blot against SUMO1/2. Ponceau S staining of the large subunit of Rubisco indicates equal loading. **(B)** The levels of free SUMO after heat shock in (A) were quantified by densitometry and expressed as a percentage decrease of the level of free SUMO in the untreated lanes.

4.3 Overexpression of SCE1 does not compensate for loss of SIZ1 function

The SUMO E3 ligase, SIZ1 has previously been shown to be the main mediator of stress-responsive SUMOylation (Miura et al, 2007) with *siz1* mutants exhibiting dramatically decreased heat stress-induced SUMO conjugation (Miura et al, 2005; Saracco et al, 2007). Since overexpression of SCE1 appears to increase global SUMOylation, *35S::FLAG-SCE1* plants were crossed to the *siz1-2* loss-of-function T-DNA insertion mutant. Confirmation of the transgene expression was confirmed in homozygous *siz1*-2 plants by Western blot against FLAG (Figure 4-2) and line #2 was chosen for its strong expression. Homozygous *siz1*-2 plants expressing the *35S::FLAG-SCE1* transgene were noticeably similar in appearance to *siz1-2* with no visible rescue of the dwarfed phenotype (Figure 4-3).

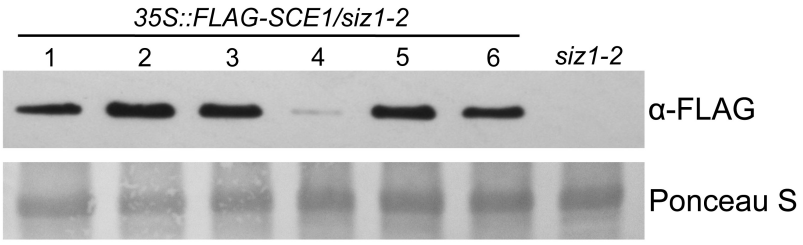

Figure 4-2 FLAG-SCE1 expression in the *siz1-2* background

Protein extracts from *35S::FLAG-SCE1* x *siz1-2* F2 plants and *siz1*-2 plants were separated by reducing SDS-PAGE and analysed by western blot against FLAG. Ponceau S staining of the large subunit of Rubisco is included as a loading control.

Figure 4-3 Overexpression of SCE1 does not rescue the dwarfed phenotype of *siz1* mutant plants

Photographs were taken of the stated lines at 4 weeks old alongside each other for comparison of size.

After isolating plants homozygous for both the *35S::FLAG-SCE1* transgene and the *siz1-2* mutation, these were used in an *in vivo* SUMOylation assay to establish if SCE1 overexpression could compensate for the reduced SUMO conjugation observed in *siz1* plants. As shown in Figure 4-4, WT and *35S::FLAG-SCE1* plants both showed efficient conjugation of SUMO after heat-shock with a consequent decrease in free SUMO levels. Again, *35S::FLAG-SCE1* plants showed less detectable free SUMO after heat shock compared to WT. In contrast, *siz1* plants showed dramatically less SUMO conjugation both basally and after heat shock. Overexpression of SCE1 appears to have no effect on SUMOylation in *siz1* plants as *35S::FLAG-SCE1*/*siz1* double mutants exhibit similar levels of SUMO conjugation. Significantly, in both *siz1* and *35S::FLAG-SCE1*/*siz1* plants, no observable change in free SUMO levels were detected after heat shock. Taken together with the developmental phenotype of *35S::FLAG*-SCE1/*siz1* plants, these results suggest that overexpression of SCE1 does not compensate for loss of SIZ1 function in the

contexts of growth, development, and heat-stress induced SUMO conjugation. However, other phenotypes of *siz1* mutant plants that were not analysed could be affected by SCE1 overexpression. These include constitutive SA-mediated defence signalling, upregulation of the abscisic acid (ABA) signalling pathway, and dysregulation of phosphate deficiency responses (Lee et al, 2007; Miura et al, 2009; Miura et al, 2005).

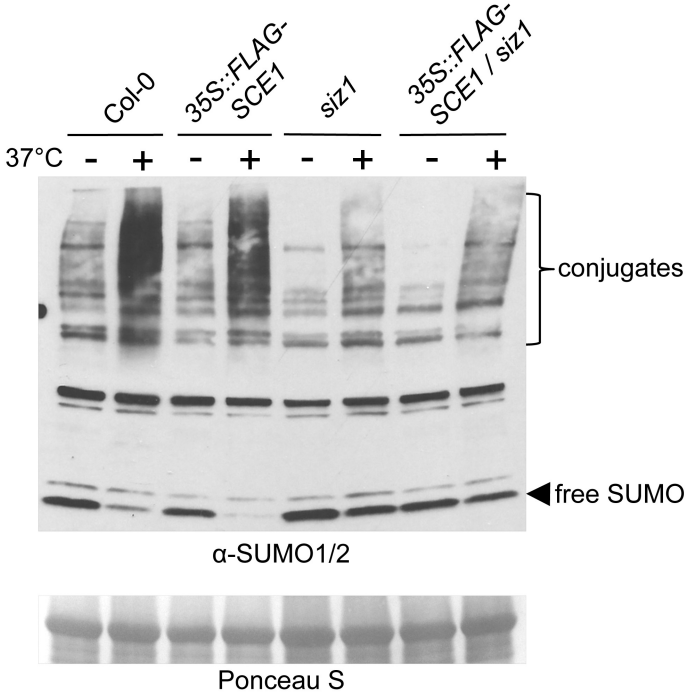

Figure 4-4 Overexpression of SCE1 in *siz1* plants has no effect on global SUMOylation in response to heat stress

Liquid-grown seedlings of the stated genotypes were either subjected to a 15 minute heat shock or incubated at RT for 15 minutes before freezing in liquid nitrogen and detecting SUMO conjugation by reducing SDS-PAGE and western blot against SUMO1/2. Ponceau S staining of the large subunit of Rubisco is included as a loading control.

4.4 Overexpression of SCE1 increases tolerance to H_2O_2

It is well established that SUMOylation is involved in general stress responses, including heat and oxidative stress. Therefore upregulation of SUMOylation through SCE1 overexpression may affect the ability of plants to tolerate exposure to these stresses. To test whether SCE1 overexpression affects oxidative stress tolerance, seeds were germinated and grown on ½ MS plates containing 2.5 mM H_2O_2 and scored for cotyledon development. As shown in Figure 4-5, *35S::FLAG-SCE1* cotyledon development was unaffected by the presence of 2.5 mM H_2O_2, whereas in WT plants, cotyledon development was reduced to ~70%. The *35S::FLAG-SCE1-C139S* line (Chapter 3) was included as an additional, independent SCE1 overexpressor line and similarly, showed significantly higher cotyledon development in the presence of 2.5 mM H_2O_2 compared to WT. This suggests that overexpression of SCE1 increases the tolerance of *Arabidopsis* to oxidative stress, reminiscent of Ubc9 overexpression in mice (Lee et al, 2011).

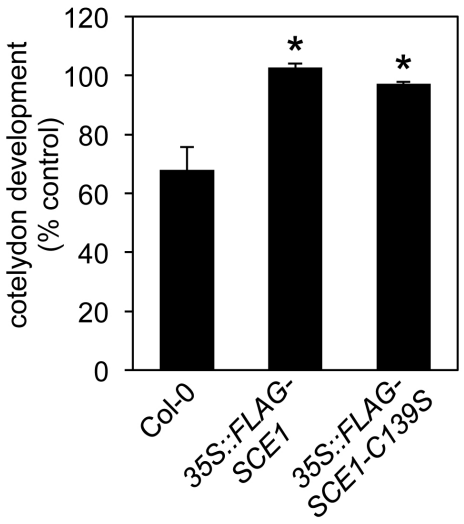

Figure 4-5 Overexpression of SCE1 enhances tolerance to H_2O_2

Seeds of the stated lines were stratified at 4°C for 2 days on ½ MS media containing 2.5 mM H_2O_2 before moving to 22°C and placing under light in long day cycles. Cotyledon development was scored within 5 days and expressed as a percentage of the score of the same plants on ½ MS media without H_2O_2. Data points represent mean ± SEM (n=3), with asterisks indicating significant difference from Col-0 (Student's *t* test, $P < 0.05$).

4.5 Discussion

4.5.1 Overexpression of SCE1 increases SUMOylation and enhances tolerance to oxidative stress

Unlike the Ub system, which has many E2 enzymes (up to 37 in *Arabidopsis*) (Vierstra, 2009), SUMO relies on a single E2 for its conjugation to target proteins. Therefore, modulation of SUMO E2s might be an efficient means to control global SUMOylation. Overexpression of SCE1 appeared to increase the levels of SUMO conjugates after heat shock in *Arabidopsis* seedlings (Figure 4-1). The levels of free SUMO also disappeared more rapidly after heat shock in *35S::FLAG-SCE1* plants

compared to WT (Figure 4-1). However, it is not clear whether the changes in free SUMO quantitatively reflect the changes in SUMO conjugate levels. It is possible that the increased levels of SCE1 are partially sequestering the pool of free SUMO. If this was the case, it would be expected that free SUMO levels in *35S::FLAG-SCE1* plants would be decreased under resting conditions compared to WT. This was not observed, with free SUMO levels consistently observed at comparable levels in untreated WT and *35S::FLAG-SCE1* plants (Figures 4-1 and 4-3). Therefore, it appears that overexpression of SCE1 in *Arabidopsis* plants increases stress-responsive, but not basal SUMO conjugation and thus serves to enhance the inherent SUMOylation response of plants to heat stress. It is becoming clear that to engineer plants with increased resistance to stresses, targeting induced responses is more likely to avoid the negative trade-offs associated with enhancing basal resistance, such as aberrant growth, development and fertility (Cabello et al, 2014).

Since SUMOylation is involved in such a diverse range of cellular processes and targets hundreds of proteins, increasing SUMOylation might have a positive effect on one cellular response but a negative effect on another. As discussed in Chapter 3, SUMOylation contributes towards suppression of immune responses and indeed, *PR-1* gene expression after *Pst* DC3000 infection was slightly decreased in *35S::FLAG-SCE1* plants compared to WT (Figure 3-21). The same *35S::FLAG-SCE1* plants showed increased tolerance to oxidative stress (Figure 4-5) demonstrating that increasing SUMOylation in *Arabidopsis* might suppress defence against bacterial pathogens but increase defence against oxidative stress. Identifying the SUMO substrates that are responsible for these phenotypes would increase the chances of specifically enhancing a particular trait. For example, identifying any

proteins that are SUMOylated in *35S::FLAG-SCE1* plants but not in WT plants grown in the presence of H_2O_2 might reveal new targets for engineering oxidative stress resistance in plants.

4.5.2 Overexpression of SCE1 does not increase global SUMOylation in *siz1* plants

The generation of *35S::FLAG-SCE1*/*siz1* plants revealed that overexpression of SCE1 does not alleviate the striking developmental phenotype, or the compromised heat-shock induced phenotype of *siz1* plants (Figures 4-3 and 4-4). The importance of SUMO E3 ligases *in vivo* are evident by the dramatic phenotypes of *siz1* and *hpy2* loss-of-function mutant plants (Miura et al, 2005; Ishida et al, 2009). To date, these are the only two SUMO E3s identified in *Arabidopsis*, compared to four in yeast and up to ten in humans (Miura and Hasegawa, 2010). SIZ1 and HPY2 are likely to SUMOylate different targets, as their heat-shock induced SUMO conjugation profile differs (Ishida et al, 2009). Other potential SUMO E3s have been identified in the *Arabidopsis* genome by sequence homology to SIZ1 domains, but have yet to be assigned a role *in vivo* (Cheong et al, 2009). It is likely that SIZ1 and HPY2 are the only functional SUMO E3 ligases *in vivo* as *siz1*/*hpy2* double mutants have been shown to be embryonic lethal (Ishida et al, 2012). The increased SUMOylation observed in *35S::FLAG-SCE1* plants appeared to be SIZ1-dependent (Figure 4-4). In agreement with this, SIZ1 has been reported to be required for efficient heat-shock induced SUMOylation (Miura et al, 2005; Saracco et al, 2007). Thus, although overexpression of SCE1 might lead to increased global SUMOylation, it requires the presence of SIZ1 for this effect. Generation of

35S::FLAG-SCE1/*hpy2* plants would reveal whether this requirement is SIZ1 specific, or if HPY2 can also provide some of the E3 activity required for SCE1 overexpression to increase SUMOylation. It is unknown whether proteins are SUMOylated *in vivo* independently of E3 activity, and due to the embryonic lethality of *siz1*/*hpy2* mutants, this is difficult to establish. Although SCE1 and other SUMO E2s can directly conjugate SUMO to lysines within the consensus SUMOylation motif ψKXE *in vitro* in the absence of E3 activity, it is unknown whether this occurs *in vivo*. In a proteomic analysis of *Arabidopsis* SUMO conjugates, 80% of the identified proteins contained at least one consensus SUMOylation motif (Miller et al, 2010), suggesting that direct SCE1-substrate binding is an important factor for SUMOylation. To establish if E3-independent SUMOylation occurs *in vivo* would require generation of an organism with mutations in all SUMO E3 ligases. In yeast, it has been reported that *siz1 siz2 mms21* triple mutants are lethal (Zhao and Blobel, 2005; Reindle et al, 2006). Thus, if loss of three of the four SUMO E3s in yeast is lethal, loss of both *Arabidopsis* SUMO E3s is lethal, and mammals have up to ten SUMO E3s, generation of an organism lacking any SUMO E3 activity is likely impossible. Because the increased SUMOylation observed in *35S::FLAG-SCE1* plants appeared to be SIZ1-dependent (Figure 4-4), it would be interesting to analyse SUMOylation profiles in plants overexpressing both SCE1 and SIZ1 to establish if SUMOylation in *35S::FLAG-SCE1* plants is limited by SIZ1 levels. In conclusion, work presented in this chapter suggests that engineering of global SUMOylation in *Arabidopsis* can be achieved by modulating SCE1 levels, but this is probably dependent on SUMO E3 ligase activity.

Chapter 5

5 Investigating the effects of GSNOR1 overexpression

5.1 Background

As discussed in Chapter 1, GSNO is a molecule thought to constitute a cellular reservoir of NO bioactivity. NO can be released from GSNO or can be directly transferred to a target by a process known as transnitrosylation (Hess et al, 2005). The enzyme responsible for controlling GSNO levels, GSNOR, consequently controls the levels of protein SNOs albeit indirectly. In *Arabidopsis*, loss of GSNOR function in the mutant line *gsnor1-3* results in elevated global SNO levels and compromises multiple modes of disease resistance (Feechan et al, 2005). This study provided evidence that SNO metabolism controlled by GSNOR plays a major role in plant immunity. Further studies have since suggested that GSNOR is a key regulator of cell death (Chen et al, 2009), thermotolerance (Lee et al, 2008), and development (Kwon et al, 2012). Many defence-related proteins have increased levels of S-nitrosylation in *gsnor1-3* mutant plants compared to WT, further confirming the importance of this enzyme in regulating global SNO levels (Skelly and Loake, 2013). Most studies of GSNOR1 function in *Arabidopsis* have relied on loss-of-function mutants, although a T-DNA insertion line, *gsnor1-1* showed increased levels of *GSNOR1* transcripts and increased GSNOR activity (Feechan et al, 2005). The T-DNA insertion in this line is located in the *GSNOR1* promoter approximately 350 bp upstream of the ATG start codon. Although the exact reason is unknown, overexpression of *GSNOR1* is presumably caused by the T-DNA insertion preventing a negative regulator of transcription from binding to the promoter. To

further examine the effect of GSNOR1 overexpression and facilitate detection of the transgenic protein, this chapter describes the generation of transgenic plants constitutively expressing FLAG-tagged GSNOR1 under the control of the *35S* promoter. Furthermore, characterization of these plants and the effect of GSNOR1 overexpression in different mutant backgrounds will be discussed.

5.2 Generation of FLAG-GSNOR1 transgenic plants

After successfully generating *35S::FLAG-SCE1* plants and using antibodies against FLAG for robust detection of the transgenic protein (Chapter 3), the same approach was adopted for GSNOR1. As well as WT plants, *gsnor1* mutant (*paraquat resistant 2* (*par2-1*)) plants were transformed with a *35S::FLAG-GSNOR1* construct to establish if the transgene could complement the *par2-1* mutation. The *par2-1* allele was chosen rather than *gsnor1-3* because it is a point mutation in *GSNOR1*, rather than a T-DNA insertion line and thus transformation will result in plants with one, rather than two T-DNA insertions thereby reducing the chances of any unwanted indirect effects of T-DNA insertion occurring. Numerous (>10) T_1 transgenic lines were obtained from transformation of WT plants, while only two lines were recovered from transformation of *par2-1*. This was unsurprising since *gsnor1-3* plants were previously shown to produce only 30% of the amount of seeds as WT (Kwon et al, 2012). After confirming that the transgenic plants contained a single copy of the transgene, the selected lines were analysed for transgene expression by western blot against FLAG. As shown in Figure 5-1, *35S::FLAG-GSNOR1* / *par2-1* line #1-3 and *35S::FLAG-GSNOR1* / Col-0 line #16-5 both express the transgene at comparable levels. The band detected is of the correct

predicted size (~45 kDa) and is absent in WT plants confirming that FLAG-GSNOR1 is expressed. These lines were then selected for analysis of *GSNOR1* expression compared to WT plants.

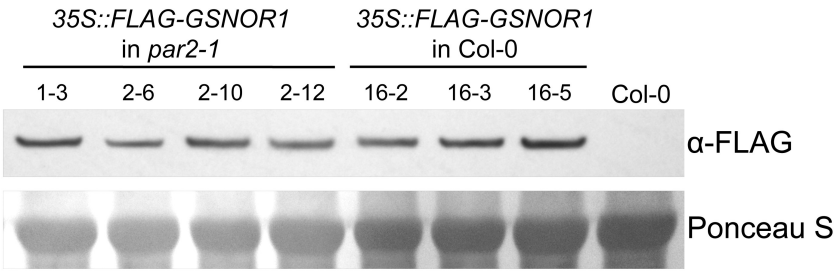

Figure 5-1 Expression of FLAG-GSNOR1 protein in transgenic lines

Protein extracts from *35S::FLAG-GSNOR1* plants in the stated genetic backgrounds were analysed by reducing SDS-PAGE and western blot against FLAG. Ponceau S staining of the large subunit of Rubisco is included as a loading control.

Since no antibodies against *Arabidopsis* GSNOR1 were available, *GSNOR1* transcript levels were analysed by semi-quantitative RT-PCR. As shown in Figure 5-2, *35S::FLAG-GSNOR1* plants accumulate more *GSNOR1* transcripts in both WT and *par2-1* backgrounds. *GSNOR1* expression was detected in *par2-1* plants, consistent with previous reports that the point mutation does not ablate gene expression but rather, results in a defective protein (Chen et al, 2009). To confirm that the *par2-1* mutation was still present in the transformed plants, genomic DNA from these lines was subjected to PCR genotyping (described in section 2.5). As shown in the top panel of Figure 5-3, genotyping for the presence of the WT version of the *PAR2* / *GSNOR1* gene with the WT-F and Rev primers amplifies a 325 bp

product from WT (lane 3), but not *par2-1* (lane 4) DNA. This PCR product includes 86 bp of the sixth intron of the gene. A smaller product is amplified from the *35S::FLAG-GSNOR1* transgene because the sixth intron is absent in this construct (lanes 1 and 2). As expected, genotyping for the *par2-1* mutation with *par2-1*-F and Rev primers amplifies a product from the two transgenic *35S::FLAG-GSNOR1* / *par2-1* lines tested (bottom panel, Figure 5-3) and from *par2-1*, but not WT DNA. Taken together, these results show that the selected transgenic plants do indeed exhibit overexpression of *GSNOR1* by means of the *35S::FLAG-GSNOR1* constructs in WT and *par2-1* backgrounds.

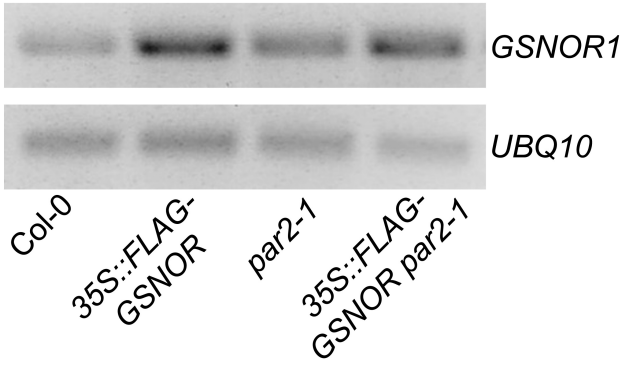

Figure 5-2 Expression of *GSNOR1* in transgenic lines

Expression of *GSNOR1* was determined in the stated lines by semi-quantitative RT-PCR. The constitutively expressed *UBQ10* was included as a loading control.

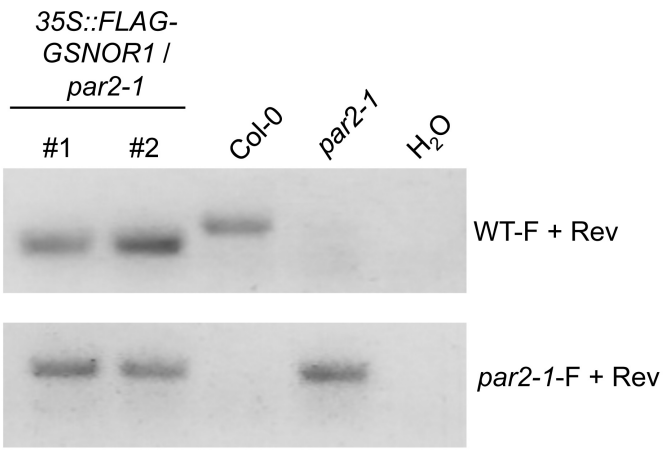

Figure 5-3 PCR genotyping of *par2-1*

Genomic DNA from the stated lines was analysed by SNP-based PCR genotyping using the stated primer pairs. H_2O was used as a negative control for the PCR reactions in the place of DNA.

5.3 FLAG-GSNOR1 is active *in vivo*

5.3.1 *35S::FLAG-GSNOR1* rescues the developmental phenotype of the *par2-1* mutant

Although data presented in section 5.2 showed that *35S::FLAG-GSNOR1* plants are indeed *GSNOR1* overexpressors, these results did not address whether the transgenic GSNOR1 protein was active *in vivo*. Active transgenic FLAG-GSNOR1 should complement the reduced apical dominance and semi-dwarf *par2-1* mutant phenotype (Chen et al, 2009) providing it is expressed at an appropriate level. As shown in Figure 5-4, the presence of the *35S::FLAG-GSNOR1* transgene does not visibly impact the appearance of WT plants but does restore the growth phenotype and loss of apical dominance displayed in *par2-1* plants, suggesting that transgenic FLAG-GSNOR1 is active *in vivo*.

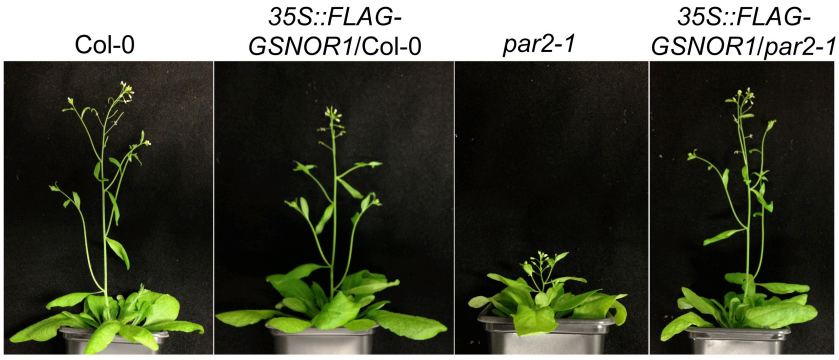

Figure 5-4 Overexpression of *GSNOR1* restores the developmental phenotype of *par2-1* plants to wild-type

6-week old plants of the stated lines were grown on soil in individual pots and photographed to compare growth between lines. Images shown are representative of >10 plants per line.

5.3.2 *35S::FLAG-GSNOR1* rescues the susceptibility of *par2-1* mutant plants to *Pst* DC3000

Since the *35S::FLAG-GSNOR1* transgene rescued the developmental phenotype of *par2-1*, the same plants were then infected with virulent *Pst* DC3000 and assayed for bacterial growth. It has previously been reported that *gsnor1-3* plants are susceptible to various pathogens including *Pst* DC3000 (Feechan et al, 2005) and so it was hypothesized that *par2-1* plants would show a similar disease phenotype. As shown in Figure 5-5, *35S::FLAG-GSNOR1* plants show increased resistance to *Pst* DC3000 compared to WT, while *par2-1* plants are clearly susceptible. Importantly, *35S::FLAG-GSNOR1*/*par2-1* plants exhibit enhanced resistance as compared to WT. Thus, overexpression of *GSNOR1* appears to increase resistance to *Pst* DC3000, in both WT and *par2-1* genetic backgrounds.

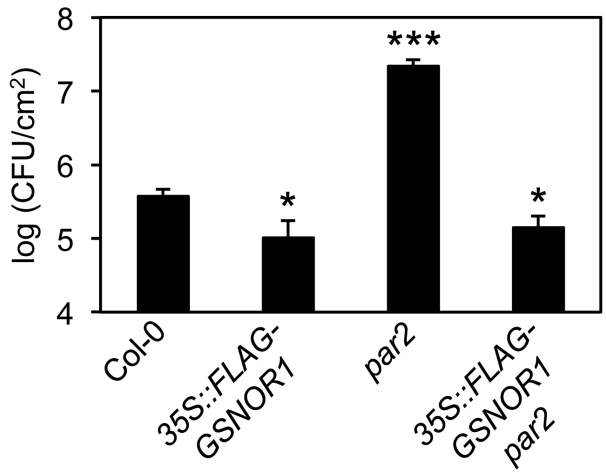

Figure 5-5 Overexpression of *GSNOR1* enhances resistance to *Pst* DC3000 and rescues the susceptibility of *par2-1* plants

The stated lines were inoculated with *Pst* DC3000 and assayed for bacterial growth at 3 dpi. Data points represent mean ± SEM (n=6), with asterisks indicating significant difference from Col-0 (Student's *t* test,* P < 0.05, *** P < 0.0001). This experiment was repeated twice with similar results.

5.4 Overexpression of GSNOR1 in *nox1* plants

Overexpression of *GSNOR1* rescued the phenotypes of a loss-of-function *gsnor1* mutant i.e. *par2-1*, demonstrating that the transgenic FLAG-GSNOR1 protein was active *in vivo* and was therefore capable of reducing the levels of protein SNOs. Many, if not all of the phenotypes of *gsnor1* loss-of-function mutants probably result from the increased levels of global S-nitrosylation. Global SNO levels are also increased in *Arabidopsis nox1* mutants (Yun et al, 2011) although through a GSNO-independent mechanism. The levels of L–arginine and citrulline are elevated in *nox1* mutants suggesting that these plants accumulate high levels of NO through a NOS-like activity (He et al, 2004). While both dramatically different from WT, the

phenotypes of loss-of-function *gsnor1* and *nox1* mutants are different from each other suggesting that elevated GSNO and elevated NO levels have different effects on growth and development. However, it is unknown whether increasing GSNOR activity could alleviate the effects of high NO levels in *nox1* plants by reducing global S-nitrosylation. To test this, *35S::FLAG-GSNOR1* plants were crossed with *nox1* plants and double homozygotes were recovered in the T_3 generation. Expression level of the transgene was confirmed in *35S::FLAG-GSNOR1*/*nox1* plants by western blot (Figure 5-6) and was similar to the parent *35S::FLAG-GSNOR1* line used for crossing.

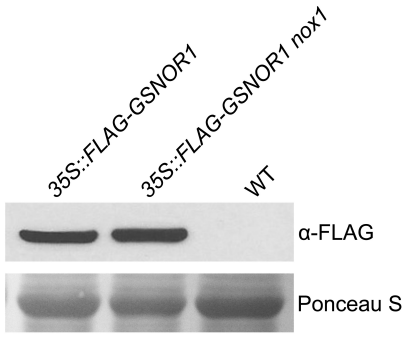

Figure 5-6 FLAG-GSNOR1 protein levels in *nox1* plants

Protein extracts from *35S::FLAG-GSNOR1* plants in WT and *nox1* genetic backgrounds were analysed by reducing SDS-PAGE and western blot against FLAG. Ponceau S staining of the large subunit of Rubisco is included as a loading control.

5.4.1 Overexpression of GSNOR1 does not affect the developmental phenotype of *nox1* plants

After isolating *35S::FLAG-GSNOR1*/*nox1* double mutant plants, it was observed that these visually resembled the single *nox1* mutant. To verify that these plants were developmentally similar, the rosette leaf area was measured every 5 days

over a 15 day period. As shown in Figure 5-7, WT, *35S::FLAG-GSNOR1* and *35S::FLAG-GSNOR1*/*par2-1* plants had a similar growth pattern over the time period tested. Growth was slower in *par2-1* and *nox1* plants, and as expected, *35S::FLAG-GSNOR1*/*nox1* plants grew at a similar rate and to a similar size as *nox1*.

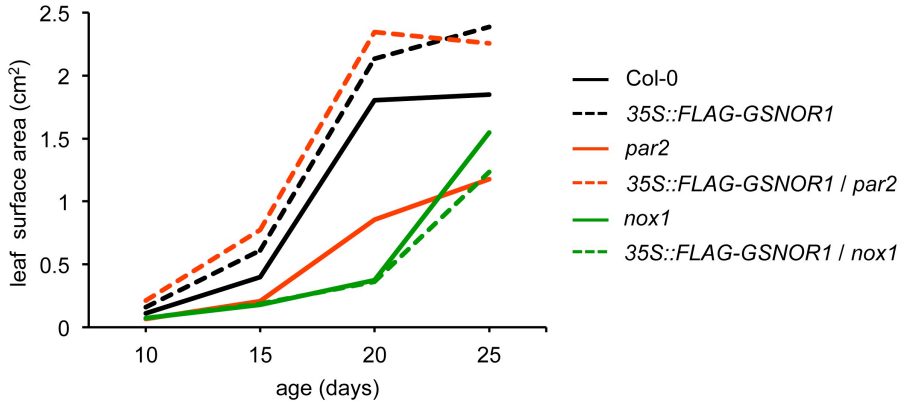

Figure 5-7 Vegetative growth rates of *35S::FLAG-GSNOR1* transgenic lines in different genetic backgrounds

Surface areas of rosette leaves were measured at 10, 15, 20 and 25 days on soil-grown plants of the stated lines. Data points represent the mean (n=4) with markers and error bars omitted for clarity.

To confirm that the *35S::FLAG*-GSNOR1 transgene did not rescue the developmental phenotype of the *nox1* mutant, the data from 25-day old plants were analysed for statistically significant differences. As shown in Figure 5-8, *35S::FLAG-GSNOR1* expression has no effect on the size of WT plants. No difference was observed between *nox1* and *35S::FLAG-GSNOR1*/*nox1* plants and as expected, *35S::FLAG-GSNOR1*/*par2* plants showed similar leaf surface areas to WT

plants. These data suggest that overexpression of GSNOR1 does not affect the developmental phenotype of *nox1* mutant plants and therefore make it likely that the high level of NO in *nox1* plants occurs independently of, and is unaffected by cellular GSNO levels.

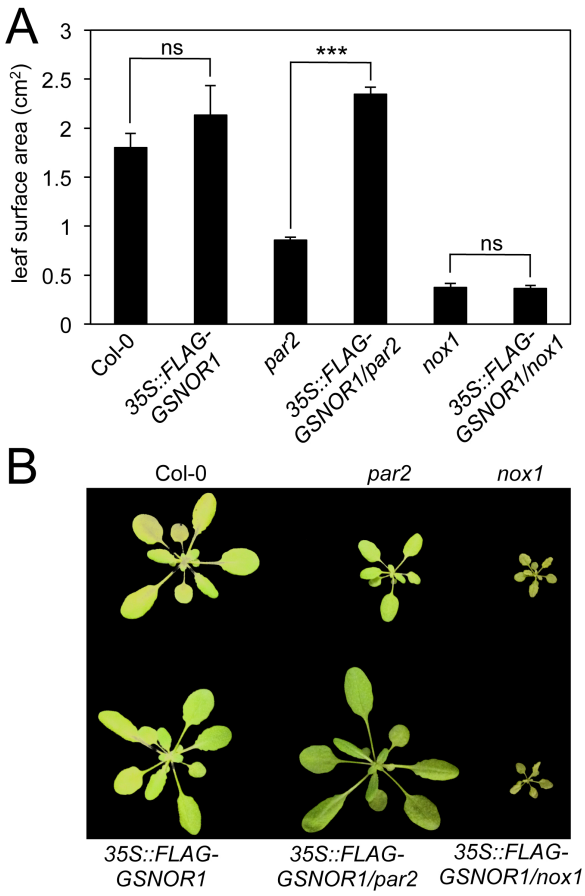

Figure 5-8 *35S::FLAG-GSNOR1* rescues the developmental phenotype of *par2-1* but not *nox1*

(A) Surface areas of rosette leaves were measured at 25 days on soil-grown plants of the stated lines. Data points represent mean ± SEM (n=4), with asterisks indicating significant difference (Student's *t* test, *** P < 0.0001) and *ns* representing not significant. **(B)** Photographs of representative plants used in (A).

5.4.2 *nox1* plants are susceptible to *Pst* DC3000 and are not rescued by *35S::FLAG-GSNOR1*

Although it has been reported that global SNO levels are elevated in *nox1* plants, and that they exhibit accelerated cell death in response to avirulent pathogens (Yun et al, 2011), it is unknown whether they are susceptible to bacterial infection. To test this and to further examine the effect of overexpressing GSNOR1 in the *nox1* background, plants were inoculated with *Pst* DC3000 and monitored for visible disease symptoms. At 4 dpi, WT and *35S::FLAG-GSNOR1* plants show no observable disease symptoms, while both *nox1* and *35S::FLAG-GSNOR1*/*nox1* plants exhibit striking discolouration and wilting of the inoculated leaves (Figure 5-9 (A)). Bacterial growth assays in these lines confirmed that both *nox1* and *35S::FLAG-GSNOR1*/*nox1* plants are susceptible to *Pst* DC3000 infection (Figure 5-9 (B)). Similar to previous experiments, *35S::FLAG-GSNOR1* plants showed increased resistance to *Pst* DC3000 compared to WT. These data suggest that *nox1* plants are compromised in resistance to *Pst* DC3000 and while *35S::FLAG-GSNOR1* expression enhances resistance in WT and *par2-1* backgrounds, it has no effect in the *nox1* background.

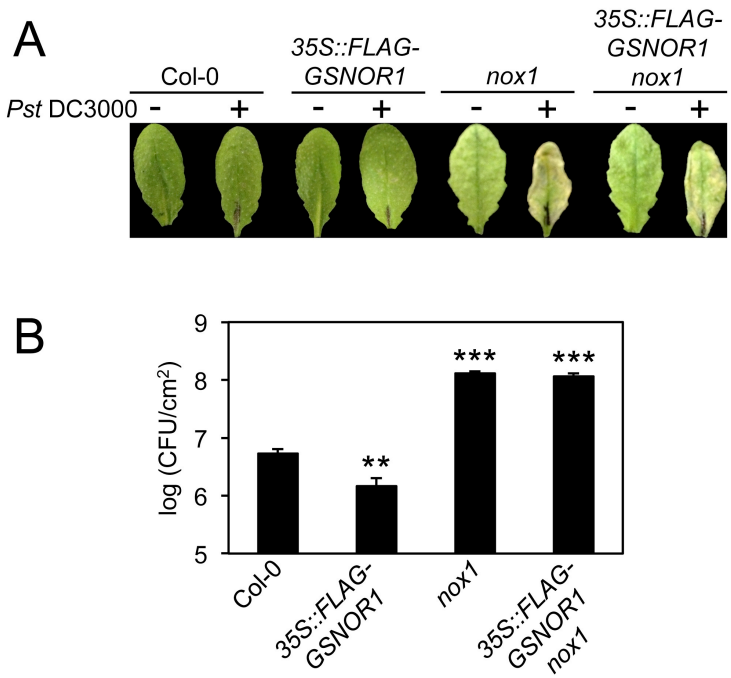

Figure 5-9 *nox1* plants are susceptible to *Pst* DC3000

(A) Disease symptoms of the stated lines at 4 dpi with *Pst* DC3000. Representative leaves from non-inoculated or inoculated plants were photographed. **(B)** The stated lines were inoculated with *Pst* DC3000 and assayed for bacterial growth at 3 dpi. Data points represent mean ± SEM (n=6), with asterisks indicating significant difference from Col-0 (Student's *t* test,** P < 0.01, *** P < 0.0001). This experiment was repeated twice with similar results.

5.4.3 GSNOR activity is increased in *35S::FLAG-GSNOR1*, but decreased in *nox1* plants

Since the presence of the *35S::FLAG-GSNOR1* transgene increased resistance to *Pst* DC3000 and rescued *par2-1* but had no effect in *nox1* plants, the specific GSNOR activity was determined in these lines. As shown in Figure 5-10, *35S::FLAG-GSNOR1* plants have increased GSNOR activity compared to WT and as expected, *par2-1* plants have very low GSNOR activity. *35S::FLAG-GSNOR1*/*par2-*

1 plants have dramatically elevated GSNOR activity compared not only to *par2-1* but also to WT and *35S::FLAG-GSNOR1* plants. This was unexpected as although the *35S::FLAG-GSNOR1* and *35S::FLAG-GSNOR1*/*par2-1* lines result from independent transformations, they both appear to express the transgene at similar levels (Figures 5-1 and 5-2). Interestingly, GSNOR activity is decreased in *nox1* plants compared to WT. Consistent with this, GSNOR activity is decreased in *35S::FLAG-GSNOR1*/*nox1* compared with *35S::FLAG-GSNOR1* plants. This suggests that the decreased GSNOR activity in *nox1* plants is due to an effect at the protein, rather than the transcriptional level.

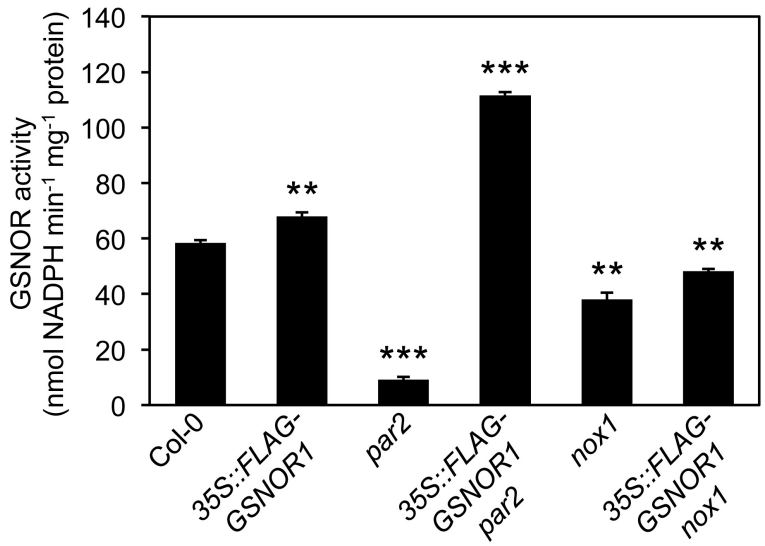

Figure 5-10 GSNOR activity of *35S::FLAG-GSNOR1* lines in various genetic backgrounds

Specific GSNOR activity was determined in protein extracts from the stated lines. Data points represent mean ± SEM (n=3), with asterisks indicating significant difference from the Col-0 sample (Student's *t* test,** $P < 0.01$, *** $P < 0.0001$).

5.5 Discussion

5.5.1 *35S::FLAG-GSNOR1* expression enhances resistance to *Pst* DC3000

After confirmation that transgenic FLAG-GSNOR1 was active *in vivo*, by rescue of the *par2-1* mutant, it was shown that *35S::FLAG-GSNOR1* plants were more resistant than WT to *Pst* DC3000 infection (Figures 5-5 and 5-9). This is consistent with a previous report that enhanced *GSNOR1* expression and GSNOR activity in *gsnor1-1* plants resulted in increased resistance against *Pst* DC3000 and upregulation of the SA-mediated defence signalling network (Feechan et al, 2005). Presumably the elevated GSNOR activity in *35S::FLAG-GSNOR1* plants is having the same effect on SA-signalling, although this was untested. It has been shown that S-nitrosylation of the transcriptional co-activator NPR1 is increased in *gsnor1-3* plants, which promotes its oligomerization in the cytoplasm. This inhibits translocation of NPR1 to the nucleus upon induction of SA-signalling and reduces the expression of NPR1-dependent defence genes (Tada et al, 2008). This molecular link between the elevated global S-nitrosylation and disease susceptibility of *gsnor1-3* mutant plants might be the same relationship linking the increased GSNOR activity to disease resistance in *35S::FLAG-GSNOR1* plants. Although global SNO levels were not measured in *35S::FLAG-GSNOR1* plants, it can be reasonably assumed that they are lower than WT since the increased GSNOR activity and enhanced disease resistance are consistent with *gsnor1-1* plants (Feechan et al 2005). Thus, perhaps S-nitrosylation of NPR1 is lessened in *35S::FLAG-GSNOR1* (and *gsnor1-1*) plants resulting in more nuclear-localized NPR1 and increased defence-gene expression.

Since overexpression of GSNOR1 in *Arabidopsis* appears to have beneficial effects in the context of disease resistance, modulating GSNOR activity might be a strategy to develop new disease resistant crop varieties. However, constitutive expression of disease resistance is often accompanied by negative fitness tradeoffs (Denance et al, 2013). Indeed, *Arabidopsis gsnor1-1* mutant plants, while showing increased disease resistance, produce less seed and have less root biomass than WT plants (Kwon et al, 2012). These traits were not analysed in *35S::FLAG-GSNOR1* plants but it is likely that they are similar to *gsnor1-1* plants.

5.5.2 *35S::FLAG-GSNOR1* expression does not rescue *nox1*

The presence of the *35S::FLAG-GSNOR1* transgene had no effect on the developmental phenotype of *nox1* plants (Figures 5-7 and 5-8). Global SNO levels are elevated in *nox1* plants (Yun et al, 2011) although the specific proteins that are more S-nitrosylated in this line are yet to be determined. As described in Chapter 1, GSNOR indirectly modulates the S-nitrosylation status of many proteins by controlling the GSNO:protein-SNO equilibrium. Since overexpression of GSNOR1 in *nox1* plants had no effect, this suggests that the pool of bioactive NO stored as GSNO does not contribute to the *nox1* phenotype. Different proteins are likely S-nitrosylated by different mechanisms, for example GSNO might directly S-nitrosylate some proteins by transnitrosylation whereas other proteins might be modified directly by free NO. A proteomic comparison of S-nitrosylated proteins in *gsnor1-3* (or *par2*-1) and *nox1* backgrounds would therefore be of great interest to identify these particular proteins with different mechanisms of S-nitrosylation.

Residues surrounding redox-active cysteines might play a role in determining the mechanisms by which NO is transferred to the modified thiol.

Interestingly, *nox1* plants showed striking susceptibility to *Pst* DC3000 (Figure 5-9). This disease susceptibility phenotype might be due to increased S-nitrosylation of proteins that have also been shown to be more S-nitrosylated in *gsnor1-3* plants, for example, NPR1. It would be expected that if this was the case, overexpression of GSNOR1 would lessen the susceptibility of *nox1* plants by indirectly reducing the level of protein SNOs. However, *35S::FLAG-GSNOR1*/*nox1* plants showed the same susceptible phenotype as *nox1*. Therefore, *nox1* plants might be more susceptible to *Pst* DC3000 infection due to effects other than elevated protein S-nitrosylation. The generation and analysis of a *gsnor1-3 nox1* double mutant would provide a useful tool to further uncover how the elevated (S)NO in these lines contributes to disease susceptibility.

5.5.3 GSNOR activity is inhibited in *nox1* plants

GSNOR activity was decreased not only in *nox1* plants compared to WT, but also in *35S::FLAG-GSNOR1*/*nox1* compared with *35S::FLAG-GSNOR1* plants. Although the *GSNOR1* gene expression was not analysed in *nox1* plants, this suggests that the decreased GSNOR activity is due to an effect at the protein level. Furthermore, GSNOR1 was not identified in a recent proteomic study, which revealed a list of 59 proteins that were differentially expressed in *nox1* plants (Hu et al, 2014). Taken together, these data suggest that both *GSNOR1* transcript and GSNOR1 protein levels are similar in WT and *nox1* plants. It is therefore possible that regulation of GSNOR1 activity by post-translational modification differs in *nox1*

and WT plants. Hypothetically, an obvious PTM that might therefore regulate GSNOR1 activity is S-nitrosylation, since *nox1* plants have elevated levels of protein-SNOs.

Chapter 6

6 Post-translational modification of GSNOR1

6.1 Background

GSNOR enzymes are highly conserved across all kingdoms and play a major role in maintaining the levels of GSNO and indirectly, protein-SNOs in bacteria, yeast, animals and plants (Liu et al, 2001; Feechan et al, 2005). Loss of GSNOR function in plants leads to compromised disease resistance and various developmental abnormalities (Feechan et al, 2005; Kwon et al, 2012), while in humans, dysregulation of GSNOR has been implicated in the etiology of pulmonary diseases, in particular, asthma (Foster et al, 2009; Que et al, 2009). Furthermore, GSNOR knockout mice show less survival after bacterial and endotoxin challenge (Liu et al, 2004) and have impaired cardiac function (Beigi et al, 2012). All of these examples demonstrate that regulation of GSNOR activity is vital to maintain normal physiological conditions in various organisms.

Data presented in the previous chapter of this thesis showed that GSNOR activity was decreased in *nox1* plants, even when GSNOR1 was constitutively expressed, suggesting that the effect is at the protein level (Figure 5-10). In collaboration with the laboratories of Dr Steven Spoel (University of Edinburgh), and Professor Ione Salgado (Universidade Estadual de Campinas, Brazil), the possibility that GSNOR is itself regulated by S-nitrosylation was tested and is presented in this chapter.

In addition, *Arabidopsis* GSNOR1 contains numerous lysine residues that could serve as potential targets for Ub or Ubl modification. Since NO was shown to

regulate SUMOylation in Chapter 3, it was hypothesised that conversely, SUMO might regulate NO-signalling by modification of GSNOR1. A link between NO and SUMOylation has previously been reported in *Arabidopsis*, as it was shown that the nitrate reductases NIA1 and NIA2 are SUMOylated by SIZ1, which dramatically increases their activity (Park et al, 2011). Mutant *siz1* plants were shown to have decreased NO production, further confirming that NO accumulation is influenced by nitrate reductase activity (Park et al, 2011). As previously discussed, GSNOR1 is a key enzyme in controlling total SNO levels in *Arabidopsis* and thus modulating its activity would provide regulatory control over global S-nitrosylation independently of NO production. Work presented in this chapter describes the production and purification of recombinant GSNOR1, and experiments designed to establish whether this enzyme is modified by SUMO both *in vitro* and *in vivo*.

6.2 GSNOR1 activity is inhibited by S-nitrosylation

Since GSNOR activity was decreased in *nox1* plants, which have increased levels of NO, it was hypothesized that NO might be directly regulating GSNOR1 through S-nitrosylation. To further test this, NO-donors were applied to protein extracts from WT plants and GSNOR activity was determined. As shown in Figure 6-1, the NO-donors, Diethylamine NONOate (DEA/NO) and Cys-NO both inhibit GSNOR activity in a dose-dependent fashion while GSH and L-cysteine have relatively little effect (Lucas Frungillo, unpublished). This suggests that the NO-donating properties of DEA/NO and Cys-NO are responsible for the inhibition of GSNOR activity.

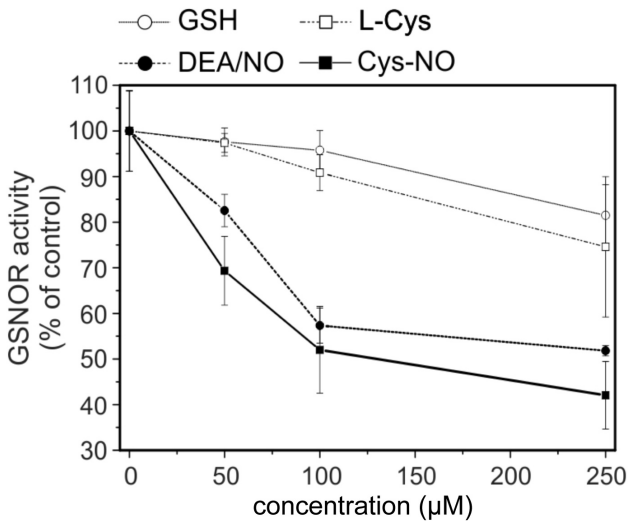

Figure 6-1 GSNOR activity is inhibited by NO-donors

Protein extracts from WT plants were incubated with the indicated compounds in the dark before these were removed by desalting. GSNOR activity was then determined and data presented as the mean ± SD (n=3).

N.B. Data shown in this figure was produced by Lucas Frungillo.

After establishing a link between NO and GSNOR1 activity, it was tested whether GSNOR1 can be S-nitrosylated *in vitro*. Protein extracts from *35S::FLAG-GSNOR1* were incubated with Cys-NO before the BST. As shown in Figure 6-2 (A), FLAG-GSNOR1 is strongly S-nitrosylated by 0.5 mM Cys-NO, and detection is completely dependent on the presence of ascorbate (Lucas Frungillo, unpublished). Since *nox1* plants have increased levels of NO and that GSNOR activity was reduced in this line, it was hypothesized that GSNOR1 might be S-nitrosylated in *nox1* plants. Indeed, *in vivo* S-nitrosylation of FLAG-GSNOR1 is readily detectable in *35S::FLAG-GSNOR1*/*nox1*, compared to *35S::FLAG-GSNOR1* plants (Figure 6-1 (B)). Taken together, this suggests that the decreased GSNOR activity observed in *nox1* plants is due to elevated S-nitrosylation of GSNOR1.

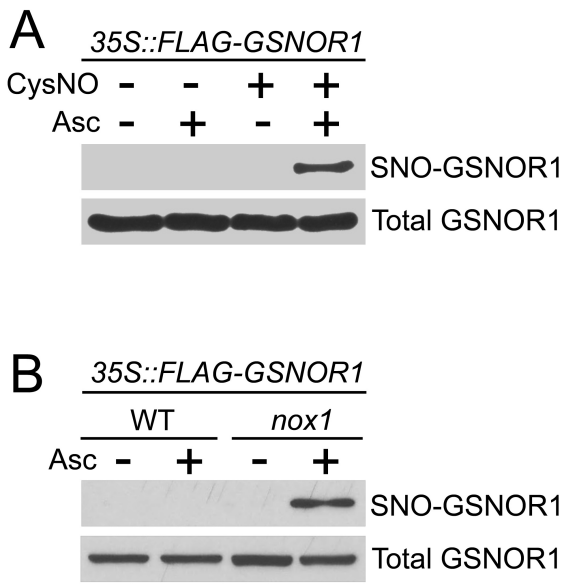

Figure 6-2 GSNOR1 is S-nitrosylated *in vitro* and *in vivo*

(A) Protein extracts from *35S::FLAG-GSNOR1* plants were subjected to the BST with or without pre-incubation with 0.5 mM CysNO. SNO-GSNOR1 and total GSNOR1 were detected by western blot against FLAG. **(B)** Protein extracts from the stated plants were subjected to the BST and GSNOR1 detected as in (A).

N.B. Data shown in part A was produced by Lucas Frungillo.

6.3 Regulation of GSNOR1 by SUMOylation

As discussed in Chapter 1, SUMOylation usually occurs at lysine residues within the consensus sequence ψKXE. The protein sequence of GSNOR1 was searched for the presence of this motif using the open access web-based software, SUMOplot. Numerous Lys residues were identified as potential SUMOylation sites with varying probabilities for modification (Figure 6-3), suggesting that GSNOR1 may indeed be a target for modification by SUMO.

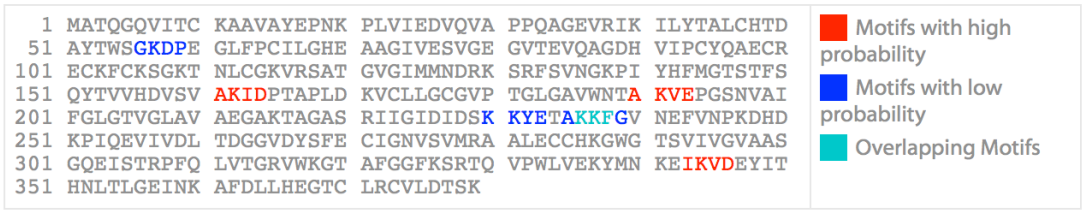

No.	Pos.	Group	Score
1	K344	YMNKE IKVD EYITH	0.94
2	K191	AVWNT AKVE PGSNV	0.79
3	K162	HDVSV AKID PTAPL	0.79
4	K57	AYTWS GKDP EGLFP	0.57

No.	Pos.	Group	Score
5	K231	IDIDS KKYE TAKKF	0.48
6	K236	KKYET AKKF GVNEF	0.44
7	K237	KYETA KKFG VNEFV	0.31

Figure 6-3 Prediction of SUMOylation sites within GSNOR1

The protein sequence of GSNOR1 was analysed with SUMOplot software (http://www.abgent.com/sumoplot) and potential SUMOylation sites are shown within the sequence and ranked by likelihood of modification below.

6.3.1 Expression and purification of GST-GSNOR1

To test whether GSNOR1 can be modified by SUMO, production of recombinant GSNOR1 with an epitope tag for detection by western blot was required. Since the SUMOylation machinery used for *in vitro* SUMOylation reactions described in Chapter 3 consists of 6xHis-tagged proteins, a different tag to allow specific detection was required. Glutathione S-transferase (GST) has successfully been used as a purification and detection method for proteins in SUMOylation assays, and although it contains 21 lysine residues, none of these conform to a consensus SUMOylation motif. A previous study showed that GST is SUMOylated at less that 1% of the levels of GST-tagged promyelocytic leukaemia protein (PML), a well-characterized mammalian SUMO substrate (Tatham et al, 2001). The coding sequence of GSNOR1 was cloned in to a bacterial expression

vector encoding an N-terminal GST-tag (See section 2.11 for details) and induction of expression was verified (Figure 6-4, left panel). Subsequently, GST-GSNOR1 was efficiently purified at the expected size of ~68 kDa (GST ≈ 26 kDa, GSNOR1 ≈ 42 kDa) (Figure 6-4, right panel).

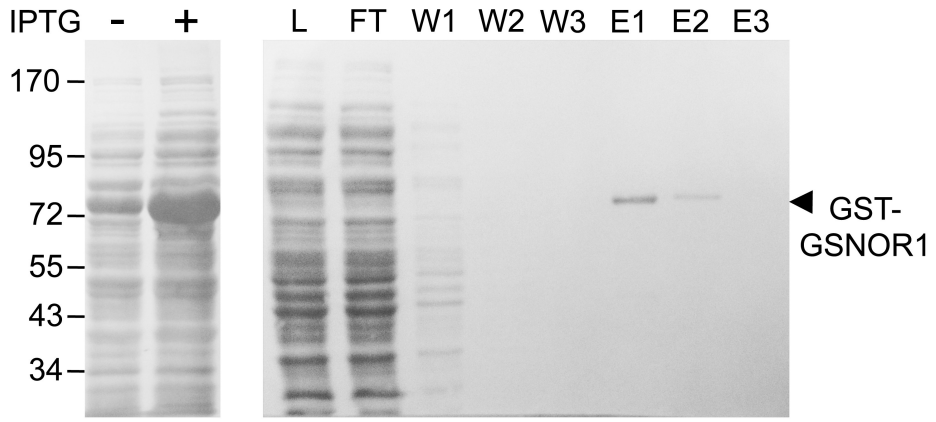

Figure 6-4 Expression and purification of GST-GSNOR1

Expression of GST-GSNOR1 was induced in *E. coli* by addition of 0.5 mM IPTG (left panel). Protein content at each step of the subsequent purification procedure was then analysed (right panel). Proteins were separated by SDS-PAGE, transferred to nitrocellulose membranes then stained with Ponceau S. L, lysate; FT, flow-through; W, wash; E, eluate.

6.3.2 GST-GSNOR1 is SUMOylated *in vitro*

After successfully producing and purifying recombinant GST-GSNOR1, this was used as a substrate in *in vitro* SUMOylation reactions. Formation of a SUMO-modified form of GST-GSNOR1 was detectable after 30 mins and increased with incubation time (Figure 6-5). Negative controls in which GST-GSNOR1, SUMO1, and ATP were omitted confirmed that this band did indeed represent SUMOylated

GST-GSNOR1. This suggests that SCE1 is capable of conjugating SUMO1 to GSNOR1 *in vitro*.

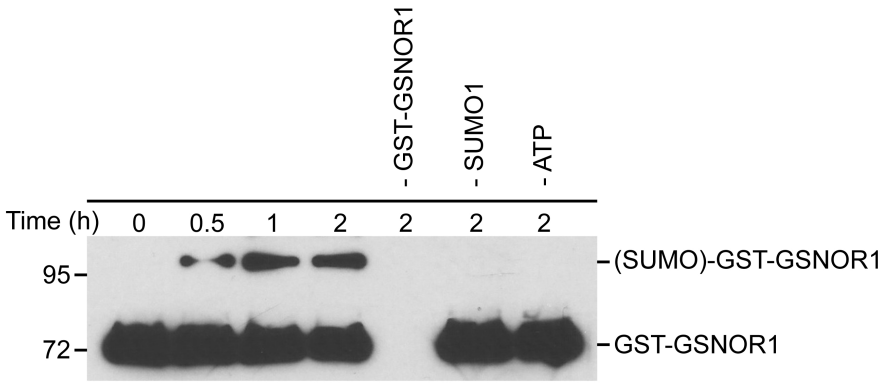

Figure 6-5 *in vitro* SUMOylation of GST-GSNOR1

GST-GSNOR1 was added to *in vitro* SUMOylation reactions and incubated at 30°C for the stated times. Negative controls were included in which the stated components were omitted. GST-GSNOR1 was detected by SDS-PAGE and western blot against GST.

6.3.3 Regulation of GSNOR1 activity by SUMOylation

To establish if SUMOylation affected GSNOR1 activity, recombinant GST-GSNOR1 was first tested for activity. Since GST is a relatively large tag it might interfere with the enzymatic activity of the enzyme. A recent study has revealed the crystal structure of tomato GSNOR (*Sl*GSNOR) (Kubienova et al, 2013), which shows high sequence similarity to *Arabidopsis* GSNOR1. Therefore it can be assumed that *Arabidopsis* GSNOR1 has a similar structure to *Sl*GSNOR. Like related alcohol dehydrogenases, *Sl*GSNOR functions as a dimer *in vivo* (Kubienova et al, 2013). The N-terminal region of *Sl*GSNOR is at a distant site to both the catalytic domain and the interface between monomers and so the presence of an N-terminal

GST-tag might not interfere with protein function. As shown in Figure 6-6 (A), GSNO-dependent NADH oxidation occurred in a linear fashion over the time course tested in the presence, but not in the absence of GST-GSNOR1. Using this assay, specific GSNOR activity was calculated, revealing that recombinant GST-GSNOR1 was highly active *in vitro* (Figure 6-6 (B)).

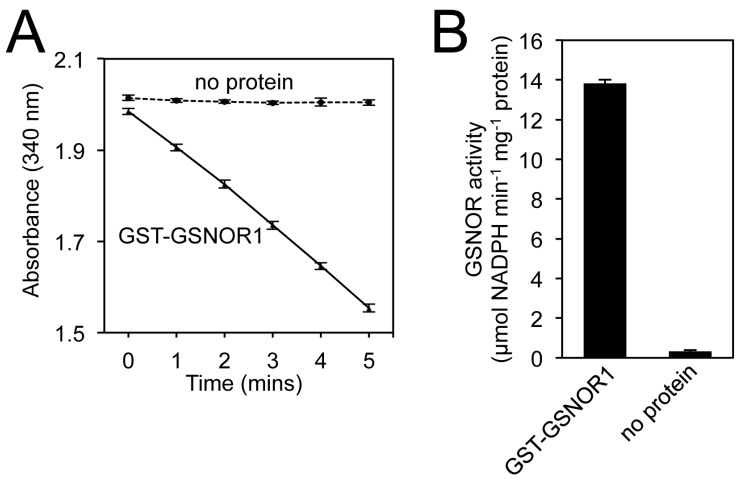

Figure 6-6 GST-GSNOR1 is active *in vitro*

(A) Rate of NADH oxidation in the presence or absence of GST-GSNOR1. **(B)** Data from (A) was used to determine specific GSNOR activity. Data points represent mean ± SEM (n=3).

After establishing that GST-GSNOR1 was active *in vitro*, it was then tested if SUMOylation affected this activity. To this end, GST-GSNOR1 was SUMOylated as previously described for 2 hours (Figure 6-5) but instead of stopping the reactions with the addition of SDS sample buffer, the reaction mixtures were passed through columns that trap small molecules and proteins with a molecular weight below 40 kDa (See section 2.19 for details). Thus, SUMO1, SCE1 and ATP are removed from

the reaction mixtures, preventing further SUMO1 conjugation. The reaction mixtures were then assayed for GSNOR activity. Strikingly, GSNOR activity was increased by ~39% in samples in which SUMO1 was conjugated to GST-GSNOR1 (Figure 6-7).

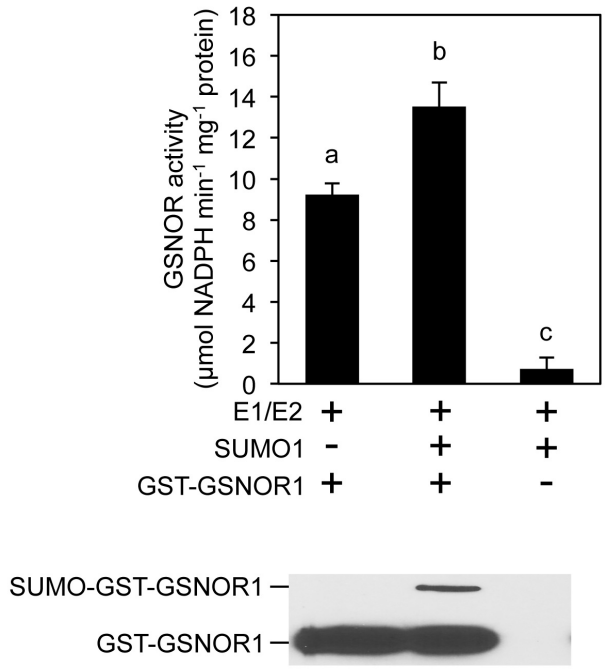

Figure 6-7 SUMOylation of GSNOR1 increases its activity *in vitro*

SUMOylation reactions with or without SUMO1 and GST-GSNOR1 were incubated for 2 hours at 30°C before being assayed for GSNOR activity. Data points represent mean ± SEM (n=3) with letters denoting statistically significant differences between samples (Student's *t* test,* $P < 0.05$). The same samples assayed for GSNOR activity were also analysed by SDS-PAGE and western blot against GST to confirm that GST-GSNOR1 was SUMOylated.

6.3.4 GSNOR1 is SUMOylated at multiple Lys residues

After uncovering a role for SUMOylation in regulating GSNOR1 activity, the next aim was to establish which Lys residue SUMO was conjugated to. A region of

mammalian Ubc9 close to its active site cysteine residue directly binds ψKXE motifs in substrates to conjugate SUMO (Bernier-Villamor et al, 2001; Lin et al, 2002; Tatham et al, 2003 (b)). Since GSNOR1 was SUMOylated *in vitro* by SCE1 without the need for an E3 ligase, it was hypothesized that the target lysine(s) would reside within a consensus ψKXE motif. Although GSNOR1 does not contain an exact SUMO consensus motif, K191 is the closest Lys conforming to this sequence (AKVE) (Figure 6-3). It has been shown that after the Lys itself, the Glu (E) residue is the second-most critical residue for SUMO conjugation (Rodriguez et al, 2001). However, the ψ is usually a large hydrophobic residue such as isoleucine, leucine or valine (Hay et al, 2005) and thus the presence of an alanine preceding K191 does not conform to this. However, it has been suggested that the ψ and X may influence the efficiency of SUMO conjugation while the K and E are strictly required in the absence of an E3 (Rodriguez et al, 2001). To determine if K191 is the site of GSNOR1 SUMOylation, this residue was mutated to an arginine and the K191R protein used as a substrate for *in vitro* SUMOylation. As shown in Figure 6-8, the K191R mutant protein is still SUMOylated but to a lesser extent that WT GST-GSNOR1 suggesting that while K191 is a target for SUMO conjugation *in vitro*, it is not the only residue that is modified.

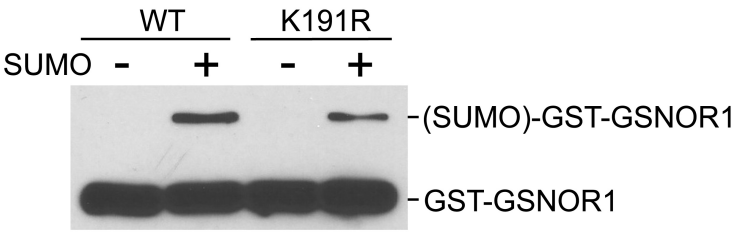

Figure 6-8 Mutation of K191 does not abolish the *in vitro* SUMOylation of GSNOR1

Either WT or K191R GST-GSNOR1 were added to *in vitro* SUMOylation reactions and incubated at 30°C for 1 hour before SDS-PAGE and western blot against GST.

6.3.5 GSNOR1 might be SUMOylated *in vivo*

After confirming that GSNOR1 is SUMOylated by SUMO1 *in vitro*, it was next tested if this is a mechanism occurring *in vivo*. To detect GSNOR1, the *35S::FLAG-GSNOR1* transgenic plants described in the previous chapter were utilized. Protein extracts from *35S::FLAG-GSNOR1* plants were immunoprecipitated using anti-FLAG antibodies to pull down GSNOR1. As shown Figure 6-9, left panel, Ponceau S staining revealed that FLAG-GSNOR1-interacting proteins are specifically pulled-down that are absent if the same immunoprecipitation is applied to WT plant extracts. Probing the immunoprecipitated proteins with anti-FLAG allows detection of FLAG-GSNOR1 and a smear of higher molecular weight proteins that could represent modified forms of FLAG-GSNOR1. Some lower molecular weight species were also detected in this western blot, perhaps representing incompletely translated FLAG-GSNOR1 (Figure 6-9, middle panel). Interestingly, probing the anti-FLAG immunoprecipitated proteins with anti-SUMO1/2 antibodies detects a smear of high molecular weight proteins that are only

detectable in extracts from *35S::FLAG-GSNOR1* plants, suggesting that they represent either SUMOylated FLAG-GSNOR1, or SUMOylated proteins that are interacting with FLAG-GSNOR1. Taken together with the fact GSNOR1 is SUMOylated *in vitro*, it is likely that this key enzyme is also regulated by SUMOylation *in vivo*.

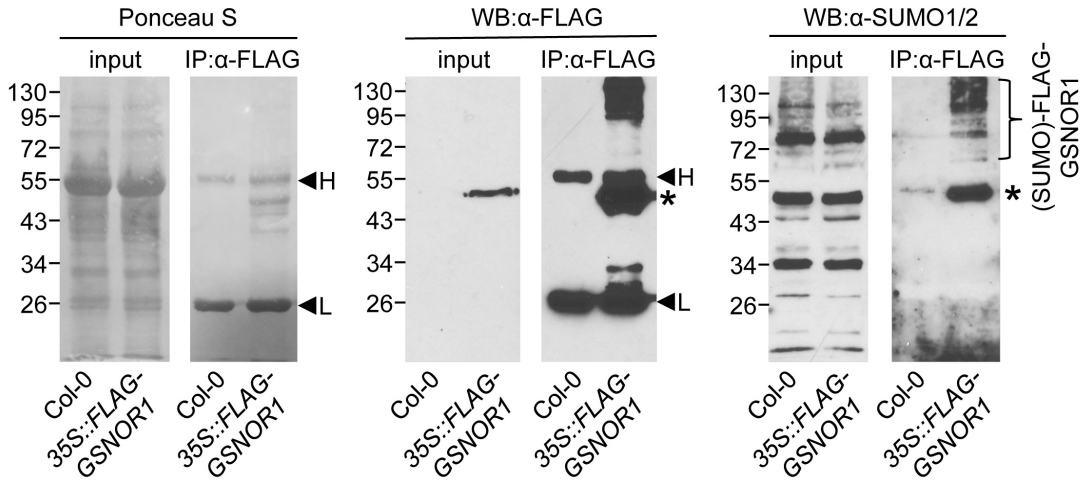

Figure 6-9 GSNOR1 might be SUMOylated *in vivo*

Protein extracts from WT or *35S::FLAG-GSNOR1* plants were subjected to FLAG immunoprecipitation before analsysis by reducing SDS-PAGE, Ponceau S staining and western blots against FLAG and SUMO1/2 as indicated. Asterisks denote FLAG-GSNOR1 while arrowheads labelled H and L denote the heavy and light chains of the anti-FLAG antibodies respectively, that were boiled with the samples after immunoprecipitation.

6.4 Discussion

6.4.1 Regulation of GSNOR1 activity by S-nitrosylation

Data presented in this thesis and work by Lucas Frungillo showed that GSNOR1 is S-nitrosylated *in vitro* and *in vivo*. Importantly, this inhibits enzyme activity as demonstrated by the pharmacological treatment of plant extracts with NO-donors and also by *nox1* plants exhibiting increased S-nitrosylation of GSNOR1 and decreased GSNOR activity (Figures 5-10, 6-1 and 6-2). Since GSNOR1 is a master regulator of GSNO and protein-SNO levels, the fact that it itself is regulated by S-nitrosylation perhaps represents a feedback mechanism by which NO controls GSNO levels. This could represent a positive feedback loop in which increasing NO levels inhibit GSNOR1 activity, leading to increased levels of bioavailable NO (GSNO). It is possible that this mechanism has evolved to increase the amplitude of NO-mediated cellular signalling. Establishing the cellular cues that lead to S-nitrosylation of GSNOR1 *in vivo* would lead to a better understanding of this regulatory mechanism.

Although numerous lines of evidence suggest that S-nitrosylation of GSNOR1 inhibits its enzymatic activity, how this occurs at the molecular level is unknown. With cysteines accounting for almost 4% of its amino acid content, this makes GSNOR1 extremely cysteine-rich in comparison with the 1.37% average cysteine content for all proteins (Xu et al, 2013). The crystal structure of *Sl*GSNOR revealed that like human GSNOR, two distinct groups of cysteine residues are involved in the coordination of zinc ions (Sanghani et al, 2002; Kubienova et al, 2013). One zinc ion is located at the active site of GSNOR1, while the other is thought to have a role in maintaining protein structure. These two distinct clusters

contain two and four cysteines respectively. S-nitrosylation of any of these cysteines could therefore directly interfere with enzymatic activity or cause inhibition by disrupting the protein structure. Alternatively, any of the other nine cysteine residues not involved in coordination of zinc ions might be targeted by S-nitrosylation. In a previous analysis of GSNOR sequences and structures, three of these cysteines were predicted to be solvent exposed (Xu et al, 2013). Furthermore, two of these are positionally conserved from humans to plants suggesting they may have important regulatory roles. In contrast to data presented in this thesis, it has been reported that S-nitrosylation of murine GSNOR increases its activity (Brown-Steinke et al, 2010). GSNOR activity was shown to be correlated to gender, with female mice exhibiting elevated GSNOR activity and increased S-nitrosylation of GSNOR compared to males. Moreover, castration of male mice increased the levels of SNO-GSNOR and increased GSNOR activity (Brown-Steinke et al, 2010). The cysteine residues that are modified by S-nitrosylation have yet to be determined in plants and animals and once identified, may reveal different mechanisms of GSNOR regulation across different species.

6.4.2 Regulation of GSNOR1 activity by SUMOylation

Data presented in this thesis showed that *Arabidopsis* GSNOR1 is SUMOylated *in vitro* and *in vivo* (Figures 6-5 and 6-9). Post-translational modification of proteins by SUMO is an essential process that has been implicated in most, if not all, important cellular processes. Proteomic analyses have revealed a vast catalogue of SUMO substrates in *Arabidopsis* and humans (Miller et al, 2010; Golebiowski, 2009), mainly located in the nucleus. However, SUMOylation of non-

nuclear proteins has been reported. *Arabidopsis* GSNOR1 is predicted to be a cytosolic enzyme (Xu et al, 2013), but human GSNOR has been reported to localize to both the cytoplasm and the nucleus (Fernandez et al, 2003). Intriguingly, the effects of SUMOylation on a target vary from protein to protein. For example, conjugation of SUMO can interfere with other PTMs, affect target localization, prevent or mediate protein-protein interactions and affect protein stability (Johnson, 2004; Hay, 2005; Miura and Hasegawa, 2010). Interestingly, SUMOylation of GSNOR1 appeared to increase its activity (Figure 6-7). However, only a small fraction of GSNOR appeared to be SUMOylated. How then does this have such a dramatic effect on the activity of GSNOR1? This phenomenon by which only a small proportion of the available target requires modification to have maximal effect is also known as the "SUMO enigma" and occurs *in vivo* (Wilkinson and Henley, 2010; Hay, 2005). The presence of a number of active SUMO proteases *in vivo* and the dynamic nature of SUMOylation/deSUMOylation can explain why only small amounts of a given protein can be detected in their SUMO-modified form at a particular time. However, this does not explain the increased GSNOR1 activity after SUMOylation observed in Figure 6-7. Since this experiment was carried out completely *in vitro* using purified recombinant proteins, it suggests that conjugation of SUMO1 to GSNOR1 is having a direct effect on its enzymatic activity.

Identification of the site(s) of SUMOylation would provide clues as to how modification of GSNOR1 leads to its increased activity. K191 was predicted to be a SUMOylation site and although mutation of this residue decreased SUMOylation, it did not completely abrogate it (Figure 6-8), suggesting that more than one lysine is modified. Two other lysines were identified as potential SUMOylation sites (K162

and K344) (Figure 6-3), although these were not mutated in the work presented in this thesis. Surface analysis of the dimeric *Sl*GSNOR reveals that K162, K191 and K344 are all located on the protein surface and are likely solvent exposed and accessible for modification (Figure 6-10). Importantly, all three of these lysines are conserved in human, tomato and *Arabidopsis* GSNOR enzymes (Kubienova et al, 2013), suggesting that they may have an important functional role. Determining which residues are SUMOylated would provide novel insights into how the activity of GSNOR is regulated and may provide new strategies to modulate the activity of this enzyme in therapeutic or plant engineering technologies.

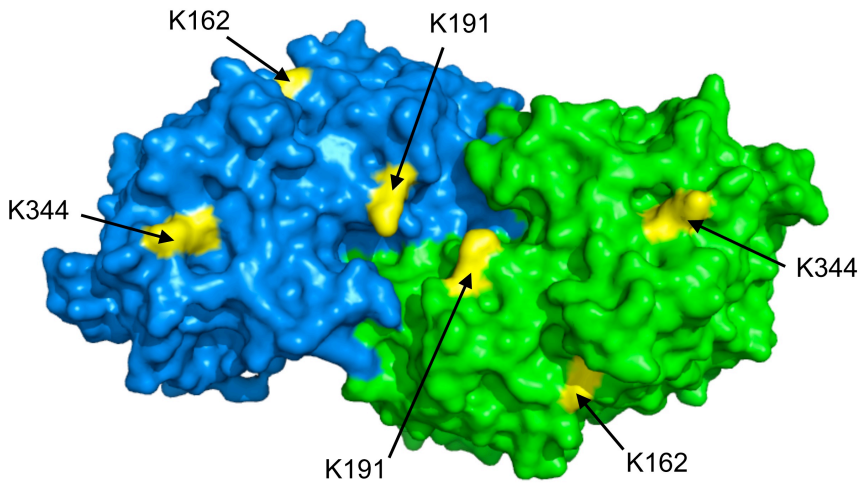

Figure 6-10 Surface locations of potential GSNOR SUMOylation sites

Surface representation of the dimeric crystal structure of *Sl*GSNOR, with each monomer coloured in blue or green. Locations of the stated lysines are shown in yellow.

Chapter 7

7 General Discussion

7.1 Interplay between S-nitrosylation and SUMOylation in plant immunity – a role for SA?

Data presented in Chapter 3 showed that after *Pst* DC3000 infection, SCE1 is S-nitrosylated, and perhaps further oxidized at Cys139. This cysteine has not been assigned a functional role in any species, yet shows high conservation among eukaryotes (Figure 3-2). Mutation of Cys139 did not affect the activity of SCE1, but did render it insensitive to inhibition by S-nitrosylation *in vitro* (Figure 3-4). The effect of mutating Cys139 *in vivo* was revealed by the generation of *35S::FLAG-SCE1-C139S* plants, which were more susceptible to *Pst* DC3000, showed delayed *PR-1* induction, and had elevated levels of SUMO conjugates after pathogen infection when compared to WT plants and transgenic controls (Figures 3-19, 3-20, 3-21 and 3-22). This suggests that SCE1 is a key regulator of SUMOylation after immune activation. However, as discussed in section 4.5.2, it is unknown whether SUMO E2 enzymes function *in vivo* independently of E3 ligase activity. Data presented in Chapter 4 suggested that SIZ1 activity is required for overexpression of SCE1 to increase global SUMOylation (Figure 4-4), at least in the context of heat stress. As discussed previously, SIZ1 appears to play a central role in plant immunity (Lee et al, 2007). However, no reports on how SIZ1 activity might be regulated after immune activation currently exist. It is likely that SIZ1 could also be a target for S-nitrosylation, as it contains 21 cysteine residues, while the other SUMO E3, HPY2

contains seven. Therefore NO-mediated regulation of SUMOylation might occur at multiple levels.

The means by which SUMOylation inhibits SA-mediated plant immunity remains a mystery. Loss of SIZ1 function results in elevated SA levels, constitutive activation of *PR* gene expression and increased resistance to *Pst* DC3000 (Lee et al, 2007). These phenotypes were reverted back to WT by expression of the bacterial salicylate hydroxylase NahG, which degrades SA, suggesting that the phenotypes of *siz1* mutant plants are due to the elevated levels of SA (Lee et al, 2007). The reduced *PR-1* expression observed in *35S::FLAG-SCE1-C139S* plants (Figure 3-21) is then perhaps explained by these plants possessing lower levels of SA. This is purely speculative, as SA levels were not determined in any of the work presented in this thesis. It is unknown why *siz1* plants accumulate high levels of SA, although possible targets upstream of SA synthesis that contain SUMOylation motifs include ENHANCED DISEASE SUSCEPTIBILITY 1 (EDS1), PHYTOALEXIN DEFICIENT 4 (PAD4), and SENESCENCE ASSOCIATED GENE 1 (SAG101) (Lee et al, 2007). These three proteins are thought to form a complex that constitutes a regulatory hub for immune signalling, required for the accumulation of SA (reviewed in Wiermer et al, 2005). Perhaps SUMOylation of any of these proteins inhibits their positive regulation of SA signalling, and loss of SIZ1 function abolishes this inhibition. Interestingly, it has been shown that translocation of EDS1 from the cytoplasm to the nucleus is required for resistance to avirulent *Pst* DC3000 and that this might be controlled by post-transcriptional regulation (García et al, 2010). SUMOylation has long been associated with nucleocytoplasmic transport in mammals and yeast (Geiss-Friedlander and Melchior, 2007; Palancade and Doye,

2008), and is likely to play a similar role in plants. Therefore, perhaps SUMOylation of EDS1 is involved in regulating its subcellular localization. The bulk of SA synthesis in plants is thought to take place in chloroplasts (Vlot et al, 2009), which might make it unlikely that SA biosynthetic enzymes would be directly modified by SUMO. However, SUMOylation of chloroplastic proteins in *Arabidopsis* has been reported (Elrouby and Coupland, 2010) so screening of enzymes involved in SA biosynthesis for SUMOylation motifs might provide insight into the molecular links between SUMOylation and inhibition of SA signalling. It was suggested that because no changes in SUMOylation levels were observed after pathogen challenge, SIZ1 might influence plant immunity in a SUMOylation-independent manner (Lee et al, 2007). However, data presented in this thesis suggests negative regulation of plant immunity does result from SUMOylation, because global SUMO conjugate levels are dramatically increased after pathogen infection in *35S::FLAG-SCE1-C139S* plants (Figure 3-22). Introducing the *35S::FLAG-SCE1-C139S* transgene into *siz1* mutant plants might therefore be informative in establishing if SIZ1 negatively regulates SA-mediated immunity in a SUMO-dependent manner.

Interestingly, S-nitrosylation has also been shown to regulate SA signalling networks, with loss of GSNOR1 function resulting in decreased SA levels and delayed activation of *PR-1* expression after *Pst* DC3000 infection (Feechan et al, 2005). Consistent with this, SA levels are also reduced in *nox1* plants (Yun et al, 2011). GSNOR1 also appears to regulate SA-signalling alongside or downstream of SA, since *PR-1* expression in response to exogenous application of SA was delayed in *gsnor1* mutant plants (Feechan et al, 2005), and further work showed that excessive S-nitrosylation of NPR1 blunted its transcription cofactor activity in

gsnor1-3 mutant plants (Tada et al, 2008). It is possible that proteins upstream of SA biosynthesis are inhibited by S-nitrosylation, either directly or indirectly. This raises a potential paradox, by which SUMOylation and S-nitrosylation both inhibit SA synthesis and its downstream signalling, but S-nitrosylation inhibits SUMOylation after immune activation. Crosstalk between these two PTMs might therefore facilitate fine-tuning of defence responses after immune activation (Figure 7-1). Proteomic screens to identify proteins that are modified by both SUMOylation and S-nitrosylation after immune activation would be informative and might identify further regulatory networks that facilitate crosstalk between the two PTMs. Data presented in Chapter 6 revealed that GSNOR1 is both S-nitrosylated and SUMOylated. However, it is unknown if this has any relevance in the context of plant immunity. Since GSNOR1 plays such a central role in plant immunity (Feechan et al, 2005; Malik et al, 2011), tight regulation of its activity is probably required in order to efficiently execute defence responses. Therefore it is likely that GSNOR1 is subject to PTMs after immune activation but this remains to be determined.

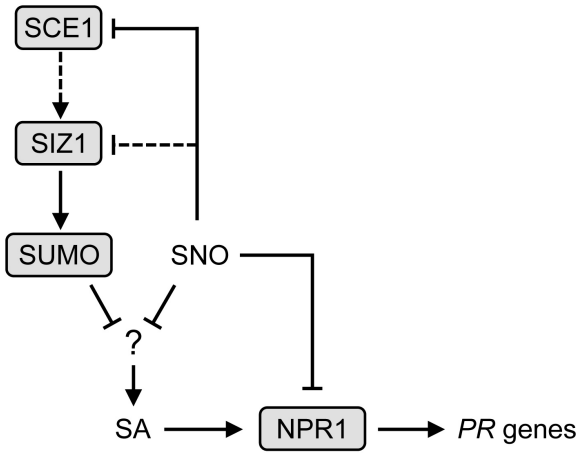

Figure 7-1 A model for interplay between S-nitrosylation and SUMOylation in SA-mediated immune signalling

SUMOylation and S-nitrosylation both appear to negatively regulate SA accumulation by unknown mechanisms. S-nitrosylation of SCE1 inhibits its activity and relieves SUMO-mediated suppression of SA-mediated immune signalling. SIZ1 might also be a target for S-nitrosylation in plant immunity. Elevated S-nitrosylation of NPR1 in *gsnor1* plants has been shown to promote its oligomerization and inhibit its transcription coactivator activity (Tada et al, 2008). Dashed lines represent hypothetical effects discussed in this chapter while solid lines represent effects previously reported or demonstrated by experimental evidence in this thesis.

7.2 SUMOylation might regulate NO synthesis and bioavailablity

Much of the work presented in this thesis focused on the regulation of SUMOylation by S-nitrosylation of SCE1 during plant immunity. Reciprocal to this, crosstalk by which SUMOylation might regulate S-nitrosylation was revealed by the identification of GSNOR1 as a substrate for SUMOylation. Interestingly, the activity of GSNOR1 was increased by SUMOylation *in vitro* (Figure 6-7). If this is also the case *in vivo*, it would be expected that SUMOylation of GSNOR1 would increase

turnover of GSNO and reduce the levels of protein SNOs. Therefore, SUMOylation might lead to decreased levels of bioactive NO. Intriguingly, it was previously shown that SIZ1-dependent SUMOylation of the nitrate reductases NIA1 and NIA2 increased their NO production (Park et al, 2011). Thus, the effect of SUMOylation might lead to opposite effects on NO-mediated signalling depending on the targeting of either GSNOR1 or NIA1/2. This is a speculative theory since it is unknown if SUMOylation of GSNOR1 has a biological function *in vivo*. Furthermore, although GSNO appears to act as a naturally occurring NO donor, signalling pathways mediated by GSNO might differ from those mediated by free NO.

7.3 Differential effects of GSNO and NO accumulation

It is well established that loss-of-function *gsnor1* mutants accumulate high levels of protein SNOs. The levels of SNOs in *nox1* plants were previously shown to accumulate to similar levels as those observed in *gsnor1-3* plants (Yun et al, 2011). Work presented in this thesis suggests that overexpression of GSNOR1 does not alleviate any phenotypes of *nox1* plants (Chapter 5). Since NO spontaneously reacts with GSH to form GSNO, it might be expected that the high levels of NO in *nox1* plants would result in increased GSNO levels. The fact that GSNOR overexpression did not affect *nox1* plants in the contexts of development and immunity suggests that high GSNO levels do not contribute to these phenotypes. It is possible then, that GSH levels are decreased in *nox1* plants, which may limit the amount of GSNO that can be formed. Determination of both GSH and GSNO levels in *nox1* plants would provide more understanding of the complexities of the balance between NO, GSH, GSNO and protein SNOs. Another possible reason that GSNOR overexpression did

not alleviate any of the phenotypes of *nox1* is because the transgenic GSNOR1 is S-nitrosylated in this mutant background (Figure 6-2 (B)). However, GSNOR activity was still increased by GSNOR1 overexpression in *nox1* plants (Figure 5-10). Furthermore, the developmental phenotypes of *gsnor1-3*/*par2-1* and *nox1* mutant plants are distinct (Kwon et al, 2012; He et al, 2004), suggesting that the accumulation of GSNO and NO impact plant development differentially.

As previously mentioned, some protein thiols might be substrates for transnitrosylation by GSNO but not for direct S-nitrosylation by free NO. Indeed, a motif has been suggested that might promote GSNO-mediated transnitrosylation in which the amine of GSNO and the carboxylate from either an aspartic acid or glutamic acid residue close to the modified cysteine engage in hydrogen bonding. This places the NO group of GSNO close to the cysteine thiol, promoting transnitrosylation (Kim et al, 2002; Hess et al, 2005). A potential example of a protein that might be S-nitrosylated by free NO but not by GSNO is GSNOR1. Since GSNO is a substrate for this enzyme, it is unlikely that transnitrosylation would occur in this instance. It would be expected that if GSNOR1 was in close proximity to GSNO within the cell, it would recognize it as an enzyme substrate and process it, rather than be subjected to transnitrosylation. Perhaps local GSNO concentrations govern the S-nitrosylation of GSNOR1 but this would be extremely difficult to study unless an inactive form of GSNOR1 was generated that could be S-nitrosylated by GSNO, but did not possess any enzymatic GSNOR activity. It is likely that many proteins can be S-nitrosylated by both GSNO and free NO, such as *Arabidopsis* RBOHD, which appears to be subjected to elevated S-nitrosylation in both *gsnor1-3* and *nox1* mutant plants (Yun et al, 2011). *Arabidopsis* SCE1 was identified as a

novel target for *in vivo* S-nitrosylation in this thesis, but it was not determined whether this is mediated by GSNO, free NO, or both. No notable differences in the SUMOylation patterns between the *gsnor1-3* mutant and WT seedlings were observed in a heat shock assay (Figure 3-23 (A)), but surprisingly, SUMOylation in *nox1* plants appeared to be increased compared to WT in a similar assay (Figure 3-23 (B)). S-nitrosylation of SCE1 was not determined in *gsnor1-3* or *nox1* plants because the *35S::FLAG-SCE1* transgene was not introduced into these mutant backgrounds, and detection of S-nitrosylation of endogenous SCE1 had already proved difficult using antibodies against SCE1, even after addition of GSNO to plant extracts (Figure 3-8 (B)). Proteomic analysis of S-nitrosylated proteins in *gsnor1-3* and *nox1* plants would provide clues as to what the determinants are for S-nitrosylation by either GSNO or NO. With recent advances in the proteomic analyses of mammalian S-nitrosylation (Wiktorowicz et al, 2011; Doulias et al, 2013), these techniques can be adapted and utilised in plants to answer these questions.

7.4 Conclusions, impact and future directions

As outlined above, work presented in this thesis has uncovered several novel mechanisms that regulate important PTMs. These findings are summarized as four key points below:

(1) S-nitrosylation of SCE1 at Cys139 was shown to provide a molecular link between the nitrosative burst and activation of *PR-1* expression after *Pst* DC3000 challenge.

(2) Overexpression of SCE1 can increase global SUMOylation in *Arabidopsis* and potentially be used to engineer stress tolerance in plants.

(3) GSNO and NO accumulation affect plants differentially and overexpression of GSNOR1 in *Arabidopsis* does not alleviate *nox1* mutant phenotypes.

(4) GSNOR1 activity is regulated by both S-nitrosylation and SUMOylation.

All four of the above points can have far reaching impact, not only in the context of plant immunity, but also in the fields of medicine and biotechnology. For example, points (1) and (4) may provide clues as to how the activities of Ubc9 and GSNOR are regulated in mammals. Since both of these enzymes, and the PTMs that they regulate have been implicated in many human diseases, designing drugs that interfere with or exploit regulatory mechanisms uncovered in this thesis might provide novel therapeutic strategies. First, it will need to be determined if these mechanisms occur in other species, but high conservation of residues that are likely to be modified by the PTMs discussed in this thesis make this likely. Point (2) could be exploited in the genetic engineering of plants to introduce stress resistance, although further characterization of *35::FLAG-SCE1 Arabidopsis* plants will be required to establish if any negative traits result from this transgene and to test resistance to other biotic and abiotic stresses. Points (1), (3), and (4) all provide new evidence of regulatory crosstalk between essential PTMs that coordinate immune responses, development and growth of plants. Future work to identify further targets, and the subcellular locations where interplay between S-nitrosylation and SUMOylation occurs will likely identify new key players in plant immunity and facilitate new research and development in to the engineering and/or breeding of disease resistance in crops.

Bibliography

Alonso, J.M. (2003). Genome-wide insertional mutagenesis of Arabidopsis thaliana (vol 301, pg 653, 2003). Science 301, 1849-1849.

Alontaga, A.Y., Bobkova, E., and Chen, Y. (2012). Biochemical analysis of protein SUMOylation. Current protocols in molecular biology / edited by Frederick M Ausubel [et al] Chapter 10, Unit10.29.

Belenghi, B., Romero-Puertas, M.C., Vercammen, D., Brackenier, A., Inzé, D., Delledonne, M., and Van Breusegem, F. (2007). Metacaspase activity of Arabidopsis thaliana is regulated by S-nitrosylation of a critical cysteine residue. J Biol Chem 282, 1352-1358.

Bencsath, K.P., Podgorski, M.S., Pagala, V.R., Slaughter, C.A., and Schulman, B.A. (2002). Identification of a multifunctional binding site on Ubc9p required for Smt3p conjugation. J Biol Chem 277, 47938-47945.

Benhar, M., Forrester, M.T., Hess, D.T., and Stamler, J.S. (2008). Regulated protein denitrosylation by cytosolic and mitochondrial thioredoxins. Science 320, 1050-1054.

Benhar, M., Thompson, J.W., Moseley, M.A., and Stamler, J.S. (2010). Identification of S-nitrosylated targets of thioredoxin using a quantitative proteomic approach. Biochemistry 49, 6963-6969.

Bernier-Villamor, V., Sampson, D.A., Matunis, M.J., and Lima, C.D. (2002). Structural basis for E2-mediated SUMO conjugation revealed by a complex between ubiquitin-conjugating enzyme Ubc9 and RanGAP1. Cell 108, 345-356.

Boggio, R., Colombo, R., Hay, R.T., Draetta, G.F., and Chiocca, S. (2004). A mechanism for inhibiting the SUMO pathway. Mol Cell 16, 549-561.

Boggio, R., Passafaro, A., and Chiocca, S. (2007). Targeting SUMO E1 to ubiquitin ligases: a viral strategy to counteract sumoylation. J Biol Chem 282, 15376-15382.

Bonfoco, E., Krainc, D., Ankarcrona, M., Nicotera, P., and Lipton, S.A. (1995). Apoptosis and necrosis: two distinct events induced, respectively, by mild and intense insults with N-methyl-D-aspartate or nitric oxide/superoxide in cortical cell cultures. Proc Natl Acad Sci U S A 92, 7162-7166.

Bossis, G., and Melchior, F. (2006a). Regulation of SUMOylation by reversible oxidation of SUMO conjugating enzymes. Mol Cell 21, 349-357.

Bossis, G., and Melchior, F. (2006b). SUMO: regulating the regulator. Cell Div 1, 13.

Bradford, M.M. (1976). A rapid and sensitive method for the quantitation of microgram quantities of protein utilizing the principle of protein-dye binding. Anal Biochem 72, 248-254.

Broniowska, K.A., Diers, A.R., and Hogg, N. (2013). S-nitrosoglutathione. Biochim Biophys Acta 1830, 3173-3181.

Brown-Steinke, K., deRonde, K., Yemen, S., and Palmer, L.A. (2010). Gender differences in S-nitrosoglutathione reductase activity in the lung. PLoS One 5, e14007.

Budhiraja, R., Hermkes, R., Müller, S., Schmidt, J., Colby, T., Panigrahi, K., Coupland, G., and Bachmair, A. (2009). Substrates related to chromatin and to RNA-dependent processes are modified by Arabidopsis SUMO isoforms that differ in a conserved residue with influence on desumoylation. Plant Physiol 149, 1529-1540.

Cabello, J.V., Lodeyro, A.F., and Zurbriggen, M.D. (2014). Novel perspectives for the engineering of abiotic stress tolerance in plants. Curr Opin Biotechnol 26C, 62-70.

Capili, A.D., and Lima, C.D. (2007). Structure and analysis of a complex between SUMO and Ubc9 illustrates features of a conserved E2-Ubl interaction. J Mol Biol 369, 608-618.

Carbia-Nagashima, A., Gerez, J., Perez-Castro, C., Paez-Pereda, M., Silberstein, S., Stalla, G.K., Holsboer, F., and Arzt, E. (2007). RSUME, a small RWD-containing protein, enhances SUMO conjugation and stabilizes HIF-1alpha during hypoxia. Cell 131, 309-323.

Castillo, A.G., Kong, L.J., Hanley-Bowdoin, L., and Bejarano, E.R. (2004). Interaction between a geminivirus replication protein and the plant sumoylation system. J Virol 78, 2758-2769.

Chen, R., Sun, S., Wang, C., Li, Y., Liang, Y., An, F., Li, C., Dong, H., Yang, X., Zhang, J., et al. (2009). The Arabidopsis PARAQUAT RESISTANT2 gene encodes

an S-nitrosoglutathione reductase that is a key regulator of cell death. Cell Res 19, 1377-1387.
Cheong, M.S., Park, H.C., Hong, M.J., Lee, J., Choi, W., Jin, J.B., Bohnert, H.J., Lee, S.Y., Bressan, R.A., and Yun, D.J. (2009). Specific domain structures control abscisic acid-, salicylic acid-, and stress-mediated SIZ1 phenotypes. Plant Physiol 151, 1930-1942.

Chosed, R., Mukherjee, S., Lois, L.M., and Orth, K. (2006). Evolution of a signalling system that incorporates both redundancy and diversity: Arabidopsis SUMOylation. Biochem J 398, 521-529.

Clough, S.J., and Bent, A.F. (1998). Floral dip: a simplified method for Agrobacterium-mediated transformation of Arabidopsis thaliana. Plant J 16, 735-743.

Colby, T., Matthaei, A., Boeckelmann, A., and Stuible, H.-P. (2006). SUMO-conjugating and SUMO-deconjugating enzymes from Arabidopsis. Plant Physiology 142, 318-332.

Cueto, M., Hernández-Perera, O., Martín, R., Bentura, M.L., Rodrigo, J., Lamas, S., and Golvano, M.P. (1996). Presence of nitric oxide synthase activity in roots and nodules of Lupinus albus. FEBS Lett 398, 159-164.

Dangl, J.L., Dietrich, R.A., and Richberg, M.H. (1996). Death Don't Have No Mercy: Cell Death Programs in Plant-Microbe Interactions. Plant Cell 8, 1793-1807.

Delledonne, M., Xia, Y., Dixon, R.A., and Lamb, C. (1998). Nitric oxide functions as a signal in plant disease resistance. Nature 394, 585-588.

Delledonne, M., Zeier, J., Marocco, A., and Lamb, C. (2001). Signal interactions between nitric oxide and reactive oxygen intermediates in the plant hypersensitive disease resistance response. Proc Natl Acad Sci U S A 98, 13454-13459.

Denancé, N., Sánchez-Vallet, A., Goffner, D., and Molina, A. (2013). Disease resistance or growth: the role of plant hormones in balancing immune responses and fitness costs. Front Plant Sci 4, 155.

Després, C., Chubak, C., Rochon, A., Clark, R., Bethune, T., Desveaux, D., and Fobert, P.R. (2003). The Arabidopsis NPR1 disease resistance protein is a novel cofactor that confers redox regulation of DNA binding activity to the basic domain/leucine zipper transcription factor TGA1. Plant Cell 15, 2181-2191.

Desterro, J.M., Rodriguez, M.S., Kemp, G.D., and Hay, R.T. (1999). Identification of the enzyme required for activation of the small ubiquitin-like protein SUMO-1. J Biol Chem 274, 10618-10624.

Deyrieux, A.F., Rosas-Acosta, G., Ozbun, M.A., and Wilson, V.G. (2007). Sumoylation dynamics during keratinocyte differentiation. J Cell Sci 120, 125-136.
Doulias, P.T., Tenopoulou, M., Raju, K., Spruce, L.A., Seeholzer, S.H., and Ischiropoulos, H. (2013). Site specific identification of endogenous S-nitrosocysteine proteomes. J Proteomics 92, 195-203.

Durner, J., Wendehenne, D., and Klessig, D.F. (1998). Defense gene induction in tobacco by nitric oxide, cyclic GMP, and cyclic ADP-ribose. Proc Natl Acad Sci U S A 95, 10328-10333.

Durrant, W.E., and Dong, X. (2004). Systemic acquired resistance. Annu Rev Phytopathol 42, 185-209.

Dye, B.T., and Schulman, B.A. (2007). Structural mechanisms underlying posttranslational modification by ubiquitin-like proteins. Annu Rev Biophys Biomol Struct 36, 131-150.

Earley, K., Haag, J., Pontes, O., Opper, K., Juehne, T., Song, K., and Pikaard, C. (2006). Gateway-compatible vectors for plant functional genomics and proteomics. Plant Journal 45, 616-629.

Einhauer, A., and Jungbauer, A. (2001). The FLAG peptide, a versatile fusion tag for the purification of recombinant proteins. J Biochem Biophys Methods 49, 455-465.

Elrouby, N., and Coupland, G. (2010). Proteome-wide screens for small ubiquitin-like modifier (SUMO) substrates identify Arabidopsis proteins implicated in diverse biological processes. Proc Natl Acad Sci U S A 107, 17415-17420.

Fares, A., Rossignol, M., and Peltier, J.B. (2011). Proteomics investigation of endogenous S-nitrosylation in Arabidopsis. Biochem Biophys Res Commun 416, 331-336.

Feechan, A., Kwon, E., Yun, B.W., Wang, Y., Pallas, J.A., and Loake, G.J. (2005). A central role for S-nitrosothiols in plant disease resistance. Proc Natl Acad Sci U S A 102, 8054-8059.

Fernández, M.R., Biosca, J.A., and Parés, X. (2003). S-nitrosoglutathione reductase activity of human and yeast glutathione-dependent formaldehyde dehydrogenase and its nuclear and cytoplasmic localisation. Cell Mol Life Sci 60, 1013-1018.

Flor, H.H. (1971). Current status of the gene-for-gene concept. Annu. Rev. Phytopathol. 9: 275-296.
Foresi, N., Correa-Aragunde, N., Parisi, G., Caló, G., Salerno, G., and Lamattina, L. (2010). Characterization of a nitric oxide synthase from the plant kingdom: NO generation from the green alga Ostreococcus tauri is light irradiance and growth phase dependent. Plant Cell 22, 3816-3830.

Forrester, M.T., Foster, M.W., Benhar, M., and Stamler, J.S. (2009). Detection of protein S-nitrosylation with the biotin-switch technique. Free Radical Biology and Medicine 46, 119-126.

Foster, M.W., Hess, D.T., and Stamler, J.S. (2009). Protein S-nitrosylation in health and disease: a current perspective. Trends Mol Med 15, 391-404.

Frederickson Matika, D.E., and Loake, G.J. (2014). Redox Regulation in Plant Immune Function. Antioxid Redox Signal.

Fröhlich, A., and Durner, J. (2011). The hunt for plant nitric oxide synthase (NOS): is one really needed? Plant Sci 181, 401-404.

Fu, Z.Q., and Dong, X. (2013). Systemic acquired resistance: turning local infection into global defense. Annu Rev Plant Biol 64, 839-863.

Fukuda, I., Ito, A., Hirai, G., Nishimura, S., Kawasaki, H., Saitoh, H., Kimura, K., Sodeoka, M., and Yoshida, M. (2009). Ginkgolic acid inhibits protein SUMOylation by blocking formation of the E1-SUMO intermediate. Chem Biol 16, 133-140.

Garcia-Dominguez, M., March-Diaz, R., and Reyes, J.C. (2008). The PHD domain of plant PIAS proteins mediates sumoylation of bromodomain GTE proteins. J Biol Chem 283, 21469-21477.

García, A.V., Blanvillain-Baufumé, S., Huibers, R.P., Wiermer, M., Li, G., Gobbato, E., Rietz, S., and Parker, J.E. (2010). Balanced nuclear and cytoplasmic activities of EDS1 are required for a complete plant innate immune response. PLoS Pathog 6, e1000970.

Geiss-Friedlander, R., and Melchior, F. (2007). Concepts in sumoylation: a decade on. Nat Rev Mol Cell Biol 8, 947-956.

Goldstein, G., Scheid, M., Hammerling, U., Schlesinger, D.H., Niall, H.D., and Boyse, E.A. (1975). Isolation of a polypeptide that has lymphocyte-differentiating properties and is probably represented universally in living cells. Proc Natl Acad Sci U S A 72, 11-15.

Golebiowski, F., Matic, I., Tatham, M.H., Cole, C., Yin, Y., Nakamura, A., Cox, J., Barton, G.J., Mann, M., and Hay, R.T. (2009). System-wide changes to SUMO modifications in response to heat shock. Sci Signal 2, ra24.

Han, S., and Kim, D. (2006). AtRTPrimer: database for Arabidopsis genome-wide homogeneous and specific RT-PCR primer-pairs. BMC Bioinformatics 7, 179.

Hanania, U., Furman-Matarasso, N., Ron, M., and Avni, A. (1999). Isolation of a novel SUMO protein from tomato that suppresses EIX-induced cell death. Plant J 19, 533-541.

Hanley-Bowdoin, L., Bejarano, E.R., Robertson, D., and Mansoor, S. (2013). Geminiviruses: masters at redirecting and reprogramming plant processes. Nat Rev Microbiol 11, 777-788.

Hay, R.T. (2005). SUMO: a history of modification. Mol Cell 18, 1-12.

He, Y., Tang, R.H., Hao, Y., Stevens, R.D., Cook, C.W., Ahn, S.M., Jing, L., Yang, Z., Chen, L., Guo, F., et al. (2004). Nitric oxide represses the Arabidopsis floral transition. Science 305, 1968-1971.

Heaton, P.R., Deyrieux, A.F., Bian, X.L., and Wilson, V.G. (2011). HPV E6 proteins target Ubc9, the SUMO conjugating enzyme. Virus Res 158, 199-208.

Hermkes, R., Fu, Y.F., Nürrenberg, K., Budhiraja, R., Schmelzer, E., Elrouby, N., Dohmen, R.J., Bachmair, A., and Coupland, G. (2011) Distinct roles for Arabidopsis SUMO protease ESD4 and its closest homolog ELS1. Planta 233, 63-73.

Hess, D.T., Matsumoto, A., Kim, S.O., Marshall, H.E., and Stamler, J.S. (2005). Protein S-nitrosylation: purview and parameters. Nat Rev Mol Cell Biol 6, 150-166.

Hietakangas, V., Anckar, J., Blomster, H.A., Fujimoto, M., Palvimo, J.J., Nakai, A., and Sistonen, L. (2006). PDSM, a motif for phosphorylation-dependent SUMO modification. Proc Natl Acad Sci U S A 103, 45-50.

Hochstrasser, M. (2009). Origin and function of ubiquitin-like proteins. Nature 458, 422-429.

Horchani, F., Prévot, M., Boscari, A., Evangelisti, E., Meilhoc, E., Bruand, C., Raymond, P., Boncompagni, E., Aschi-Smiti, S., Puppo, A., et al. (2011). Both plant and bacterial nitrate reductases contribute to nitric oxide production in Medicago truncatula nitrogen-fixing nodules. Plant Physiol 155, 1023-1036.

Hotson, A., Chosed, R., Shu, H., Orth, K., and Mudgett, M.B. (2003). Xanthomonas type III effector XopD targets SUMO-conjugated proteins in planta. Mol Microbiol 50, 377-389.

Hsieh, Y.L., Kuo, H.Y., Chang, C.C., Naik, M.T., Liao, P.H., Ho, C.C., Huang, T.C., Jeng, J.C., Hsu, P.H., Tsai, M.D., et al. (2013). Ubc9 acetylation modulates distinct SUMO target modification and hypoxia response. EMBO J 32, 791-804.

Hu, W.J., Chen, J., Liu, T.W., Liu, X., Wu, F.H., Wang, W.H., He, J.X., Xiao, Q., and Zheng, H.L. (2014). Comparative proteomic analysis on wild type and nitric oxide-overproducing mutant (nox1) of Arabidopsis thaliana. Nitric Oxide 36, 19-30.

Ishida, T., Fujiwara, S., Miura, K., Stacey, N., Yoshimura, M., Schneider, K., Adachi, S., Minamisawa, K., Umeda, M., and Sugimoto, K. (2009). SUMO E3 ligase HIGH PLOIDY2 regulates endocycle onset and meristem maintenance in Arabidopsis. Plant Cell 21, 2284-2297.

Ishida, T., Yoshimura, M., Miura, K., and Sugimoto, K. (2012). MMS21/HPY2 and SIZ1, two Arabidopsis SUMO E3 ligases, have distinct functions in development. PLoS One 7, e46897.

Jaffrey, S.R., and Snyder, S.H. (2001). The biotin switch method for the detection of S-nitrosylated proteins. Sci STKE 2001, pl1.

Jensen, O.N. (2004). Modification-specific proteomics: characterization of post-translational modifications by mass spectrometry. Current Opinion in Chemical Biology 8, 33-41.

Jing, B., Xu, S., Xu, M., Li, Y., Li, S., Ding, J., and Zhang, Y. (2011). Brush and spray: a high-throughput systemic acquired resistance assay suitable for large-scale genetic screening. Plant Physiol 157, 973-980.

Jones, J.D., and Dangl, J.L. (2006). The plant immune system. Nature 444, 323-329.
Kachroo, A., and Robin, G.P. (2013). Systemic signaling during plant defense. Curr Opin Plant Biol 16, 527-533.

Kelley, L.A., and Sternberg, M.J. (2009). Protein structure prediction on the Web: a case study using the Phyre server. Nat Protoc 4, 363-371.

Kim, J.G., Stork, W., and Mudgett, M.B. (2013). Xanthomonas type III effector XopD desumoylates tomato transcription factor SlERF4 to suppress ethylene responses and promote pathogen growth. Cell Host Microbe 13, 143-154.

Kim, J.G., Taylor, K.W., Hotson, A., Keegan, M., Schmelz, E.A., and Mudgett, M.B. (2008). XopD SUMO protease affects host transcription, promotes pathogen growth, and delays symptom development in xanthomonas-infected tomato leaves. Plant Cell 20, 1915-1929.

Kim, S.O., Merchant, K., Nudelman, R., Beyer, W.F., Keng, T., DeAngelo, J., Hausladen, A., and Stamler, J.S. (2002). OxyR: a molecular code for redox-related signaling. Cell 109, 383-396.

Kleinboelting, N., Huep, G., Kloetgen, A., Viehoever, P., and Weisshaar, B. (2012). GABI-Kat SimpleSearch: new features of the Arabidopsis thaliana T-DNA mutant database. Nucleic Acids Research 40, D1211-D1215.

Klug, H., Xaver, M., Chaugule, V.K., Koidl, S., Mittler, G., Klein, F., and Pichler, A. (2013). Ubc9 sumoylation controls SUMO chain formation and meiotic synapsis in Saccharomyces cerevisiae. Mol Cell 50, 625-636.

Knipscheer, P., Flotho, A., Klug, H., Olsen, J.V., van Dijk, W.J., Fish, A., Johnson, E.S., Mann, M., Sixma, T.K., and Pichler, A. (2008). Ubc9 sumoylation regulates SUMO target discrimination. Mol Cell 31, 371-382.

Knipscheer, P., van Dijk, W.J., Olsen, J.V., Mann, M., and Sixma, T.K. (2007). Noncovalent interaction between Ubc9 and SUMO promotes SUMO chain formation. EMBO J 26, 2797-2807.

Komander, D., and Rape, M. (2012). The ubiquitin code. Annu Rev Biochem 81, 203-229.

KONCZ, C., and SCHELL, J. (1986). The promoter of TL-DNA gene 5 controls the tissue-specific expression of chimeric genes carried by a novel type of Agrobacterium binary vector. Molecular & General Genetics 204, 383-396.

Kubienová, L., Kopečný, D., Tylichová, M., Briozzo, P., Skopalová, J., Šebela, M., Navrátil, M., Tâche, R., Luhová, L., Barroso, J.B., et al. (2013). Structural and

functional characterization of a plant S-nitrosoglutathione reductase from Solanum lycopersicum. Biochimie 95, 889-902.

Kurepa, J., Walker, J.M., Smalle, J., Gosink, M.M., Davis, S.J., Durham, T.L., Sung, D.Y., and Vierstra, R.D. (2003). The small ubiquitin-like modifier (SUMO) protein modification system in Arabidopsis. Accumulation of SUMO1 and -2 conjugates is increased by stress. J Biol Chem 278, 6862-6872.

Kwon, E., Feechan, A., Yun, B.W., Hwang, B.H., Pallas, J.A., Kang, J.G., and Loake, G.J. (2012). AtGSNOR1 function is required for multiple developmental programs in Arabidopsis. Planta 236, 887-900.

Lai, Z., Vinod, K., Zheng, Z., Fan, B., and Chen, Z. (2008). Roles of Arabidopsis WRKY3 and WRKY4 transcription factors in plant responses to pathogens. BMC Plant Biol 8, 68.

Laloi, C., Mestres-Ortega, D., Marco, Y., Meyer, Y., and Reichheld, J.P. (2004). The Arabidopsis cytosolic thioredoxin h5 gene induction by oxidative stress and its W-box-mediated response to pathogen elicitor. Plant Physiol 134, 1006-1016.

Larkin, M.A., Blackshields, G., Brown, N.P., Chenna, R., McGettigan, P.A., McWilliam, H., Valentin, F., Wallace, I.M., Wilm, A., Lopez, R., et al. (2007). Clustal W and Clustal X version 2.0. Bioinformatics 23, 2947-2948.

Lee, J., Nam, J., Park, H.C., Na, G., Miura, K., Jin, J.B., Yoo, C.Y., Baek, D., Kim, D.H., Jeong, J.C., et al. (2007). Salicylic acid-mediated innate immunity in Arabidopsis is regulated by SIZ1 SUMO E3 ligase. Plant J 49, 79-90.

Lee, U., Wie, C., Fernandez, B.O., Feelisch, M., and Vierling, E. (2008). Modulation of nitrosative stress by S-nitrosoglutathione reductase is critical for thermotolerance and plant growth in Arabidopsis. Plant Cell 20, 786-802.

Lee, Y.J., Mou, Y., Maric, D., Klimanis, D., Auh, S., and Hallenbeck, J.M. (2011). Elevated Global SUMOylation in Ubc9 Transgenic Mice Protects Their Brains against Focal Cerebral Ischemic Damage. PLoS One 6, e25852.

Leitner, M., Vandelle, E., Gaupels, F., Bellin, D., and Delledonne, M. (2009). NO signals in the haze: nitric oxide signalling in plant defence. Curr Opin Plant Biol 12, 451-458.

Lin, D., Tatham, M.H., Yu, B., Kim, S., Hay, R.T., and Chen, Y. (2002). Identification of a substrate recognition site on Ubc9. J Biol Chem 277, 21740-21748.

Lindermayr, C., Saalbach, G., and Durner, J. (2005). Proteomic identification of S-nitrosylated proteins in Arabidopsis. Plant Physiol 137, 921-930.

Lindermayr, C., Sell, S., Müller, B., Leister, D., and Durner, J. (2010). Redox regulation of the NPR1-TGA1 system of Arabidopsis thaliana by nitric oxide. Plant Cell 22, 2894-2907.

Liu, L., Hausladen, A., Zeng, M., Que, L., Heitman, J., and Stamler, J.S. (2001). A metabolic enzyme for S-nitrosothiol conserved from bacteria to humans. Nature 410, 490-494.

Liu, L., Yan, Y., Zeng, M., Zhang, J., Hanes, M.A., Ahearn, G., McMahon, T.J., Dickfeld, T., Marshall, H.E., Que, L.G., et al. (2004). Essential roles of S-nitrosothiols in vascular homeostasis and endotoxic shock. Cell 116, 617-628.

Livak, K.J., and Schmittgen, T.D. (2001). Analysis of relative gene expression data using real-time quantitative PCR and the 2(-Delta Delta C(T)) Method. Methods 25, 402-408.

Loake, G., and Grant, M. (2007). Salicylic acid in plant defence--the players and protagonists. Curr Opin Plant Biol 10, 466-472.

Lois, L.M., Lima, C.D., and Chua, N.H. (2003). Small ubiquitin-like modifier modulates abscisic acid signaling in Arabidopsis. Plant Cell 15, 1347-1359.

Lozano-Durán, R., Rosas-Díaz, T., Gusmaroli, G., Luna, A.P., Taconnat, L., Deng, X.W., and Bejarano, E.R. (2011). Geminiviruses subvert ubiquitination by altering CSN-mediated derubylation of SCF E3 ligase complexes and inhibit jasmonate signaling in Arabidopsis thaliana. Plant Cell 23, 1014-1032.

Mahajan, R., Delphin, C., Guan, T., Gerace, L., and Melchior, F. (1997). A small ubiquitin-related polypeptide involved in targeting RanGAP1 to nuclear pore complex protein RanBP2. Cell 88, 97-107.

Malik, S.I., Hussain, A., Yun, B.W., Spoel, S.H., and Loake, G.J. (2011). GSNOR-mediated de-nitrosylation in the plant defence response. Plant Sci 181, 540-544.

Mannick, J.B., Hausladen, A., Liu, L., Hess, D.T., Zeng, M., Miao, Q.X., Kane, L.S., Gow, A.J., and Stamler, J.S. (1999). Fas-induced caspase denitrosylation. Science 284, 651-654.

Mansoor, S., Zafar, Y., and Briddon, R.W. (2006). Geminivirus disease complexes: the threat is spreading. Trends Plant Sci 11, 209-212.

Miller, M.J., Barrett-Wilt, G.A., Hua, Z., and Vierstra, R.D. (2010). Proteomic analyses identify a diverse array of nuclear processes affected by small ubiquitin-like modifier conjugation in Arabidopsis. Proc Natl Acad Sci U S A 107, 16512-16517.

Mishina, T.E., and Zeier, J. (2007). Pathogen-associated molecular pattern recognition rather than development of tissue necrosis contributes to bacterial induction of systemic acquired resistance in Arabidopsis. Plant J 50, 500-513.

Miura, K., and Hasegawa, P.M. (2010). Sumoylation and other ubiquitin-like post-translational modifications in plants. Trends Cell Biol 20, 223-232.

Miura, K., Jin, J.B., and Hasegawa, P.M. (2007). Sumoylation, a post-translational regulatory process in plants. Curr Opin Plant Biol 10, 495-502.

Miura, K., Lee, J., Jin, J.B., Yoo, C.Y., Miura, T., and Hasegawa, P.M. (2009). Sumoylation of ABI5 by the Arabidopsis SUMO E3 ligase SIZ1 negatively regulates abscisic acid signaling. Proc Natl Acad Sci U S A 106, 5418-5423.

Miura, K., Rus, A., Sharkhuu, A., Yokoi, S., Karthikeyan, A.S., Raghothama, K.G., Baek, D., Koo, Y.D., Jin, J.B., Bressan, R.A., et al. (2005). The Arabidopsis SUMO E3 ligase SIZ1 controls phosphate deficiency responses. Proc Natl Acad Sci U S A 102, 7760-7765.

Mo, Y.Y., Yu, Y., Shen, Z., and Beck, W.T. (2002). Nucleolar delocalization of human topoisomerase I in response to topotecan correlates with sumoylation of the protein. J Biol Chem 277, 2958-2964.

Moschos, S.J., Jukic, D.M., Athanassiou, C., Bhargava, R., Dacic, S., Wang, X., Kuan, S.F., Fayewicz, S.L., Galambos, C., Acquafondata, M., et al. (2010). Expression analysis of Ubc9, the single small ubiquitin-like modifier (SUMO) E2 conjugating enzyme, in normal and malignant tissues. Hum Pathol 41, 1286-1298.

Mou, Z., Fan, W., and Dong, X. (2003). Inducers of plant systemic acquired resistance regulate NPR1 function through redox changes. Cell 113, 935-944.

Murashige, T., and Skoog, F. (1962). A revised medium for rapid growth and bio assays with tobacco tissue cultures. Physiologia Plantarum 15, 473-497.

Murtas, G., Reeves, P.H., Fu, Y.F., Bancroft, I., Dean, C., and Coupland, G. (2003) A nuclear protease required for flowering-time regulation in Arabidopsis reduces the abundance of SMALL UBIQUITIN-RELATED MODIFIER conjugates. Plant Cell 15, 2308-19.

Ninnemann, H., and Maier, J. (1996). Indications for the occurrence of nitric oxide synthases in fungi and plants and the involvement in photoconidiation of Neurospora crassa. Photochem Photobiol 64, 393-398.

Oerke, E.C. (2006). Crop losses to pests. Journal of Agricultural Science 144, 31-43.

Palancade, B., and Doye, V. (2008). Sumoylating and desumoylating enzymes at nuclear pores: underpinning their unexpected duties? Trends Cell Biol 18, 174-183.
Park, B.S., Song, J.T., and Seo, H.S. (2011). Arabidopsis nitrate reductase activity is stimulated by the E3 SUMO ligase AtSIZ1. Nat Commun 2, 400.

Prabakaran, S., Lippens, G., Steen, H., and Gunawardena, J. (2012). Post-translational modification: nature's escape from genetic imprisonment and the basis for dynamic information encoding. Wiley Interdisciplinary Reviews-Systems Biology and Medicine 4, 565-583.

Prudden, J., Perry, J.J., Arvai, A.S., Tainer, J.A., and Boddy, M.N. (2009). Molecular mimicry of SUMO promotes DNA repair. Nat Struct Mol Biol 16, 509-516.

Puyaubert, J., Fares, A., Rézé, N., Peltier, J.B., and Baudouin, E. (2014). Identification of endogenously S-nitrosylated proteins in Arabidopsis plantlets: effect of cold stress on cysteine nitrosylation level. Plant Sci 215-216, 150-156.

Qu, J., Liu, G.H., Wu, K., Han, P., Wang, P., Li, J., Zhang, X., and Chen, C. (2007). Nitric oxide destabilizes Pias3 and regulates sumoylation. PLoS One 2, e1085.

Que, L.G., Yang, Z., Stamler, J.S., Lugogo, N.L., and Kraft, M. (2009). S-nitrosoglutathione reductase: an important regulator in human asthma. Am J Respir Crit Care Med 180, 226-231.

Reindle, A., Belichenko, I., Bylebyl, G.R., Chen, X.L., Gandhi, N., and Johnson, E.S. (2006). Multiple domains in Siz SUMO ligases contribute to substrate selectivity. J Cell Sci 119, 4749-4757.

Rockel, P., Strube, F., Rockel, A., Wildt, J., and Kaiser, W.M. (2002). Regulation of nitric oxide (NO) production by plant nitrate reductase in vivo and in vitro. J Exp Bot 53, 103-110.

Rodriguez, M.S., Dargemont, C., and Hay, R.T. (2001). SUMO-1 conjugation in vivo requires both a consensus modification motif and nuclear targeting. J Biol Chem 276, 12654-12659.

Romero-Puertas, M.C., Campostrini, N., Mattè, A., Righetti, P.G., Perazzolli, M., Zolla, L., Roepstorff, P., and Delledonne, M. (2008). Proteomic analysis of S-nitrosylated proteins in Arabidopsis thaliana undergoing hypersensitive response. Proteomics 8, 1459-1469.

Romero-Puertas, M.C., Laxa, M., Mattè, A., Zaninotto, F., Finkemeier, I., Jones, A.M., Perazzolli, M., Vandelle, E., Dietz, K.J., and Delledonne, M. (2007). S-nitrosylation of peroxiredoxin II E promotes peroxynitrite-mediated tyrosine nitration. Plant Cell 19, 4120-4130.

Ronald, P. (2011). Plant genetics, sustainable agriculture and global food security. Genetics 188, 11-20.

Ross, A.F. (1961). Systemic acquired resistance induced by localized virus infections in plants. Virology 14, 340-358.

Saitoh, H., and Hinchey, J. (2000). Functional heterogeneity of small ubiquitin-related protein modifiers SUMO-1 versus SUMO-2/3. J Biol Chem 275, 6252-6258.

Sanghani, P.C., Bosron, W.F., and Hurley, T.D. (2002). Human glutathione-dependent formaldehyde dehydrogenase. Structural changes associated with ternary complex formation. Biochemistry 41, 15189-15194.

Saracco, S.A., Miller, M.J., Kurepa, J., and Vierstra, R.D. (2007). Genetic analysis of SUMOylation in Arabidopsis: conjugation of SUMO1 and SUMO2 to nuclear proteins is essential. Plant Physiol 145, 119-134.

Scheler, C., Durner, J., and Astier, J. (2013). Nitric oxide and reactive oxygen species in plant biotic interactions. Curr Opin Plant Biol 16, 534-539.

Schneider, C.A., Rasband, W.S., and Eliceiri, K.W. (2012). NIH Image to ImageJ: 25 years of image analysis. Nat Methods 9, 671-675.

Schreiter, E.R., Rodríguez, M.M., Weichsel, A., Montfort, W.R., and Bonaventura, J. (2007). S-nitrosylation-induced conformational change in blackfin tuna myoglobin. J Biol Chem 282, 19773-19780.

Skelly, M.J., and Loake, G.J. (2013). Synthesis of redox-active molecules and their signaling functions during the expression of plant disease resistance. Antioxid Redox Signal 19, 990-997.

Slaymaker, D.H., Navarre, D.A., Clark, D., del Pozo, O., Martin, G.B., and Klessig, D.F. (2002). The tobacco salicylic acid-binding protein 3 (SABP3) is the chloroplast carbonic anhydrase, which exhibits antioxidant activity and plays a role in the hypersensitive defense response. Proc Natl Acad Sci U S A 99, 11640-11645.

Spadaro, D., Yun, B.W., Spoel, S.H., Chu, C., Wang, Y.Q., and Loake, G.J. (2010). The redox switch: dynamic regulation of protein function by cysteine modifications. Physiol Plant 138, 360-371.

Spoel, S.H., and Loake, G.J. (2011). Redox-based protein modifications: the missing link in plant immune signalling. Curr Opin Plant Biol.

Spoel, S.H., Mou, Z., Tada, Y., Spivey, N.W., Genschik, P., and Dong, X. (2009). Proteasome-mediated turnover of the transcription coactivator NPR1 plays dual roles in regulating plant immunity. Cell 137, 860-872.

Stamler, J.S., Simon, D.I., Osborne, J.A., Mullins, M.E., Jaraki, O., Michel, T., Singel, D.J., and Loscalzo, J. (1992). S-nitrosylation of proteins with nitric oxide: synthesis and characterization of biologically active compounds. Proc Natl Acad Sci U S A 89, 444-448.

Streatfield, S.J., Weber, A., Kinsman, E.A., Häusler, R.E., Li, J., Post-Beittenmiller, D., Kaiser, W.M., Pyke, K.A., Flügge, U.I., and Chory, J. (1999). The phosphoenolpyruvate/phosphate translocator is required for phenolic metabolism, palisade cell development, and plastid-dependent nuclear gene expression. Plant Cell 11, 1609-1622.

Su, Y.F., Yang, T., Huang, H., Liu, L.F., and Hwang, J. (2012). Phosphorylation of Ubc9 by Cdk1 enhances SUMOylation activity. PLoS One 7, e34250.

Sweat, T.A., and Wolpert, T.J. (2007). Thioredoxin h5 is required for victorin sensitivity mediated by a CC-NBS-LRR gene in Arabidopsis. Plant Cell 19, 673-687.

Sánchez-Durán, M.A., Dallas, M.B., Ascencio-Ibañez, J.T., Reyes, M.I., Arroyo-Mateos, M., Ruiz-Albert, J., Hanley-Bowdoin, L., and Bejarano, E.R. (2011). Interaction between geminivirus replication protein and the SUMO-conjugating enzyme is required for viral infection. J Virol 85, 9789-9800.

Tada, Y., Spoel, S.H., Pajerowska-Mukhtar, K., Mou, Z., Song, J., Wang, C., Zuo, J., and Dong, X. (2008). Plant immunity requires conformational changes [corrected] of NPR1 via S-nitrosylation and thioredoxins. Science 321, 952-956.

Tatham, M.H., Chen, Y., and Hay, R.T. (2003a). Role of two residues proximal to the active site of Ubc9 in substrate recognition by the Ubc9.SUMO-1 thiolester complex. Biochemistry 42, 3168-3179.

Tatham, M.H., Jaffray, E., Vaughan, O.A., Desterro, J.M.P., Botting, C.H., Naismith, J.H., and Hay, R.T. (2001). Polymeric chains of SUMO-2 and SUMO-3 are conjugated to protein substrates by SAE1/SAE2 and Ubc9. J Biol Chem 276, 35368-35374.

Tatham, M.H., Kim, S., Yu, B., Jaffray, E., Song, J., Zheng, J., Rodriguez, M.S., Hay, R.T., and Chen, Y. (2003b). Role of an N-terminal site of Ubc9 in SUMO-1, -2, and -3 binding and conjugation. Biochemistry 42, 9959-9969.

Tomanov, K., Hardtke, C., Budhiraja, R., Hermkes, R., Coupland, G., and Bachmair, A. (2013). Small ubiquitin-like modifier conjugating enzyme with active site mutation acts as dominant negative inhibitor of SUMO conjugation in arabidopsis(F). J Integr Plant Biol 55, 75-82.

Tong, H., Hateboer, G., Perrakis, A., Bernards, R., and Sixma, T.K. (1997). Crystal structure of murine/human Ubc9 provides insight into the variability of the ubiquitin-conjugating system. J Biol Chem 272, 21381-21387.

Torres, M.A., and Dangl, J.L. (2005). Functions of the respiratory burst oxidase in biotic interactions, abiotic stress and development. Curr Opin Plant Biol 8, 397-403.

Torres, M.A., Dangl, J.L., and Jones, J.D. (2002). Arabidopsis gp91phox homologues AtrbohD and AtrbohF are required for accumulation of reactive oxygen intermediates in the plant defense response. Proc Natl Acad Sci U S A 99, 517-522.

Truong, K., Lee, T.D., and Chen, Y. (2012). Small ubiquitin-like modifier (SUMO) modification of E1 Cys domain inhibits E1 Cys domain enzymatic activity. J Biol Chem 287, 15154-15163.

van den Burg, H.A., Kini, R.K., Schuurink, R.C., and Takken, F.L. (2010). Arabidopsis small ubiquitin-like modifier paralogs have distinct functions in development and defense. Plant Cell 22, 1998-2016.

van den Burg, H.A., and Takken, F.L. (2010). SUMO-, MAPK-, and resistance protein-signaling converge at transcription complexes that regulate plant innate immunity. Plant Signal Behav 5, 1597-1601.

van Loon, L.C., and van Kammen, A. (1970). Polyacrylamide disc electrophoresis of the soluble leaf proteins from Nicotiana tabacum var. "Samsun" and "Samsun NN". II. Changes in protein constitution after infection with tobacco mosaic virus. Virology 40, 190-211.

Verhage, A., van Wees, S.C., and Pieterse, C.M. (2010). Plant immunity: it's the hormones talking, but what do they say? Plant Physiol 154, 536-540.

Vernooij, B., Friedrich, L., Morse, A., Reist, R., Kolditz-Jawhar, R., Ward, E., Uknes, S., Kessmann, H., and Ryals, J. (1994). Salicylic Acid Is Not the Translocated Signal Responsible for Inducing Systemic Acquired Resistance but Is Required in Signal Transduction. Plant Cell 6, 959-965.

Vierstra, R.D. (2009). The ubiquitin-26S proteasome system at the nexus of plant biology. Nat Rev Mol Cell Biol 10, 385-397.

Vlot, A.C., Dempsey, D.A., and Klessig, D.F. (2009). Salicylic Acid, a multifaceted hormone to combat disease. Annu Rev Phytopathol 47, 177-206.

Wang, Y., Yun, B.W., Kwon, E., Hong, J.K., Yoon, J., and Loake, G.J. (2006). S-nitrosylation: an emerging redox-based post-translational modification in plants. J Exp Bot 57, 1777-1784.

Wang, Y.Q., Feechan, A., Yun, B.W., Shafiei, R., Hofmann, A., Taylor, P., Xue, P., Yang, F.Q., Xie, Z.S., Pallas, J.A., et al. (2009). S-nitrosylation of AtSABP3 antagonizes the expression of plant immunity. J Biol Chem 284, 2131-2137.

Wiermer, M., Feys, B.J., and Parker, J.E. (2005). Plant immunity: the EDS1 regulatory node. Curr Opin Plant Biol 8, 383-389.

Wiktorowicz, J.E., Stafford, S., Rea, H., Urvil, P., Soman, K., Kurosky, A., Perez-Polo, J.R., and Savidge, T.C. (2011). Quantification of cysteinyl S-nitrosylation by fluorescence in unbiased proteomic studies. Biochemistry 50, 5601-5614.

Wilkinson, J.Q., and Crawford, N.M. (1991). Identification of the Arabidopsis CHL3 gene as the nitrate reductase structural gene NIA2. Plant Cell 3, 461-471.

Wilkinson, K.A., and Henley, J.M. (2010). Mechanisms, regulation and consequences of protein SUMOylation. Biochem J 428, 133-145.

Wu, F.H., Shen, S.C., Lee, L.Y., Lee, S.H., Chan, M.T., and Lin, C.S. (2009). Tape-Arabidopsis Sandwich - a simpler Arabidopsis protoplast isolation method. Plant Methods 5, 16.

Xiong, R., and Wang, A. (2013). SCE1, the SUMO-conjugating enzyme in plants that interacts with NIb, the RNA-dependent RNA polymerase of Turnip mosaic virus, is required for viral infection. J Virol 87, 4704-4715.

Xu, S., Guerra, D., Lee, U., and Vierling, E. (2013). S-nitrosoglutathione reductases are low-copy number, cysteine-rich proteins in plants that control multiple developmental and defense responses in Arabidopsis. Front Plant Sci 4, 430.

Yang, S.H., and Sharrocks, A.D. (2006). Convergence of the SUMO and MAPK pathways on the ETS-domain transcription factor Elk-1. Biochem Soc Symp, 121-129.

Yu, M., Lamattina, L., Spoel, S.H., and Loake, G.J. (2014). Nitric oxide function in plant biology: a redox cue in deconvolution. New Phytol.

Yun, B.W., Feechan, A., Yin, M., Saidi, N.B., Le Bihan, T., Yu, M., Moore, J.W., Kang, J.G., Kwon, E., Spoel, S.H., et al. (2011). S-nitrosylation of NADPH oxidase regulates cell death in plant immunity. Nature 478, 264-268.

Zhao, X., and Blobel, G. (2005). A SUMO ligase is part of a nuclear multiprotein complex that affects DNA repair and chromosomal organization. Proc Natl Acad Sci U S A 102, 4777-4782.

Zhu, S., Sachdeva, M., Wu, F., Lu, Z., and Mo, Y.Y. (2010). Ubc9 promotes breast cell invasion and metastasis in a sumoylation-independent manner. Oncogene 29, 1763-1772.